Chapter 10

DYNAMICS OF ELECTROMECHANICAL CONTINUA

10.0 INTRODUCTION

In Chapter 9 we treated simple examples of mechanical continua to establish the basic techniques of making mathematical models and to illustrate the kinds of dynamic behavior and the mathematical methods needed in analyses. In that chapter simple elastic continua at rest were excited at boundaries so that the resulting continuum dynamics were determined by mechanical characteristics alone.

In this chapter we still restrict our attention to simple elastic continua but we generalize on the treatment of Chapter 9 to include the effects of distributed forces of electric origin and material motion. By the use of simple models we illustrate the basic phenomena that occur in a wide variety of physical systems and the analytical techniques used in their mathematical description. In spite of the diversity of physical situations in which continuum electromechanical interactions are important, a unity results from mathematical techniques that are common to all of the situations. It is our purpose here to illuminate, in the simplest context possible, these mathematical techniques and the physical phenomena they describe.

As stated earlier, the techniques presented are fundamental to a wide variety of physical situations. It is therefore helpful for the purpose of appreciating our objectives to review some of the technical areas concerned with continuum electromechanics.

Magnetohydrodynamics (*MHD*) is concerned with the interactions of free currents and magnetic fields in fluids (liquids and gases) which have high enough electrical conductivity that a quasi-static magnetic field model is appropriate for describing the electromagnetic part of the system. To reflect more accurately the nature of the mechanical medium this area is sometimes referred to as *magnetogasdynamics* (*MGD*) or as *magnetofluiddynamics* (*MFD*). Areas of application include pumping and levitation of liquids (usually

metals), orientation and confinement of extremely hot ionized gases or plasmas, as, for example, in thermonuclear fusion experiments,* electric power generation from ionized gases produced by combustion of fossil fuels or from heat produced in a fission reactor,† and space propulsion achieved by electromagnetic acceleration of ionized gases.‡ Scientific interest in this area includes such geophysical and astrophysical topics as the origin of the earth's magnetic field in its liquid metal core and the dynamics of stellar structures composed of highly ionized gases.

A similar area is *ferrohydrodynamics*, which is concerned with magnetization interactions of magnetic fields with a ferromagnetic fluid.§

Electrohydrodynamics (EHD) is concerned with interaction between electric fields and free or bound (polarization) charges in fluids. The fluids may be extremely good insulators, slightly conducting, or even highly conducting. The distinguishing feature is that the electromagnetic part of the system is described by a quasi-static electric field model. Applications of EHD include pumping and levitation of liquids and gases, extraction of contaminants from gases such as smoke,** mixing of liquids, orientation of liquids in near-zero-gravity environments, augmentation of heat transfer, and property measurements in fluid systems. EHD interactions also occur in meteorology, in which charge distribution in the atmosphere (as in a thunderstorm) is important, and in surface physics, in which the distribution of charges at an interface is significant, as in frictional electrification.††

The engineering and scientific applications of *electron and ion beams* involve continuum electromechanical interactions. Electron beams, confined by magnetic fields and interacting through electric fields with distributed electric circuits, are commonly used to generate power at microwave frequencies.‡‡ In such applications the beam is represented by quasi-static equations, but the distributed electric circuits support electromagnetic waves and are not amenable to quasi-static analysis. Electron beams are also used for heating, welding, forming, and purifying metals. Charged particle beams, electrons and ions, are used for medical treatment, for measuring collision cross sections, and for heating plasmas.§§

* D. J. Rose and M. Clark, Jr., *Plasmas and Controlled Fusion*, M.I.T. Press and Wiley, New York, 1961.

† G. W. Sutton and A. Sherman, *Engineering Magnetohydrodynamics*, McGraw-Hill, New York, 1965.

‡ *Ibid.*, p. 447.

§ R. E. Rosensweig, "Magnetic Fluids," *Intern. Sci. Technol.*, **55**, 48–56, 90 (July 1966).

** H. J. White, *Industrial Electrostatic Precipitation*, Addison-Wesley, Reading, Mass., 1963.

†† L. B. Loeb, *Static Electrification*, Springer, Berlin, 1958.

‡‡ C. C. Johnson, *Field and Wave Electrodynamics*, McGraw-Hill, New York, 1965, p. 275.

§§ T. H. Stix, *The Theory of Plasma Waves*, McGraw-Hill, New York, 1962, p. 107.

*Plasma dynamics** is concerned with the behavior of gases composed at least in part of charged particles. Thus continuum electromechanical interactions will affect the behavior of a plasma. Probably the most common example of a plasma is the ionized gas in a fluorescent lamp. Other examples are gas-filled rectifiers, flames such as rocket exhausts, and the sun. The physical characteristics of ionized gases can assume many forms. In certain cases, such as proposed fusion devices and MHD generators, the plasma behaves as a highly conducting fluid and its dynamic behavior is described by a magnetohydrodynamic approximation. In other cases the plasma is only slightly ionized and the electrohydrodynamic equations are appropriate. In still other cases the plasma may be so tenuous that it is best described as a collection of noninteracting particles in imposed magnetic and electric fields. In all of these regimes the plasma exhibits the basic phenomena of wave propagation and instability, subjects that are treated in this chapter.

Electrons and holes in semiconductors, usefully modeled as plasmas, give rise to the name *solid-state plasmas.*† These charges behave collectively like gaseous plasmas and are thus amenable to analysis with the same types of mathematical model. Electromechanical interactions in solid-state plasmas are used to achieve microwave power generation and to make electronic components with a variety of useful terminal characteristics.

Electromechanical interactions of several types occur with elastic solids and lead to useful devices such as transducers. *Electroelasticity* and *piezoelectricity*‡ result from polarization interactions in elastic dielectrics and are modeled as quasi-static electric field systems. *Magnetoelasticity* and *piezomagnetics*§ result from magnetization interactions in elastic solids and are modeled as quasi-static magnetic field systems. Magnetoelastic phenomena have found applications in *microwave magnetics*** in which electromechanical interactions lead to useful microwave components.

The foregoing examples illustrate the diversity of physical situations, in which continuum electromechanical interactions are important, and the variety of applications resulting therefrom. We now proceed to study the kinds of dynamical phenomena that can result from these interactions.

In the study of lumped parameter systems defined by linear, constant-coefficient equations, the temporal behavior is characterized by e^{st}, as illustrated in Chapter 5. Similarly, the dynamics of a continuum with a single

* L. Spitzer, Jr., *Physics of Fully Ionized Gases*, Interscience, New York, 1956. (The plasma, as defined on p. 17 of this reference, is somewhat more specifically defined then in our discussion.)

† R. Bowers and M. C. Steele, *Proc. I.E.E.E.*, **52,** 1105 (1964).

‡ W. P. Mason, *Physical Acoustics*, Vol. 1, Part A, Academic, New York (1964, pp. 169–270).

§ *Ibid.*

** W. F. Brown, *Micromagnetics*, Interscience, New York, 1963.

space dependence x can be represented in terms of solutions in the form*

$$\xi = \text{Re}\, \hat{\xi} e^{j(\omega t - kx)}. \tag{10.0.1}$$

The (angular) frequency ω can, in general, be complex

$$\omega = \omega_r + j\omega_i, \tag{10.0.2}$$

just as s can be complex in the lumped-parameter case. As we shall see, the physical significance of a complex ω is not so clear as it is in the lumped-parameter case because the temporal dependence is only part of the story. The wavenumber k, which represents the spatial dependence, can also be complex:

$$k = k_r + jk_i. \tag{10.0.3}$$

The sections that follow have the objective of imparting some physical and mathematical insight as to how wave solutions in the form of (10.0.1) are used to describe the dynamics of one-dimensional continuous media.

10.1 WAVES AND INSTABILITIES IN STATIONARY MEDIA

It is the purpose of this chapter to illustrate the dynamics of electromechanical continua. This is done by making use of the one-dimensional model for the wire and membrane, introduced in Chapter 9. It should be evident from the introduction that the cases considered in the following sections illustrate the dynamics of a variety of purely mechanical and purely electrical as well as electromechanical systems. A salient feature of the dynamics of systems involving continuous media is the effect of material motion. Our development in this section is confined to the dynamics of systems in which the mechanical medium is at rest. The effect of convection, or gross material motion, on these systems is taken up in the next section.

It is helpful to associate fundamental types of dynamical behavior with a particular physical situation. One of the simplest we can imagine for this purpose is the "string" or wire under tension. If the wire has an equilibrium tension f and a mass per unit length m, its transverse deflections are governed by the equation

$$m\frac{\partial^2 \xi}{\partial t^2} = f\frac{\partial^2 \xi}{\partial x^2} + S_z, \tag{10.1.1}$$

where S_z is a transverse force per unit length (see Table 9.2). In the sections that follow we consider electromechanical coupling to the string through

* The use of $j\omega$ rather than s is simply a matter of convention.

S_z. Before embarking on this development it would be helpful to recall the essential features of the string dynamics in the absence of coupling.

10.1.1 Waves without Dispersion

In the absence of external forces the string deflections $\xi(x, t)$ must satisfy the wave equation [(10.1.1) with $S_z = 0$]

$$\frac{\partial^2 \xi}{\partial t^2} = v_s^2 \frac{\partial^2 \xi}{\partial x^2}, \tag{10.1.2}$$

where $v_s = \sqrt{f/m}$. In Section 9.2.1 we found both the sinusoidal steady-state and the transient response (normal modes) of the string by making appropriate use of solutions in the form of (10.0.1). Substitution of the assumed solution into the equation of motion (10.1.2) shows that ω and k must be related by the dispersion equation

$$\omega^2 = v_s^2 k^2. \tag{10.1.3}$$

Thus the ω-k plot for waves on the simple string appears as shown in Fig. 10.1.1. For the real value of frequency ω shown in the figure there are two solutions ($\pm\beta$) to (10.1.3) for the wavenumber k.

From the form of the wave solution (10.0.1) it follows that points of constant phase move along the x-axis with a phase velocity

$$v_p = \frac{\omega}{k}. \tag{10.1.4}$$

Figure 10.1.1 shows that for a given frequency there are two waves with phase velocities that are negatives. Note that the phase velocities of the waves are

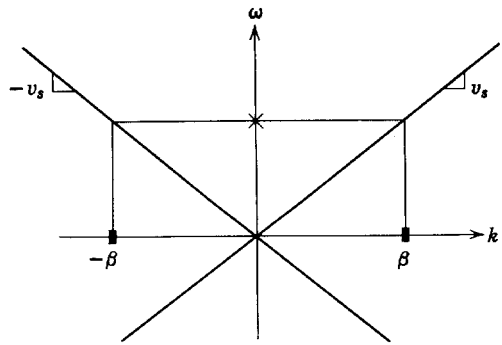

Fig. 10.1.1 Dispersion equation for waves on the simple string.

simply $\pm v_s$ and are independent of the frequency; that is, the dispersion equation for a given wave is a linear relationship between ω and k. For the simple string, waves with differing frequencies (or wavenumbers) propagate with the same phase velocity and are therefore said to propagate without dispersion.

10.1.2 Cutoff or Evanescent Waves

The string, described by (10.1.1), can be a taut conducting wire (or tightly wound helical spring) carrying a current that interacts with a magnetic field (Fig. 10.1.2). Here the string is stretched along the x-axis between two magnet coils arranged to give a null in magnetic field along the x-axis. The wire is free to vibrate in the horizontal plane of the magnet coils. For small excursions from the x-axis the wire experiences a magnetic flux density $\mathbf{B}$, which is essentially a linear function of ξ. Hence, when a current I is passed through the wire in the direction shown, a restoring force per unit length $\mathbf{I} \times \mathbf{B}$ tends to return the wire to the x-axis:

$$S_z \mathbf{i}_z = \mathbf{I} \times \mathbf{B} = -Ib\xi \mathbf{i}_z; \tag{10.1.5}$$

b is shown in Fig. 10.1.2*b*. This is the force-displacement relationship of a simple spring. The current $\mathbf{I}$ and flux density $\mathbf{B}$ interact to produce a spring-like force per unit length that tends to return the wire to its equilibrium position.

With the addition of coupling to the magnetic field, the equation of motion

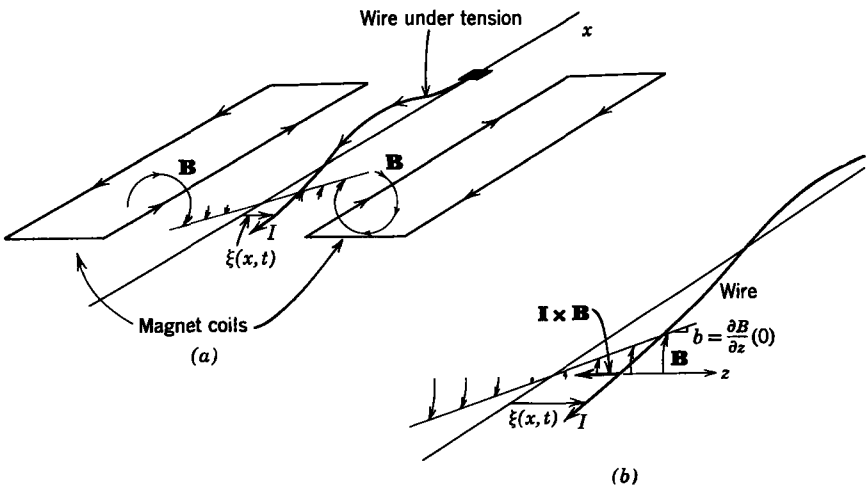

Fig. 10.1.2 (*a*) A conducting wire is stretched along the x-axis and is free to undergo transverse motions in the horizontal plane. Magnet coils produce a field $\mathbf{B}$ which is zero along the x-axis; (*b*) the wire carries a current I so that deflections from the x-axis result in a force that tends to restore the wire to its equilibrium position.

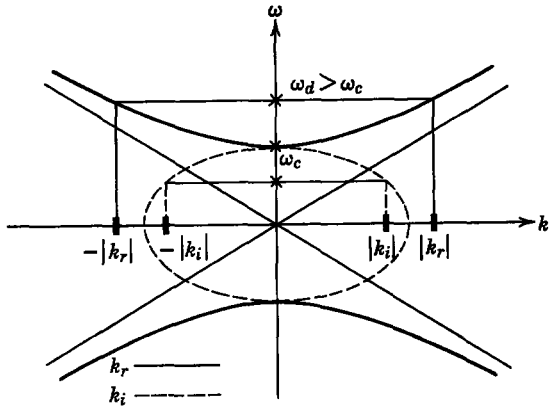

Fig. 10.1.3 Dispersion relation for the wire subject to a restoring force distributed along its length (for the case shown in Fig. 10.1.2). Complex values of k are shown as functions of real values of ω.

(10.1.1) becomes

$$\frac{\partial^2 \xi}{\partial t^2} = v_s^2 \frac{\partial^2 \xi}{\partial x^2} - \omega_c^2 \xi, \qquad \omega_c^2 = \frac{Ib}{m}. \tag{10.1.6}$$

Now, substitution of solutions in the form of (10.0.1) gives a dispersion equation that is not simply the linear relationship between ω and k of (10.1.3). Rather

$$\omega^2 = v_s^2 k^2 + \omega_c^2. \tag{10.1.7}$$

For large values of k, ω does not depend significantly on ω_c, hence the asymptotes of an ω-k plot are simply the two straight lines of the ω-k plot with $\omega_c = 0$ (Fig. 10.1.1). If we note further that $\omega = \pm\omega_c$, where $k = 0$, the ω-k plot of Fig. 10.1.3 can be easily sketched. The effect of the current I is to evolve a pair of hyperbolas from the two straight lines of Fig. 10.1.1. As the current I is raised (with B fixed), the intersections ω_c move out along the ω-axis.

The dispersion equation is quadratic in both ω and k. Hence for each real value of k two values of ω can be seen from the solid curves of Fig. 10.1.3 always to be real. This relationship, however is not true if ω and k are interchanged. Real values of ω give real values of k only if $|\omega| > \omega_c$, as can also be seen in the figure. Solution of (10.1.7) shows that in the range $|\omega| < \omega_c$ the dispersion equation gives imaginary values of k represented by the dashed curve in Fig. 10.1.3. Note that when $k = jk_i$ in (10.1.7) the analytical geometric relation between ω and k_i is an ellipse; for example at the points at which $\omega = 0$ (10.1.7) shows that $k = \pm j\omega_c/v_s$.

The most evident consequences of introducing the additional force, which we can think of as resulting because of the current I, are illustrated by

considering the response to a sinusoidal, steady-state driving function. For purposes of illustration the spring is fixed at $x = 0$ and given a sinusoidal displacement at $x = -l$:

$$\xi(0, t) = 0, \tag{10.1.8}$$

$$\xi(-l, t) = \xi_d \sin \omega_d t. \tag{10.1.9}$$

These conditions are the same as those considered in Section 9.2.1*a* for the wire with no external force.

To match the driving condition the frequency ω of the dispersion equation is taken as ω_d, and solutions have the form of (10.0.1) for two values of k which can be found by solving (10.1.7).

$$k = \pm \frac{\sqrt{\omega_d^2 - \omega_c^2}}{v_s}. \tag{10.1.10}$$

These wavenumbers are shown graphically in Fig. 10.1.3.

To avoid ambiguity the wavenumbers consistent with the frequency $\omega = \omega_d$, given by (10.1.10) are written as

$$\begin{aligned} k &= \pm |k_r|, \qquad \omega_d > \omega_c, \\ k &= \pm j |k_i|, \qquad \omega_d < \omega_c. \end{aligned} \tag{10.1.11}$$

This is the notation used in Fig. 10.1.3. At this point we have established that there are two waves on the wire with the frequency ω_d, and the boundary conditions are satisfied by taking a linear combination of these waves. For $\omega_d > \omega_c$

$$\xi = \text{Re}\,(Ce^{-j|k_r|x} + De^{j|k_r|x})e^{j\omega_d t} \tag{10.1.12}$$

and a similar equation with $|k_r| \to j|k_i|$ for $\omega_d < \omega_c$. The constants C and D are determined by the boundary conditions (10.1.8) and (10.1.9). It follows that for

$$\omega_d > \omega_c, \xi = -\xi_d \frac{\sin |k_r| x}{\sin |k_r| l} \sin \omega_d t, \tag{10.1.13}$$

and for

$$\omega_d < \omega_c, \xi = -\xi_d \frac{\sinh |k_i| x}{\sinh |k_i| l} \sin \omega_d t, \tag{10.1.14}$$

The significance of the imaginary wavenumbers is now apparent. Figure 10.1.4 shows the effect of raising the current I (i.e., ω_c) with the driving frequency ω_d fixed. With no current, waves on the wire have the same familiar appearance as in Section 9.2.1*a* (see Fig. 9.2.6). As long as $\omega_d > \omega_c$, this same general appearance prevails and the wire tends to bow outward and assume the shape usually found with standing waves. When ω_c has been raised to the point at which it coincides with ω_d, the wire takes on the appearance shown in Fig. 10.1.4*b*. Here the effect of inertia, which tends to make the wire bow outward,

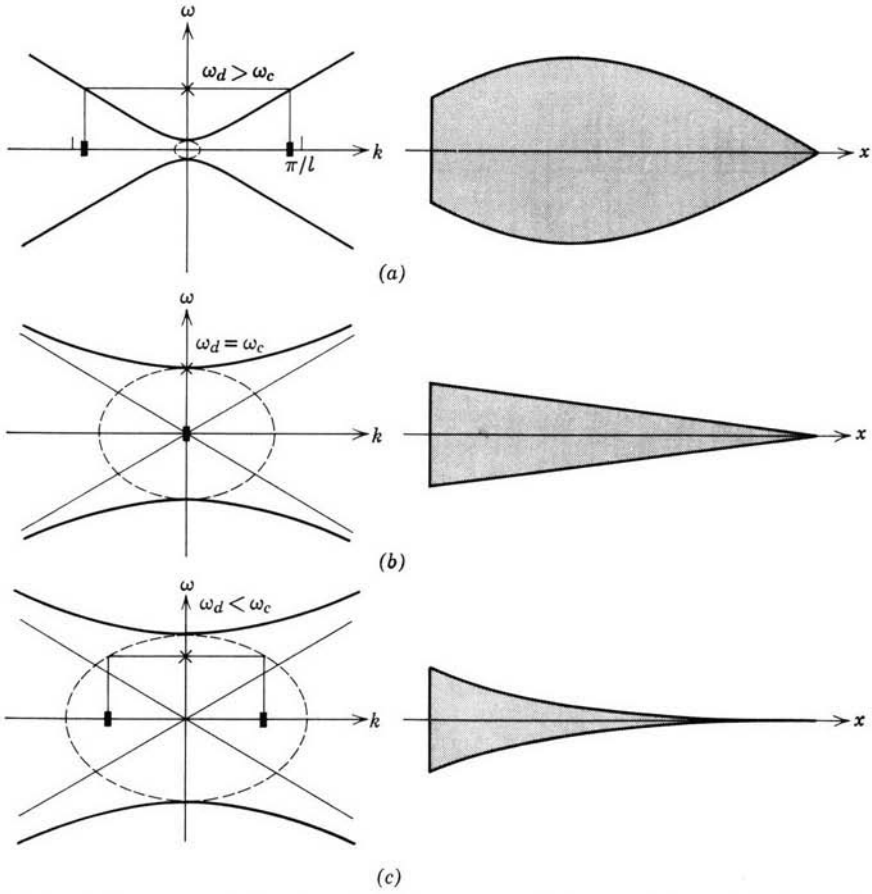

Fig. 10.1.4 Envelope of wire deflection in magnetic field. The wire is fixed at the right end and driven at a fixed sinusoidal frequency at the left end. The ω-k plots show the effect of the current I on the dispersion equation. The current I (or cutoff frequency ω_c) is being raised so that (*a*), $I \approx 0$, (*b*) I is sufficient just to cut off the propagation ($\omega_d = \omega_c$), and (*c*) the waves are evanescent, $\omega_d < \omega_c$. This experiment can be seen in the film "Complex Waves I," produced for the National Committee on Electrical Engineering films by Education Development Center, Newton, Mass.

is just canceled by the restoring force due to I. The wavenumbers are zero and the envelope of the wire deflection is a linear function of x. The limit of either (10.1.13) or (10.1.14) as $k \to 0$ yields

$$\xi = -\xi_d\left(\frac{x}{l}\right) \sin \omega_d t. \tag{10.1.15}$$

This is called the cutoff condition, hence ω_c is the *cutoff frequency*. As ω_c is raised still further, the wire bows inward, as shown in Fig. 10.1.4*c*. Here the

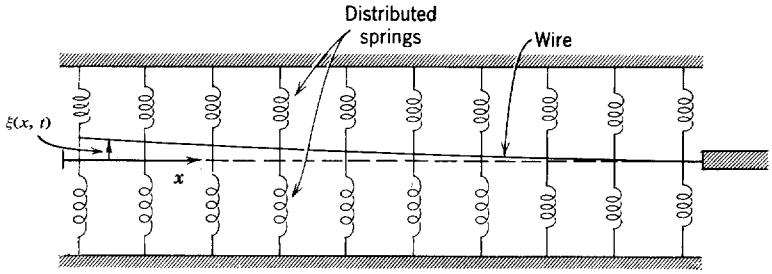

Fig. 10.1.5 With the current as shown, the system in Fig. 10.1.2 gives rise to forces on the wire that are equivalent to springs distributed along the length of the wire.

deflection amplitude simply decays spatially as we move away from the point of excitation. The spatial dependence of (10.1.14) is monotonic in x, so that the wire deflections have the same phase as the excitation. Note that these decaying or *evanescent* waves do not involve dissipation. They are present here because each segment of the wire is subject to a springlike restoring force that tends to push it toward the x-axis. An equivalent physical situation is shown in Fig. 10.1.5. Without recourse to mathematics we expect that when the left end of the wire is slowly displaced upward the wire tends to bow inward toward the x-axis. This is all that (10.1.14) is telling us. The restoring force that we would feel in slowly displacing the end of the wire would be the same as if we were displacing the end of a spring.

As we shall see, continuous media excited in the sinusoidal steady state can also support spatially decaying waves because of damping (dissipation of energy). Even more interesting are situations in which complex wavenumbers mean that waves grow spatially rather than decaying. Both cases, which are considered in later sections, involve dispersion equations that give complex values of k for real values of ω, just as we have here, and it is important to establish a physical picture of their significance.

Evanescent or cutoff waves are often found in studies of propagation through guiding structures. We shall see this in Section 10.4.1 in which waves that propagate in the x-direction on a membrane fixed along its edges at $y = 0$ and $y = b$ have a cutoff frequency below which they are evanescent. This is an example of a wide class of two- and three-dimensional situations in which propagation in a longitudinal (x) direction is restricted by boundary conditions in the transverse directions (y and z). The transverse boundaries restrict (or squash) the dynamical motions, just as they do in Fig. 10.1.5. Before propagation can take place the frequency of the drive must exceed some cutoff value in which the constraints produced by the transverse boundaries are canceled by a dynamic effect such as that resulting here from inertia. This is illustrated for waves in elastic structures in Sections 11.4.2b and 11.4.3.

Cutoff waves are found also in electromagnetic waveguides,* in which they are of considerable significance in establishing the propagation of a single mode (all modes but one are cutoff) and in which they are sometimes used to make microwave attenuators.

When an electromagnetic wave propagates through a medium, such as a plasma, it is possible that the medium will have the same effect on the waves as the springs of Fig. 10.1.5 have on waves propagating on the string. Hence cutoff or evanescent waves are of considerable importance in studies of wave propagation through plasmas.† Example 10.1.1 considers a situation, similar to that found in studies of the hydromagnetic equilibrium of fusion machines, in which evanescent waves account for the stabilizing (stiffening) influence of transverse boundaries.

Before considering what happens when I is reversed, it would be worthwhile to draw attention to the effect of the current I shown in Fig. 10.1.2 on the natural modes of vibration. Remember (from Section 9.2.1*b*) that it is these modes that characterize the response of the wire to initial conditions.

To find the eigenfrequencies with both ends ($x = 0$ and $x = -l$) of the string fixed, we once again take a linear combination of waves with wavenumbers k found from the dispersion equation (10.1.7) for a given value of ω. At the outset this frequency ω remains to be found.

$$\xi = \text{Re}\,(Ce^{-j\beta x} + De^{j\beta x})e^{j\omega t}. \tag{10.1.16}$$

For convenience we have written the two values of k as $k = \pm\beta$, with β defined as

$$\beta = \frac{\sqrt{\omega^2 - \omega_c^2}}{v_s}. \tag{10.1.17}$$

It is clear that to satisfy the boundary condition $\xi(0, t) = 0$, the constants C and D are related by $C = -D$, so that (10.1.16) becomes

$$\xi = \text{Re}\,\hat{\xi} \sin \beta x e^{j\omega t}, \tag{10.1.18}$$

where $\hat{\xi}$ includes the remaining arbitrary constant. Then to satisfy the boundary condition $\xi(-l, t) = 0$ it follows from (10.1.18) that

$$\sin \beta l = 0. \tag{10.1.19}$$

* See R. B. Adler, L. J. Chu, and R. M. Fano, *Electromagnetic Energy Transmission and Radiation*, Wiley, New York, 1960, pp. 369–378, or S. Ramo, J. R. Whinnery, and T. Van Duzer, *Fields and Waves in Communications and Electronics*, Wiley, New York, 1965, p. 420.

† See T. H. Stix, *The Theory of Plasma Waves*, McGraw-Hill, New York, 1962, p. 13, or W. P. Allis, S. J. Buchsbaum, and A. Bers, *Waves in Anisotropic Plasmas*, M.I.T. Press, Cambridge, Mass., 1963, p. 13.

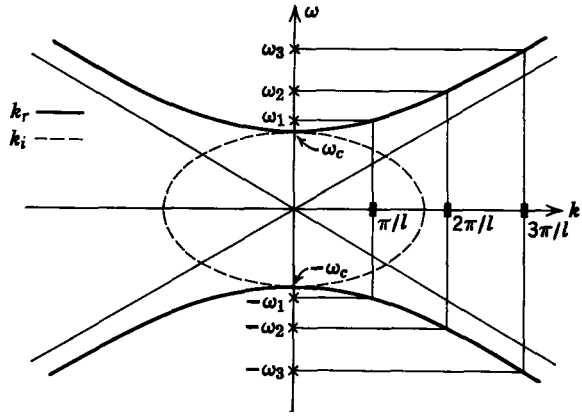

Fig. 10.1.6 A dispersion equation for waves on the wire in Fig. 10.1.2 showing the relationship between the eigenfrequencies ω_n and the eigenvalues $k = n\pi/l$.

This eigenvalue equation is the same as that for a wire without the magnetic force. It has solutions

$$\beta l = n\pi, \qquad n = 1, 2, 3, \ldots . \tag{10.1.20}$$

Now that we have seen a case in which complex wavenumbers have physical significance it is worthwhile to observe that the solutions to (10.1.19), given by (10.1.20), are the only solutions and that they constrain β to be real. We have omitted negative values of n, for the modes represented by these roots are redundant. Note that $n = 0$ is not included because it leads to an eigenvalue $\beta = 0$; hence from (10.1.18) it leads to no deflection. Solutions to the eigenvalue equation of this type, which lead to a vanishing eigenfunction, are referred to as trivial solutions. Now that the eigenvalues have been determined, (10.1.20), we can solve (10.1.17) for the corresponding eigenfrequencies:

$$\omega = \pm\omega_n = \pm\left[\left(\frac{n\pi}{l}\right)^2 + \omega_c^2\right]^{1/2}. \tag{10.1.21}$$

These are the natural frequencies of the wire in the presence of the magnetic force. The natural modes can be seen from (10.1.18) to have the same form as those for the wire with $I = 0$:

$$\xi = \mathrm{Re}\,(A_n^+ e^{j\omega_n t} + A_n^- e^{-j\omega_n t}) \sin\frac{n\pi x}{l}. \tag{10.1.22}$$

Note, however, that the frequencies ω_n are affected by the current I. Their relationship to the dispersion equation is shown graphically in Fig. 10.1.6. The eigenvalues are indicated along the k-axis. (Note that taking negative values of k results in redundant frequencies.) The corresponding eigenfrequencies are increased in magnitude by an increase in the current (increase

in ω_c). As should be expected, the magnetic force has a tendency to stiffen the wire, with the largest effect on the longest wavelengths or lowest frequencies (those least affected by the tension of the wire). The most significant effect of the current is on the lowest eigenfrequency ω_1, which approaches ω_c more rapidly than the other frequencies as the current is increased. Note that because of the current the eigenfrequencies are no longer harmonically related.

Because the natural frequencies are purely real, they appear as resonances of the driven response. This was discussed in detail in Section 9.2.1*a* for the wire without magnetic coupling. It could have been discerned earlier in this section by observing the possibility of a finite response from (10.1.13), even as $\xi_d \to 0$, if the denominator also approaches zero. This requires that

$$\sin |k_r| \, l = 0, \tag{10.1.23}$$

which is the same condition as that in (10.1.19) except that $|k_r|$ is a function of ω_d (the driving frequency) rather than an unspecified ω. Hence, if the frequency ω_d is tuned to one of the eigenfrequencies, there is a resonance in the response. The resonance frequencies of the wire are shifted upward by increasing the current I (or increasing the cutoff frequency ω_c).

Example 10.1.1. Magnetic fields are sometimes used to contain and orient highly conducting media; for example, in devices proposed to achieve thermonuclear fusion the magnetic field is used to make a "bottle" for the plasma. For many purposes this plasma, or highly ionized gas, can be considered as a perfectly conducting fluid. The example discussed here illustrates the continuum dynamics of a medium which, like the plasma, is assumed to have an infinite conductivity.

A perfectly conducting membrane forms the deformable part of the system shown in Fig. 10.1.7. When the membrane is undeformed, it lies in the x-y plane and is immersed in a uniform constant magnetic field $\mathbf{H} = H_0\mathbf{i}_x$. We consider deformations of the membrane

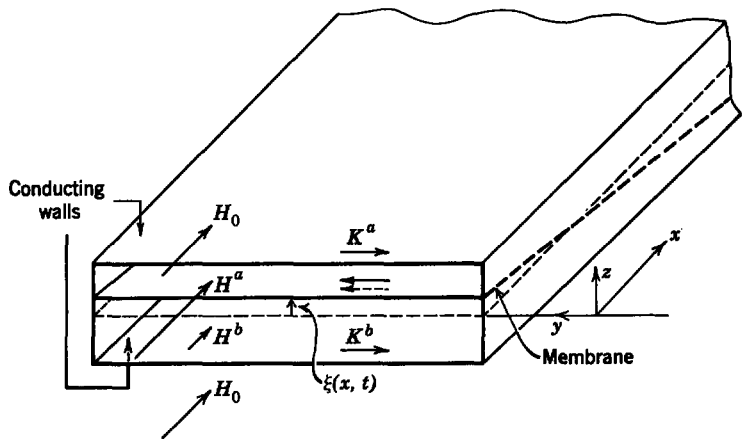

Fig. 10.1.7 A perfectly conducting membrane is bounded from above and below by fixed conducting walls and is immersed in an initially uniform magnetic field H_0.

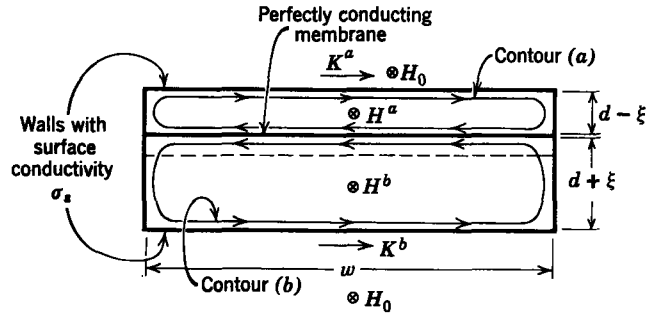

Fig. 10.1.8 Cross-sectional view of the apparatus shown in Fig. 10.1.7. The current loops (*a*) and (*b*), with the imposed magnetic field H_0, couple the membrane to the upper and lower conducting walls.

$\xi(x, t)$ that do not depend on y; hence the membrane has the general appearance shown in Fig. 10.1.7.

The membrane has a width w with its edges making electrical contact with the walls of a rectangular conducting conduit. Thus the membrane and the upper wall form a conducting loop [contour (*a*) shown in Fig. 10.1.8]. Similarly, the lower wall and membrane form the conducting loop (*b*). In the limit in which the conductivity of the walls (σ_s) is infinite the magnetic flux linked by each of these circuits must remain constant. Hence an upward deflection is accompanied by an increase in the field intensity above the membrane and a decrease in the field intensity below it. The conservation of flux is realized because of the flow of surface currents K^a and K^b as shown. This type of flux conservation dynamics is familiar from Section 5.1.3, in which it was encountered in the context of lumped-parameter dynamics.

The induced currents shown in Fig. 10.1.8 are responsible for creating a magnetic force on the membrane that tends to restore it to the plane of zero deflection. Therefore we can expect from the outset to obtain an equation of motion similar to (10.1.6).

The equation of motion for the membrane is

$$\sigma_m \frac{\partial^2 \xi}{\partial t^2} = S \frac{\partial^2 \xi}{\partial x^2} + T_z, \tag{a}$$

where T_z is the force per unit area acting in the z-direction (see Table 9.2). The magnetic field intensity above the membrane (a) and below the membrane (b) can be written as

$$\mathbf{H}^a = [H_0 + h^a(x, t)]\mathbf{i}_x, \tag{b}$$

$$\mathbf{H}^b = [H_0 + h^b(x, t)]\mathbf{i}_x, \tag{c}$$

where h^a and h^b represent perturbations from the equilibrium magnetic field intensity caused by deflections of the membrane. We assume that the transverse displacements $\xi(x, t)$ vary slowly enough with x that at each cross section of the system shown in Fig. 10.1.7 the magnetic field is essentially x-directed and is independent of y and z.

Ampère's law requires that the jump in magnetic field intensity on the upper and lower plates be equal to their respective surface currents. Hence

$$h^a = K^a, \tag{d}$$

$$h^b = -K^b, \tag{e}$$

and we can find the perturbation field intensities by writing circuit equations for the currents K^a and K^b. The integral law of induction used in conjunction with the contour (a) of Fig. 10.1.8 is

$$\oint_{C_a} \mathbf{E}' \cdot d\mathbf{l} = -\frac{\partial}{\partial t} \int_{S_a} \mu_0 \mathbf{H} \cdot \mathbf{n}\, da, \tag{f}$$

where the time derivative is written as a partial because the flux is a function of the longitudinal position x of the cross-sectional surface of integration S_a enclosed by the contour C_a. To evaluate the integral on the left note that $\mathbf{E}'$ is zero both in the perfectly conducting membrane and in the perfectly conducting end walls. In the upper plate the surface current density and electric field are related by Ohm's law, which takes the form

$$\mathbf{K}^a = \sigma_s \mathbf{E} \tag{g}$$

because the upper wall is fixed. Equation f then becomes

$$\frac{wK^a}{\sigma_s} = -\frac{\partial}{\partial t}[w(d - \xi)\,\mu_0(H_0 + h^a)]. \tag{h}$$

Similar arguments, used with contour (b) in Fig. 10.1.8, produce the electrical equation

$$\frac{wK^b}{\sigma_s} = \frac{\partial}{\partial t}[w(d + \xi)\,\mu_0(H_0 + h^b)]. \tag{i}$$

We confine our attention to small displacements of the membrane so that it is appropriate to linearize these last two equations, which in view of (d) and (e) become

$$\frac{h^a}{\sigma_s} = -\frac{\partial}{\partial t}(\mu_0 d h^a - \mu_0 H_0 \xi), \tag{j}$$

$$-\frac{h^b}{\sigma_s} = \frac{\partial}{\partial t}(\mu_0 d h^b + \mu_0 H_0 \xi). \tag{k}$$

These expressions are the required electrical equations of motion that relate the field intensities above and below the membrane to the displacement ξ. The remaining equation is (a), with T_z written in terms of h^a and h^b.

To find T_z, the surface force density is related to the Maxwell stress T^*_{mn} by (8.4.2)

$$T_z = (T_{zm}{}^a - T_{zm}{}^b)n_m, \tag{l}$$

where $\mathbf{n}$ is the vector normal to the membrane surface. Because $\mathbf{n} \approx i_z$, the summation on m has only one contribution, $m = z$, and (l) reduces to

$$T_z = T_{zz}{}^a - T_{zz}{}^b = -\tfrac{1}{2}\mu_0[(H^a)^2 - (H^b)^2]. \tag{m}$$

Now, if we introduce (b) and (c), this expression can be linearized to obtain

$$T_z = -\mu_0 H_0(h^a - h^b). \tag{n}$$

* Alternatively, the surface force density can be derived by using the energy method of Chapter 3 and viewing each section of the membrane as forming a pair of parallel plate inductors with the side walls. If this is done, remember that in addition to the two terminal pairs for these inductors there is a third terminal pair, constrained to constant current, for the magnet that makes H_0.

The effect of finite conductivity in the walls has been included up to this point because it offers the possibility of illustrating at least two important dynamical effects. These are discussed when this example is continued in Sections 10.1.4 and 10.2.4. For now, we consider the limit in which σ_s is large enough that the fluxes linked by contours (*a*) and (*b*) remain essentially constant. Because the quantities in parentheses in (j) and (k) are the flux perturbations, they must therefore be zero and it follows that

$$h^b = \frac{H_0 \xi}{d}, \tag{o}$$

$$h^b = \frac{-H_0 \xi}{d}. \tag{p}$$

If we combine these expressions with (n) and (a), an equation of motion results:

$$\frac{\partial^2 \xi}{\partial t^2} = v_s^2 \frac{\partial^2 \xi}{\partial x^2} - \omega_c^2 \xi, \tag{q}$$

where

$$v_s = \left(\frac{S}{\sigma_m}\right)^{1/2},$$

$$\omega_c^2 = \frac{2\mu_0 H_0^2}{\sigma_m d}.$$

This expression has the same form as (10.1.6), and we can conclude that in the limit in which $\sigma_s \to \infty$ the membrane of Fig. 10.1.7 will have the same dynamical behavior found for the wire shown in Fig. 10.1.5.

10.1.3 Absolute or Nonconvective Instability

When the current is reversed in the experiment of Fig. 10.1.2, the wire dynamics are found to be altogether different from those described in the preceding section. As the current I (shown in Fig. 10.1.9) is raised, there is a threshold beyond which the wire bows outward. Under this condition, no matter how carefully the wire is placed on the center line between the coils, it bows outward when it is released.

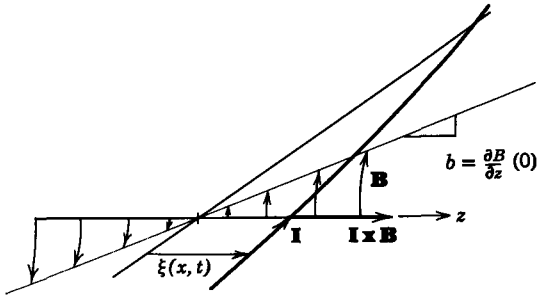

Fig. 10.1.9 Wire carrying current I in a magnetic field that is zero along the axis $\xi = 0$. Current is reversed from the situation shown in Fig. 10.1.2.

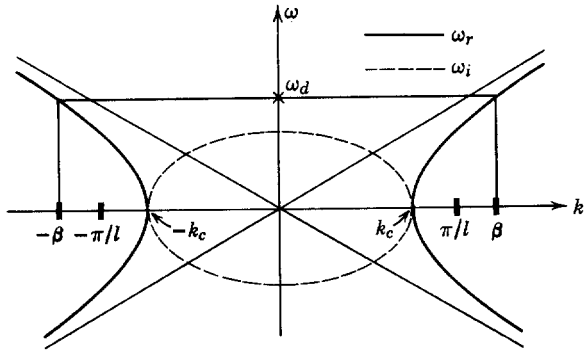

Fig. 10.1.10 Plot of the dispersion equation for physical situation shown in Fig. 10.1.2 with the current reversed, as in Fig. 10.1.9. Complex values of ω are shown for real values of k.

This might be expected. Reversing the current gives rise to a magnetic force, as in (10.1.5) with $I \rightarrow -I$, that tends to carry the wire in the same direction as the displacement. Hence it tends to produce an instability that is the continuum analogue of the static instability of lumped-parameter systems described in Section 5.1.2*a*. A transverse deflection, shown in Fig. 10.1.9, leads to a magnetic force that tends to make the deflection even larger.

The equation of motion is again (10.1.1), but now S_z is

$$S_z = Ib\xi \tag{10.1.24}$$

and the equation governing deflections of the wire is

$$\frac{1}{v_s^2}\frac{\partial^2 \xi}{\partial t^2} = \frac{\partial^2 \xi}{\partial x^2} + k_c^2 \xi, \tag{10.1.25}$$

where

$$k_c^2 = \frac{Ib}{f}.$$

Again, the dispersion equation is found by substituting (10.0.1) into this equation of motion to obtain

$$\omega^2 = v_s^2(k^2 - k_c^2). \tag{10.1.26}$$

The asymptotes of this expression, plotted in the ω-k plane, are again straight lines with slopes $\pm v_s$. The two branches of the plot, however, now pass through the k-axis, as can be seen by setting $\omega = 0$ and solving (10.1.26) to obtain $k = \pm k_c$. Hence the real values of ω, as a function of real values of k, appear as shown by the solid lines in Fig. 10.1.10. For each value of ω there is a corresponding pair of real wavenumbers k. This is evident either from Fig. 10.1.10 or from (10.1.26) solved for k. By contrast only real values of k with a magnitude greater than k_c lead to real values of ω.

Note that the roles of ω and k are the reverse of what they were in the preceding section. Now, it is appropriate to plot complex values of ω for real values of k, and this is the significance of the broken line in Fig. 10.1.10. In the range of wavenumbers $-k_c < k < k_c$ the frequency ω is purely imaginary. Substitution of $\omega = j\omega_i$ in (10.1.26) shows that the relation between ω_i and k is an ellipse (Fig. 10.1.10).

Consider first the sinusoidal steady-state vibrations with the same boundary conditions (10.1.8) and (10.1.9) used in the preceding section. Then the same steps used to compute (10.1.13) give

$$\xi = -\xi_d \frac{\sin \beta x}{\sin \beta l} \sin \omega_d t, \tag{10.1.27}$$

where

$$\beta = \left(\frac{\omega_d^2}{v_s^2} + k_c^2\right)^{1/2}. \tag{10.1.28}$$

This solution to (10.1.25) is simply a linear combination of waves for which the two wavenumbers $k = \pm\beta$ are found by solving the dispersion equation (10.1.26) with $\omega = \omega_d$. These solutions are shown graphically in Fig. 10.1.10.

The sinusoidal steady-state vibrations have the same general spatial appearance as the wire with no magnetic force. The frequency response, however, has been altered by the current I. As in Section 10.1.2, there are resonances in this response at the natural frequencies. They occur when the denominator of (10.1.27) goes to zero or when $\beta l = n\pi$, $n = 1, 2, 3, \ldots$. It follows from (10.1.28) that the resonance frequencies are

$$\omega_d = \pm v_s \left[\left(\frac{n\pi}{l}\right)^2 - k_c^2\right]^{1/2}, \quad n = 1, 2, 3, \ldots. \tag{10.1.29}$$

Remember that k_c can be increased by increasing the current I. The equation shows that the response frequencies are reduced by the interaction with the magnetic field. This is just the opposite of the effect found in the preceding section, in which these resonance frequencies were increased by the magnetic interaction.

As the current I is increased, the point is reached at which the lowest resonance frequency is reduced to zero. From (10.1.29) this critical condition occurs when

$$k_c = \frac{\pi}{l} \tag{10.1.30}$$

For larger values of k_c the lowest resonance frequency is no longer real. Because this resonance results when the driving frequency is tuned to the natural frequency, we suspect that the lowest natural frequency is complex after k_c exceeds π/l. Note that the driven response given by (10.1.27) is still perfectly valid even if k_c is larger than the critical value given by (10.1.30).

It is of crucial importance to recognize that once k_c exceeds π/l the sinusoidal steady-state response is of little significance. The lowest natural mode of the system is unstable and the transient solution, initiated by the initial conditions, eventually dominates the driven response. To see this we now consider the natural modes of the wire with both ends fixed.

The steps used in Section 10.1.2 in going from (10.1.18) to (10.1.22) are equally valid here. Hence the eigenmodes are given by (10.1.22). Now, however, the eigenfrequencies are given by the revised dispersion equation (10.1.26) with $k^2 = (n\pi/l)^2$.

$$\omega = \pm\omega_n = \pm v_s\left[\left(\frac{n\pi}{l}\right)^2 - k_c^2\right]^{1/2}. \tag{10.1.31}$$

These eigenfrequencies are shown in Fig. 10.1.11, in which a graphical representation of the dispersion equation shows how the discrete values of k allowed by the fixed ends of the spring are related to the ω_n's. From the figure it can readily be visualized how the frequencies of each mode shift inward as $k_c(I)$ is increased. As k_c is increased beyond $n\pi/l$, the frequencies of the nth mode move onto the ellipse and take the form

$$\omega_n = j\,|\omega_i|,$$

as can be seen from (10.1.31). The negative imaginary eigenfrequency gives rise to an eigenmode (10.1.22) that has an exponentially increasing amplitude.

In Section 9.2.1*b* we saw that the eigenmodes were orthogonal. Physically this meant that if initial conditions were such that only one of the modes was excited that mode would persist indefinitely without involving the others. [See Example (9.2.1) for a particular illustration of this point.] Suppose that

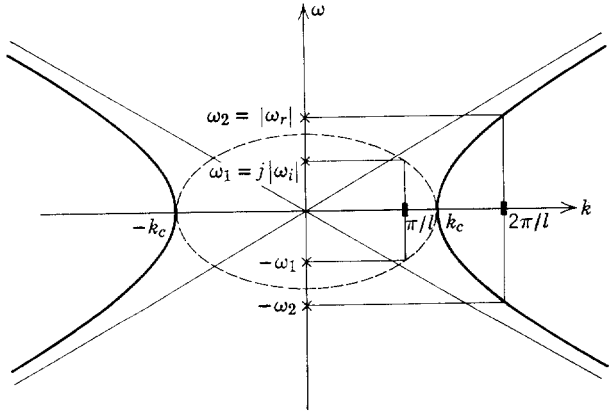

Fig. 10.1.11 The dispersion equation for the system of Fig. 10.1.2 with current as shown in Fig. 10.1.9. Complex values of ω are shown for real values of k. The allowed values of k give rise to the eigenfrequencies as shown.

the A_n's in (10.1.22) were adjusted so that just the lowest mode was initiated. Then, with $k_c < \pi/l$, the vibrations of the wire would have the oscillatory dependence on x and t shown in Fig. 10.1.12*a*. With $k_c > \pi/l$, wire displacements would appear as the instability shown in Fig. 10.1.12*b*. This is an example of an absolute or nonconvective instability because, unlike instabilities that we shall study in Section 10.2, it involves deflections that become unbounded as time increases at a fixed point in space; That is, if the wire extended to $x = \pm\infty$ and a pulse were initiated at $x = 0$, the deflection at $x = 0$ would become unbounded with time.

The "unboundedness" of the unstable deflections is, of course, a prediction of the mathematical model that sooner or later is not accurate because of nonlinear effects that were neglected in both the derivation of the equation of motion for the wire and in writing S_z as in (10.1.24). This same limitation was involved in the lumped-parameter, linear stability theory of Section 5.1.2.

The dynamics that determine when the deflections will become large vary from the mundane to the spectacular and from the disasterous to the useful. In the system of Fig. 10.1.9 the deflections may increase until the wire encounters one of the magnet coils or they may simply reach some saturation

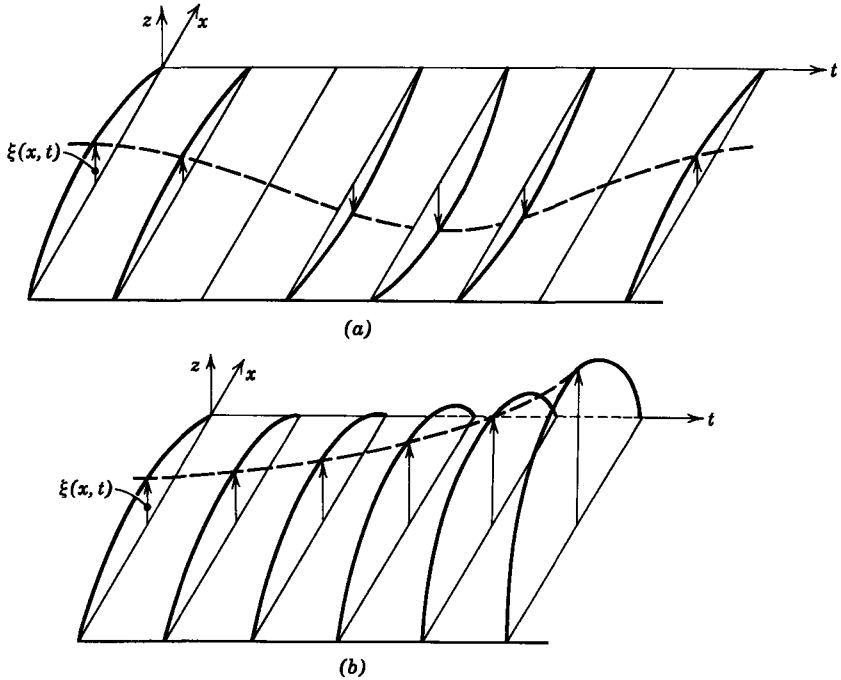

Fig. 10.1.12 Space-time dependence of lowest eigenmode: (*a*) $k_c < \pi/l$, stable; (*b*) $k_c > \pi/l$, unstable.

amplitude dictated by the large amplitude variation of the magnetic field. In Section 10.4.3 we shall see a grossly nonlinear consequence of absolute instability—the destruction of the system. On the other hand, as discussed later, instabilities of some types form the basis for making oscillators.

The example of instability presented in this section has the virtue of being extremely simple to understand mathematically, by comparison with instabilities often found in continuous media.* Nevertheless, there are practical situations in which this model has engineering significance. Example 10.1.2 considers how instability, predicted by this simple model, imposes a limitation on the levitation of continuous media with an electric field.

Absolute instability is of great interest to those concerned with fluid dynamics and the dynamics of elastic media. A classic example in the first category, which is closely related to the case considered in this section, is shown in Fig. 10.1.13. In Fig. 10.1.13*a* a heavy fluid (which is dark) is supported on a lighter fluid (which is clear) by hydrostatic pressure. In this initial equilibrium state each element of the fluid is in force equilibrium. With the heavy fluid on top, however, the equilibrium is unstable in the same sense that the wire of Fig. 10.1.9 was unstable. The only reason that the heavy fluid holds the position shown in Fig. 10.1.13*a* is that it is subject to an electric field, which induces polarization forces (discussed in Section 8.5) that stabilize the equilibrium. When this electric field is removed, the equilibrium becomes unstable, as shown in Figs. 10.1.13*b–e*, and the heavier fluid falls to the bottom of the tank. This is called a Rayleigh-Taylor† instability, and although the three-dimensional fluid motions are more complicated mathematically than those of the wire considered here the properties of these instabilities are in many ways similar. Both are absolute instabilities, and both instabilities have small amplitude motions characterized by a purely exponential growth with time.

Rayleigh-Taylor types of instability are found in a variety of situations. Many found in the hydromagnetic equilibria of fusion machines have characteristics similar to the heavy fluid on top of the light fluid.‡ This connection is explored further in Section 10.4.3. Figure 10.1.13 actually illustrates an electrohydrodynamic situation in which an electric field prevents instability (although we must leave the details of this situation for further reading§).

* The downward shift of the natural frequencies and instability of the lowest mode are illustrated in the film "Complex Waves I" produced by the Education Development Center, Newton, Mass., for the National Committee on Electrical Engineering Films.

† S. Chandrasekhar, *Hydrodynamic and Hydromagnetic Stability*, Oxford, 1961, p. 428.

‡ D. J. Rose and M. Clark, Jr., *Plasmas and Controlled Fusion*, M.I.T. Press and Wiley, New York, 1961, p. 258.

§ J. R. Melcher and M. Hurwitz, "Gradient Stabilization of Electrohydrodynamically Oriented Liquids," *J. Spacecraft Rockets*, **4**, No. 7, 864–881 (July 1967).

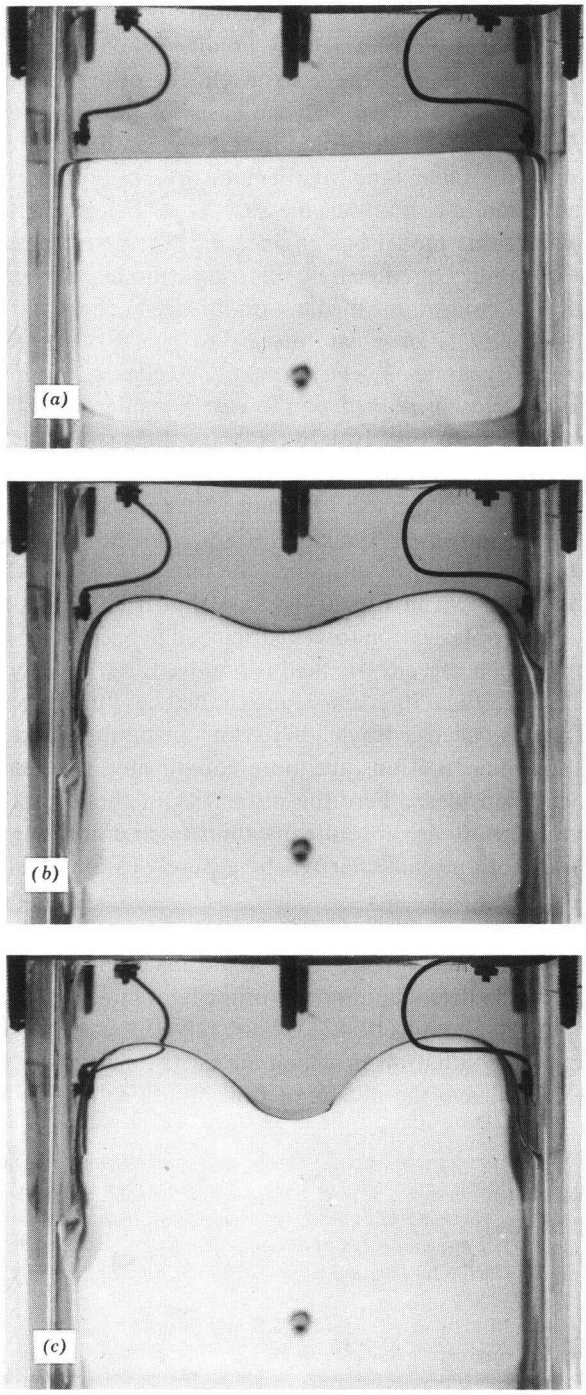

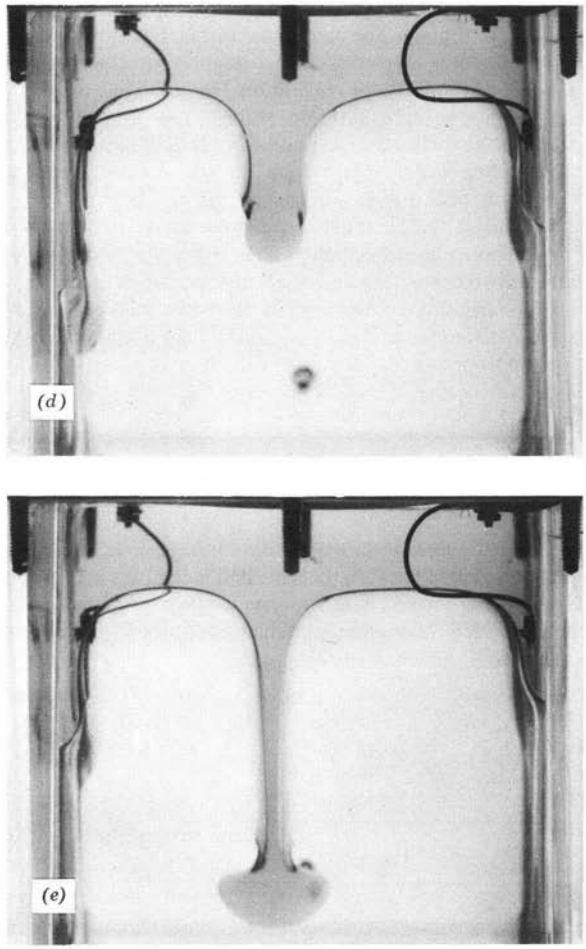

Fig. 10.1.13 (*a*) A heavy (dark) liquid is supported above a light (clear) liquid by hydrostatic pressure; (*b* – *e*) show growth of Rayleigh-Taylor instability resulting after stabilizing electric polarization forces in (*a*) are removed. (Photograph courtesy of Dynatech Corp., Cambridge, Mass.) This phenomenon can be seen in the film, "Complex Waves II," available from Education Development Center, Inc., Newton, Mass.

Electric fields most often produce instabilities. The literature of plasma dynamics abounds in illustrations of absolute instabilities.*

Example 10.1.2. Electric and magnetic fields are often used to separate, levitate, or confine continuous media. A simple example of levitation is given in Fig. 10.1.14. An electrically conducting elastic film (membrane), with a mass per unit area σ_m, is stretched horizontally with equilibrium tension S between two rigid supports. With no other forces acting, the gravitational force makes the membrane sag in the middle. We propose to remove the sag without making physical contact with the membrane by placing a parallel conducting electrode, as shown in Fig. 10.1.14, and applying a potential difference between the membrane and the fixed plate. The membrane can be placed in a perfectly horizontal static equilibrium by providing an electrostatic attraction force per unit area between the plate and the membrane just equal to the gravitational force per unit area $\sigma_m g$. An important question, however, is this: Is the equilibrium stable? That is, can we expect that small transverse deflections of the surface due to noise will not become continuously larger? The electromechanical coupling occurs everywhere on the surface; hence to answer this question we must analyze a distributed surface-coupled problem.

It is assumed at the outset that the transverse displacements of the membrane, which are critical, do not depend on the y-coordinate. This is justified if the y-dimension of the membrane is small compared with l. In an actual situation this would mean that the tension in the y-direction of the membrane shown in Fig. 10.1.14 would be considerably less than the tension S in the x-direction, a fact that would make a one-dimensional membrane equation even more appropriate.

Because there is a gravitational force per unit area $\sigma_m g$ acting in the $-z$-direction, the equation of motion (9.2.3a) becomes

$$\sigma_m \frac{\partial^2 \xi}{\partial t^2} = S \frac{\partial^2 \xi}{\partial x^2} - \sigma_m g + T_z^e, \tag{a}$$

where T_z^e is the transverse force per unit area due to the electric field.

The electric field in the region between the plate and membrane is in general a function of both x and z. We restrict our interest here, however, to the "long-wave limit" (see Example 6.2.4) in which the slope $\partial \xi / \partial x$ is small enough that the electric field is essentially z-directed. Hence we write the electric field intensity as

$$\mathbf{E} = \frac{V}{d - \xi} \mathbf{i}_z. \tag{b}$$

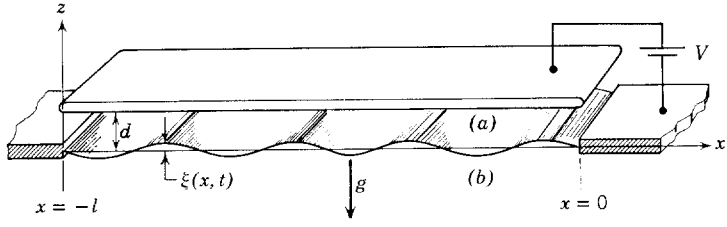

Fig. 10.1.14 Conducting elastic membrane held horizontal in a gravitational field by an electrostatic force.

* J. G. Linhart, *Plasma Physics*, North-Holland, Amsterdam, 1960, p. 101.

We have used the assumption that the membrane and the fixed plate are equipotentials; that is, the conductivities are high enough to allow charges to relax from one position to another on the conductors in a time that is short compared with a characteristic time of the mechanical motions (e.g., period of oscillation of the membrane or, as we shall see, time constant for instability). This is the idealization of the zero electric Reynolds number discussed in Section 7.2.

The force per unit area in the z-direction on a surface with the normal vector $\mathbf{n}$ is in general [from (8.4.2)]

$$T_z^e = (T_{zm}^a - T_{zm}^b)n_m. \tag{c}$$

Because $n_m \cong n_z \cong 1$ and there is no electric field below the membrane, this reduces to

$$T_z^e = T_{zz}^{(a)}. \tag{d}$$

Recall from (8.3.10) that because $E_x \approx 0$ and $E_y \approx 0$ the component of the stress tensor T_{zz} is

$$T_{zz} = \tfrac{1}{2}\epsilon_0 E_z^2, \tag{e}$$

and it follows from (b), (d), and (e) that

$$T_z^e = \tfrac{1}{2}\epsilon_0\left(\frac{V}{d-\xi}\right)^2. \tag{f}$$

Expansion of this surface force density in a Taylor series about the equilibrium position $\xi = 0$ and retention of only linear terms in displacement yield

$$T_z^e = \frac{\epsilon_0}{2d^2}V^2 + \frac{\epsilon_0}{d^3}V^2\xi. \tag{g}$$

This result is now substituted into (a) to obtain the differential equation of motion

$$\sigma_m\frac{\partial^2\xi}{\partial t^2} = S\frac{\partial^2\xi}{\partial x^2} - \sigma_m g + \frac{\epsilon_0 V^2}{2d^2} + \frac{\epsilon_0}{d^3}V^2\xi. \tag{h}$$

It is desired that the voltage V be adjusted so that in static equilibrium the membrane has no sag ($\xi = 0$). In this case, (h) reduces to

$$-\sigma_m g + \frac{\epsilon_0 V^2}{2d^2} = 0, \tag{i}$$

which simply states that the net electrical force upward (the upward attraction of the upper plate) must balance the downward force of gravity.

Subtraction of the equilibrium equation (i) from (h) gives an expression that must be satisfied by the perturbation deflections

$$\frac{1}{v_s^2}\frac{\partial^2\xi}{\partial t^2} = \frac{\partial^2\xi}{\partial x^2} + k_c^2\xi, \tag{j}$$

where

$$v_s = \left(\frac{S}{\sigma_m}\right)^{1/2} \tag{k}$$

$$k_c^2 = \frac{\epsilon_0 V^2}{Sd^3}. \tag{l}$$

This equation has the same form as (10.1.25). We can immediately conclude that because the boundary conditions are also the same as those considered in writing (10.1.30) the equilibrium is stable if

$$\frac{\epsilon_0 V^2}{Sd^3} < \left(\frac{\pi}{l}\right)^2. \tag{m}$$

This institutes an upper bound on the voltage V consistent with stability. If we recognize that a requirement is also imposed on the voltage by the levitation condition (i), it follows that a largest mass-per-unit-area σ_m can be levitated by an apparatus with given dimensions and membrane tension S. This follows by eliminating V^2 from (m) and (i):

$$\sigma_m < \left(\frac{\pi}{l}\right)^2 \frac{Sd}{2g}. \tag{n}$$

It is a limitation of this kind that absolute instability often imposes on practical systems.

In an actual design a further restriction on allowable voltages arises because the material between the plate and membrane in Fig. 10.1.14 will be able to withstand only a finite electric field intensity; for example, if this region is filled with air at atmospheric pressure, the electric field intensity cannot exceed about 3×10^6 V/m.*

10.1.4 Waves with Damping, Diffusion Waves

Any real system is affected to some extent by energy dissipative effects, whether they take the form of mechanical friction or are caused by resistive heating. This fact alone would justify at least brief attention to the dynamics of a continuum influenced by losses. Even more important, however, are the physical situations in which the effect of energy dissipation is essential. This was seen in Chapter 7, in which magnetic diffusion and charge relaxation were governed by loss-dominated continuum equations. The discussion presented in this section adds further physical significance to the diffusion equation, which in Chapter 7 represented the dynamics of the magnetic field in a conducting material and in this section the dynamics of a string in a viscous fluid. One of our reasons for introducing this topic here becomes even more evident in Section 10.2.4, in which the simple ideas introduced are extended to show how losses, in conjunction with material convection, can give rise to a class of instabilities. These "resistive wall" instabilities assume importance in a variety of situations.

For purposes of illustration suppose that the wire is immersed in a viscous liquid. Then transverse deflections ξ produce a viscous drag on each section of the wire which is analogous in its effect to the viscous damper (see Section 2.2.1*b*) of lumped-parameter systems. A small section of the wire, shown in Fig. 10.1.15, experiences a (retarding) force per unit length to oppose the

* A. E. Knowlton, *Standard Handbook for Electrical Engineers*, McGraw-Hill, 9th ed., 1957, p. 416.

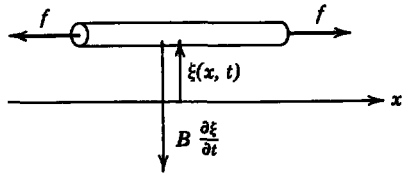

Fig. 10.1.15 A viscous drag per unit length acts to retard the motion of each element of the wire.

motion. If the velocity is low enough (or the viscosity is high enough*), this force is simply proportional to the transverse velocity; that is,

$$S_z = -B\frac{\partial \xi}{\partial t}, \tag{10.1.32}$$

where B is a damping coefficient per unit length.

With this type of force acting on the string, the equation of motion (10.1.1) becomes

$$\frac{\partial^2 \xi}{\partial t^2} = v_s^2 \frac{\partial^2 \xi}{\partial x^2} - \nu \frac{\partial \xi}{\partial t}, \tag{10.1.33}$$

where, as before,

$$v_s = \left(\frac{f}{m}\right)^{1/2} \tag{10.1.34}$$

and a normalized "damping frequency" has been defined as

$$\nu = \frac{B}{m}. \tag{10.1.35}$$

Now substitution of the standard form of solution (10.0.1) into (10.1.33) gives the dispersion equation

$$\omega^2 = v_s^2 k^2 + j\nu\omega. \tag{10.1.36}$$

This equation, like those considered in the preceding sections, is a simple quadratic either for ω or for k. Note that by contrast with the preceding cases, which did not involve dissipation, the dispersion equation now has a complex coefficient. Although the problem is formally no more complicated than it was before, the complex coefficient is responsible for making the algebra more involved.

First of all, consider the driven response to a sinusoidal steady-state excitation with the frequency $\omega = \omega_d$. Then it is appropriate to solve the dispersion

* The drag on a cylinder in a liquid obeys this law, provided the Reynolds number is small enough. See H. Rouse, *Elementary Mechanics of Fluids*, Wiley, New York, 1946, p. 247.

equation (10.1.36) for k, given that the frequency is ω_d:

$$k = \pm \frac{\sqrt{\omega_d^2 - jv\omega_d}}{v_s} \tag{10.1.37}$$

The radical makes it convenient to recognize that this expression has the form

$$k = \pm(|k_r| - j|k_i|). \tag{10.1.38}$$

The graphical construction in the complex plane (Fig. 10.1.16) shows how $|k_r|$ and $|k_i|$ are related to the driving frequency ω_d. The vectors provide a convenient way to picture the result of taking the square root of (10.1.37).

In view of the possible wavenumbers expressed by (10.1.38), the driven response is made up of two waves with amplitudes A^+ and A^- determined by the boundary conditions.

$$\xi = \text{Re}\,[A^+e^{-j(|k_r|-j|k_i|)x} + A^-e^{j(|k_r|-j|k_i|)x}]e^{j\omega_d t}. \tag{10.1.39}$$

Remember that the real part of the wavenumber contains information about the periodicity and the phase velocity of the wave. Hence the first term in (10.1.39) represents a wave with the wavelength (measured between points of zero phase)

$$\lambda = \frac{2\pi}{|k_r|} \tag{10.1.40}$$

and a phase velocity (again for points of zero phase) of

$$v_p = \frac{\omega_d}{|k_r|}. \tag{10.1.41}$$

These points of zero phase propagate in the positive x-direction. From the form of (10.1.39) it is also clear that this wave decays in the positive x-direction at a rate determined by $|k_i|$. The A^- wave has a similar physical significance,

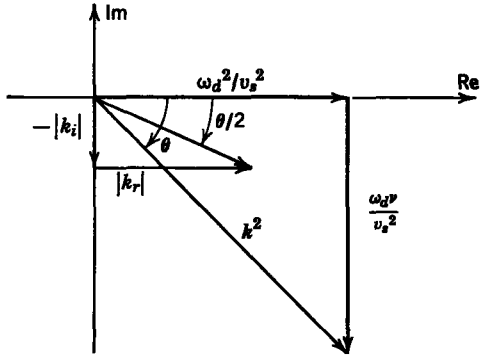

Fig. 10.1.16 Graphical solution of (10.1.37) to show complex nature of k.

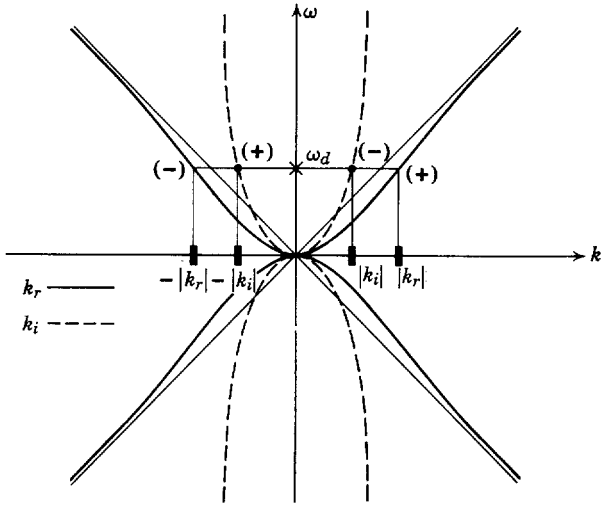

Fig. 10.1.17 Dispersion equation (10.1.37) for a string immersed in a viscous liquid, showing complex values of k for real values of ω.

with points of zero phase propagating in the $-x$-direction and an amplitude that decays also in the $-x$-direction.

What we have found is not too surprising. The effect of the damping on the driven waves is to produce a spatial decay in the direction of propagation. Figure 10.1.17 shows the ω-k plot predicted by (10.1.37). Here we are considering the driven response and plot complex values of k for real values of ω. Note that the positive real part of k (corresponding to a given frequency $\omega = \omega_d$) goes with a negative imaginary part of k on this diagram. As the driving frequency is raised, the real parts of k approach the same values they would have in the absence of damping whereas the imaginary parts (which reflect the spatial rate of decay) reach the asymptotic value $|k_i| = \nu/2v_s$.

The terms in (10.1.36) have the same physical significance as the corresponding terms in (10.1.33); that is, the ω^2 on the left represents the effects of inertia, whereas $v_s^2k^2$ and $j\nu\omega$, respectively, symbolize effects of the tension and viscous drag. If the damping is sufficiently large that

$$\nu \gg \omega_d, \tag{10.1.42}$$

the effect of damping dominates that of the inertia and the ω^2 term in (10.1.36) can be ignored. (This is similar to the class of dynamics discussed in Section 5.2.2 in the context of lumped parameters.) The resulting dispersion equation takes the form

$$k^2 = -\frac{j\omega_d\nu}{v_s^2} \tag{10.1.43}$$

In this simple form the radical found in solving for k [as in (10.1.37)] can be taken to obtain

$$k = \pm\left(\frac{-j\omega_d\nu}{v_s^2}\right)^{1/2} = \pm\left(\frac{\omega_d\nu}{2v_s^2}\right)^{1/2}(1-j). \tag{10.1.44}$$

This simplified dispersion equation is familiar from Section 7.1.3*a* [see (7.1.70)], where it was found in discussing the sinusoidal steady-state behavior of a magnetic field in a conducting medium. Instead of the magnetic skin depth δ, we now have $\delta \to \sqrt{2v_s^2/\omega_d\nu}$. The mathematical analogy between the viscous dominated spring and the magnetic diffusion could have been seen at the outset by comparing the one-dimensional form of (7.1.11) with (10.1.33), with the inertia term omitted. Both systems are represented by the diffusion equation.*

The value in recognizing the analogy between the deflection of the spring as it "oozes" through the viscous liquid and the magnetic diffusion through a conducting material is not confined to the mathematics. We can obtain a good physical "feel" for the diffusion process as it occurs in a diversity of situations by keeping in mind that the dynamics are similar to those found in the experiment shown in Fig. 10.1.18. Here a tightly wound helical spring (which is equivalent to a wire or string with a small tension f) is fixed at one end and driven up and down in a sinusoidal fashion at the other. The spring is immersed in glycerin. If we were to produce this excitation by hand, we would be most aware of a viscous retarding force. This is in contrast to the force required to excite the evanescent waves of Section 10.1.2, which was of the same nature as that required to compress a spring. (The comparison is worthy of note, for in both cases we are concerned with waves that decay spatially away from the point of excitation.)

The dispersion relation for the diffusion wave is characterized by equal real and imaginary parts of k for real values of ω. This is the region near the origin in Fig. 10.1.17, as is evident either from the ω-k plot or from the condition of (10.1.42).

In the preceding sections reference has been made to the effect of damping on the natural frequencies. This effect was clearly necessary for an accurate picture of the transient dynamics over many oscillations of the string. With the ends of the string fixed (as in the last two sections), the natural modes are found by again recognizing that solutions for k have the form $k = \pm\beta$ (where ω is now unknown and (10.1.36) is solved for k) and writing solutions in the form of (10.1.16). The same arguments used then, lead to the conclusion that

$$\beta = \frac{n\pi}{l}, \qquad n = 1, 2, 3, \ldots, \tag{10.1.45}$$

* Reference to other systems represented by this equation was made in the footnote to (7.1.11).

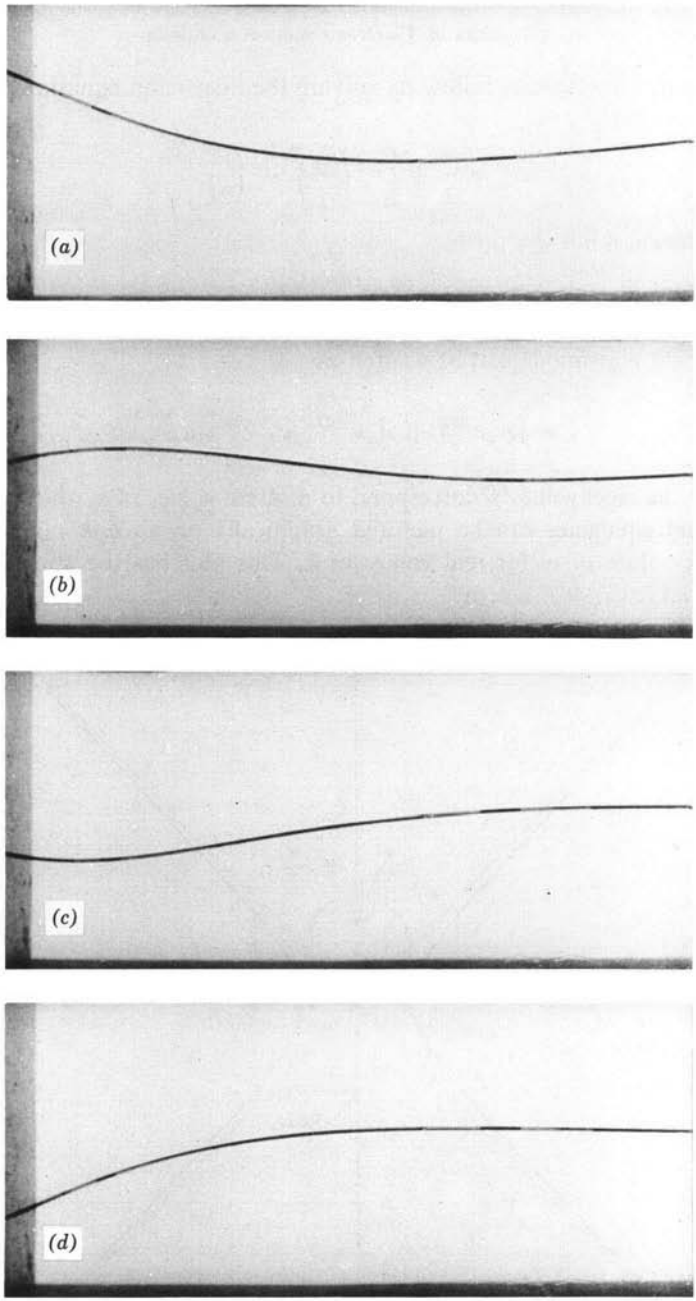

Fig. 10.1.18 A spring under tension is driven sinusoidally at the left end and fixed at the right end. It is immersed in glycerine which is sufficiently viscous that the effect of damping exceeds that of inertia. Hence the resulting motions which are shown in sequence over about one half cycle exemplify diffusion waves (or skin effect waves) in the sinusoidal steady state. (From four-minute film "Diffusion Waves" made for M.I.T. by Education Development Center, Inc., Newton, Mass.)

and the eigenfrequencies follow by solving the dispersion equation (10.1.36) with $k^2 = (n\pi/l)^2$.

$$\omega_n^{\pm} = \frac{jv}{2} \pm \left[v_s^2 \left(\frac{n\pi}{l}\right)^2 - \left(\frac{v}{2}\right)^2 \right]^{1/2}. \tag{10.1.46}$$

This expression has the form

$$\omega_n^{\pm} = \frac{jv}{2} \pm \Omega_n, \tag{10.1.47}$$

and the nth eigenmode can be written as

$$\xi = [A_n^+ e^{j\Omega_n t} + A_n^- e^{-j\Omega_n t}] e^{-(v/2)t} \sin \frac{n\pi x}{l}. \tag{10.1.48}$$

Because the eigenvalues β correspond to discrete values of k which are real, the eigenfrequencies can be pictured graphically on an ω-k plot to show complex values of ω for real values of k. This plot has the appearance of Fig. 10.1.19.

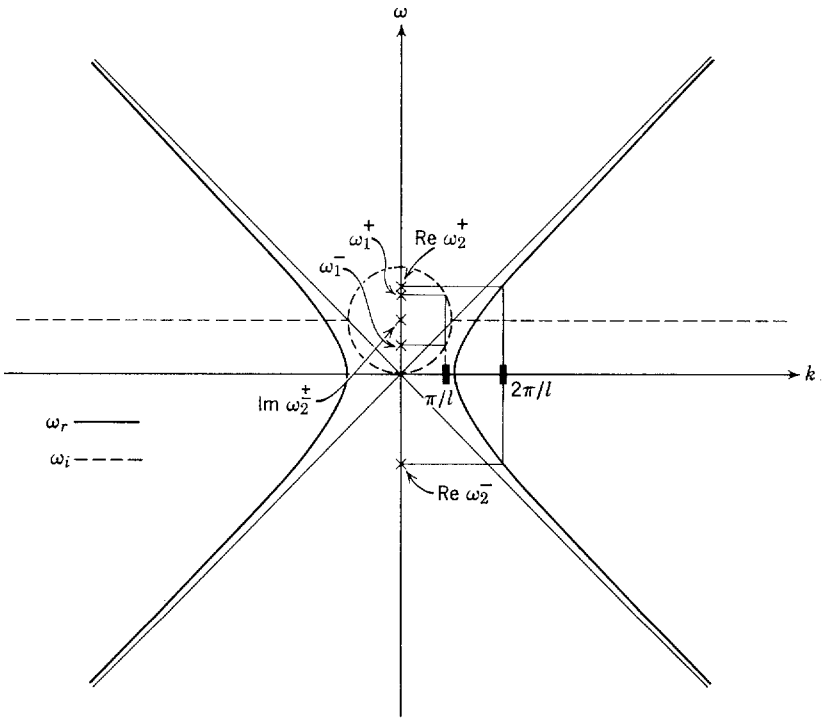

Fig. 10.1.19 Dispersion equation for string in a viscous liquid showing complex values of ω for real values of k. The lowest pairs of eigenfrequencies for a string fixed at each end are shown.

Note that for a given mode n both eigenfrequencies are imaginary (and represent pure damping) if the second (viscous drag) term under the radical in (10.1.46) exceeds the first (tension) term; for example, in Fig. 10.1.19 the $n = 1$ mode is characterized by two exponentially decaying deflections whereas the $n = 2$ mode takes the form of two oscillating deflections with amplitudes with a temporally decaying envelope. In this case we say that the lowest mode is overdamped and the others are underdamped.

Example 10.1.3. Of course, the damping can occur because of electrical as well as mechanical dissipation. The system introduced in Example 10.1.1 serves as an illustration of this fact. Suppose that the conducting top and bottom walls in Fig. 10.1.7 are so highly resistive that the voltage induced by the motion of the membrane is entirely absorbed by the resistance of the plates. This is the opposite extreme to the case considered in Example 10.1.1 in which this voltage was absorbed by the self-inductance of the current loops (*a*) and (*b*) shown in Fig. 10.1.8. (These extremes were discussed in the context of lumped parameters in Section 5.1.3.) Then, in writing the electrical loop equations (j) and (k) of Example 10.1.1, we can make the approximation that

$$\left|\frac{h^a}{\sigma_s}\right| \gg \left|\frac{\partial}{\partial t}\mu_0\, dh^a\right|, \tag{a}$$

$$\left|\frac{h^b}{\sigma_s}\right| \gg \left|\frac{\partial}{\partial t}\mu_0\, dh^b\right|, \tag{b}$$

to obtain

$$h^a = \sigma_s\mu_0 H_0\frac{\partial \xi}{\partial t}, \tag{c}$$

$$h^b = -\sigma_s\mu_0 H_0\frac{\partial \xi}{\partial t}. \tag{d}$$

The equation of motion is obtained by combining (a) and (n) in Example 10.1.1 with the last two equations:

$$\frac{\partial^2 \xi}{\partial t^2} = v_s^2\frac{\partial^2 \xi}{\partial x^2} - \nu\frac{\partial \xi}{\partial t}, \tag{e}$$

where

$$v_s = \left(\frac{S}{\sigma_m}\right)^{1/2} \tag{f}$$

$$\nu = \frac{2\sigma_s(\mu_0 H_0)^2}{\sigma_m}. \tag{g}$$

Hence in the limit in which the upper and lower walls in Fig. 10.1.7 are very lossy, the effect of the magnetic field is to damp the transverse motions of the perfectly conducting membrane. It is clear from (e) that the discussion of this section applies equally well to the resistively loaded membrane in which the damping is of electrical origin.

This example is continued in Section 10.2.4, in which the effects of electrical damping are exhibited in a considerably less obvious way than found here.

10.2 WAVES AND INSTABILITIES IN THE PRESENCE OF MATERIAL MOTION

We are concerned in this chapter with continuous media and have confined our interest so far to cases in which the continuum is initially at rest or in

static equilibrium. Gross motion of a medium can have a profound effect on the dynamics found, for example, when attempts are made to carry on a conversation in a high wind. In this section we use strings and membranes as models for introducing concepts related to the dynamics of media initially in a state of uniform motion. Again, our remarks are related to particular physical situations chosen for their simplicity, but with implications for a wide range of physical situations; for example, the string might be replaced by a beam of electrons in vacuum, by a stream of holes in a semiconductor, or by a streaming gas or plasma.

The systems to be considered now have the same basic physical nature as those in Section 10.1. The mechanical continuum is a string or a membrane undergoing one-dimensional transverse displacements $\xi(x, t)$. Now we introduce a new ingredient and specify that the continuum is moving in the longitudinal (x) direction with an equilibrium velocity U. Although the remarks that follow use the string as an example, it should be clear that they also apply directly to the one-dimensional motion of a membrane.

Our interest here is in exciting the moving string at a fixed point and in describing the dynamical behavior as viewed from a fixed frame. Consequently, the equation of motion developed in Section 9.2 is not adequate because it does not account for the equilibrium velocity (convection) of the continuum. It does, however, give a proper description of the string viewed from a reference frame moving in the x-direction with a velocity U because in that frame the string has no velocity in the x-direction. We denote variables (both independent and dependent) measured in this moving frame by primes and write (10.1.1) for string deflections ξ' in the moving frame as

$$m\frac{\partial^2\xi'}{\partial t'^2} = f\frac{\partial^2\xi'}{\partial x'^2} + S_z'. \tag{10.2.1}$$

We are dealing with velocities much lower than the velocity of light; consequently we use Fig. 10.2.1 to relate the coordinates and time in the two frames by the Galilean transformation*:

$$x = x' + Ut', \tag{10.2.2}$$

$$z = z' \tag{10.2.3}$$

$$t = t'. \tag{10.2.4}$$

It follows from (10.2.3) that $\xi = \xi'$ and because the moving frame is not accelerating, we can also say that $S_z' = S_z$. Hence to write (10.2.1) in the fixed

* This discussion represents a review of ideas developed in Section 6.1, now applied to transforming mechanical rather than electrical equations of motion. Hence once again we encounter the substantial or convective derivative.

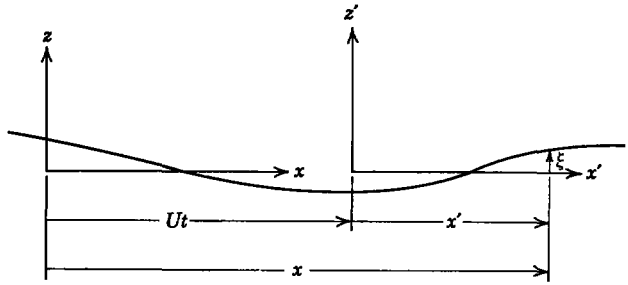

Fig. 10.2.1 The fixed coordinate system x, y, z or the moving coordinate system x', y', z' can be used to define a given position along the equilibrium axis of the string. Because the moving coordinate system has the same velocity U in the x-direction as the string, the string appears to move only in the z'-direction when viewed from the primed frame.

frame we need only compute the derivatives in terms of (x, t); that is

$$\frac{\partial \xi}{\partial t'} = \frac{\partial \xi}{\partial t}\frac{\partial t}{\partial t'} + \frac{\partial \xi}{\partial x}\frac{\partial x}{\partial t'} = \frac{\partial \xi}{\partial t} + U\frac{\partial \xi}{\partial x}. \tag{10.2.5}$$

Repeating this procedure, we have

$$\frac{\partial^2 \xi}{\partial t'^2} = \frac{\partial}{\partial t}\left(\frac{\partial \xi}{\partial t} + U\frac{\partial \xi}{\partial x}\right) + U\frac{\partial}{\partial x}\left(\frac{\partial \xi}{\partial t} + U\frac{\partial \xi}{\partial x}\right). \tag{10.2.6}$$

The space derivative is found in the same way to be

$$\frac{\partial^2 \xi}{\partial x'^2} = \frac{\partial^2 \xi}{\partial x^2}, \tag{10.2.7}$$

hence (10.2.1) becomes

$$m\left(\frac{\partial}{\partial t} + U\frac{\partial}{\partial x}\right)^2 \xi = f\frac{\partial^2 \xi}{\partial x^2} + S_z, \tag{10.2.8}$$

where the quantity in brackets on the left is recognized as the one-dimensional form of the substantial or convective derivative operating twice on ξ.* Remember from Section 6.1 (6.1.19) that the substantial or convective derivative is the time rate of change viewed from a frame moving with the velocity U. Our derivation of (10.2.8) makes this interpretation apparent once again. Here the convective derivative provides the means of expressing the equation of motion in the fixed frame.

* From the derivation $\left(\frac{\partial}{\partial t} + U\frac{\partial}{\partial x}\right)^2 \xi \equiv \frac{\partial^2 \xi}{\partial t^2} + 2U\frac{\partial^2 \xi}{\partial x\,\partial t} + U^2\frac{\partial^2 \xi}{\partial x^2}$.

10.2.1 Fast and Slow Waves

Before introducing further complications, it is worthwhile to consider the nature of waves that propagate on a convecting string with no electromechanical coupling. Thus we set $S_e = 0$ and (10.2.8) becomes

$$\left(\frac{\partial}{\partial t} + U\frac{\partial}{\partial x}\right)^2 \xi = v_s^2 \frac{\partial^2 \xi}{\partial x^2}, \tag{10.2.9}$$

where once again $v_s = \sqrt{f/m}$.

10.2.1a Traveling Waves

Now, if $U = 0$, the problem is mathematically identical to the one discussed in Section 9.1.1 in which we also found that the wave equation was pertinent and that deflections took the form of waves (9.1.14). We expect that in the moving frame shown in Fig. 10.2.1 solutions will have this same form and that we can now write solutions as

$$\xi = \xi_+(\alpha) + \xi_-(\beta), \tag{10.2.10}$$

where

$$\alpha = x' - v_s t', \qquad C^+, \tag{10.2.11}$$

$$\beta = x' + v_s t', \qquad C^-. \tag{10.2.12}$$

The parameters α and β can be written in terms of the fixed frame variables (x, t) by using the transformation equations (10.2.2) to (10.2.4):

$$\alpha = x - (v_s + U)t, \qquad C^+, \tag{10.2.13}$$

$$\beta = x + (v_s - U)t, \qquad C^-, \tag{10.2.14}$$

and direct substitution into (10.2.9) shows that (10.2.10) is indeed a solution.

Equations 10.2.13 and 10.2.14 for α and β are recognized as the characteristics discussed in Section 9.1.1*a* but altered by the convection. The convection increases the velocity of waves propagating in the positive x-direction along C^+ characteristic lines and decreases the velocity of waves propagating in the negative x-direction along C^- characteristics.

The characteristic lines that originate at $x = 0$ when $t = 0$ (α and β equal to zero in (10.2.13) and (10.2.14)) are shown in Fig. 10.2.2. In (*a*) of this figure waves propagate relative to the string with a velocity exceeding $U(v_s = 2U)$. Note that the slopes of the characteristics are the velocities of propagation for the forward and backward waves ξ_+ and ξ_-. Hence the wave propagating in the $+x$-direction does so more rapidly than the wave propagating against the convection in the $-x$-direction.

By contrast Fig. 10.2.2*b* shows the case in which the convection makes both characteristics point downstream ($+x$-direction) as time increases. Hence a

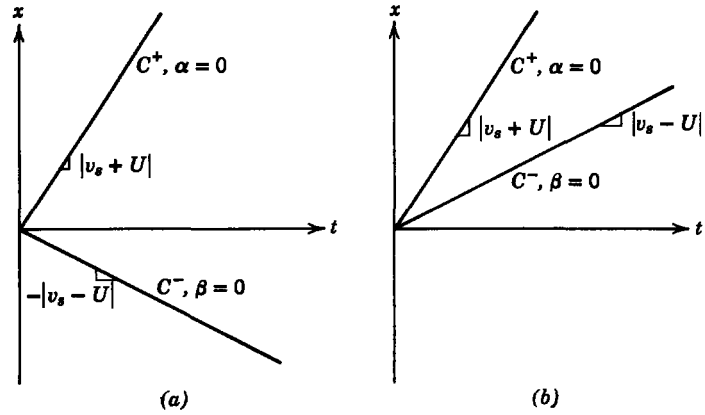

Fig. 10.2.2 Characteristic lines in the space-time plane along which a disturbance at $x = 0$ when $t = 0$ will propagate: (*a*) when $v_s = 2U$; (*b*) when $v_s = U/2$.

disturbance at $x = 0$ when $t = 0$ will result in two waves that propagate in the $+x$-direction. There is no effect from such a distrubance on that part of the string in which $x < 0$. As we shall find in Chapter 13, sound waves in a gas have a behavior analogous to that of the elastic waves considered here. In the language of gas dynamics we say that the two cases of Fig. 10.2.2 are "subsonic" and "supersonic," respectively.

An example serves to clarify further the effect of material convection on waves.

Example 10.2.1. In Example 9.1.2 of Section 9.1.1*a* we studied the behavior of an initially static pulse propagating on an elastic rod. A mathematically similar problem is now considered in which the string is given an initial displacement and velocity and we inquire about the resulting motions; that is, we are given

$$\xi(x, 0) = \xi_0(x), \tag{a}$$

$$\frac{\partial \xi}{\partial t}(x, 0) = \dot{\xi}_0(x). \tag{b}$$

We can evaluate ξ_+ and ξ_- by using the initial conditions. This is done by taking the derivative of (10.2.10) with respect to x and using (a). (Here we use the fact that $\partial\alpha/\partial x = \partial\beta/\partial x = 1$.)

$$\frac{d\xi_+}{d\alpha} + \frac{d\xi_-}{d\beta} = \frac{d\xi_0}{dx}. \tag{c}$$

Similarly, the use of the time derivative of (10.2.10) with (b) gives

$$-(v_s + U)\frac{d\xi_+}{d\alpha} + (v_s - U)\frac{d\xi_-}{d\beta} = \dot{\xi}_0(x). \tag{d}$$

Simultaneous solution of (c) and (d) yields

$$\frac{d\xi_+}{d\alpha} = \left(\frac{v_s - U}{2v_s}\right)\frac{d\xi_0}{dx} - \frac{1}{2v_s}\dot{\xi}_0(x), \tag{e}$$

$$\frac{d\xi_-}{d\beta} = \left(\frac{v_s + U}{2v_s}\right)\frac{d\xi_0}{dx} + \frac{1}{2v_s}\dot{\xi}_0(x). \tag{f}$$

Remember that in (e) and (f) x is the position along the string when t = 0. To find the solution at a general point C in space and time, as shown in Fig. 10.2.3, we use (e) with x evaluated at A, where $x = \alpha$. In the same way (f) is evaluated at point B, where $x = \beta$. Then (e) provides $d\xi_+/d\alpha$ anywhere along the C^+ characteristic shown in Fig. 10.2.3. The particular values of α and β required to give characteristics passing through the point $C(x, t)$ are given by (10.2.13) and (10.2.14). The space derivative of (10.2.10) can now be evaluated in terms of the initial conditions by using (e) and (f).

$$\frac{\partial \xi}{\partial x}(x, t) = \left(\frac{v_s - U}{2v_s}\right)\frac{d\xi_0}{dx}(\alpha) + \left(\frac{v_s + U}{2v_s}\right)\frac{d\xi_0}{dx}(\beta) - \frac{\dot{\xi}_0(\alpha) - \dot{\xi}_0(\beta)}{2v_s}. \tag{g}$$

Suppose that when $t = 0$ the string is static ($\dot{\xi}_0 = 0$) and the displacement is a uniform pulse of magnitude A distributed between $x = -a$ and $x = a$. Then we have

$$\frac{d\xi_0}{dx}(x) = A[u_0(x + a) - u_0(x - a)], \tag{h}$$

where $u_0(x + a)$ is a unit impulse at the position $x = -a$. The resulting space derivative of the displacement follows from (g) which becomes

$$\frac{\partial \xi}{\partial x}(x, t) = A\left\{\frac{(v_s + U)}{2v_s}[u_0(\beta + a) - u_0(\beta - a)] + \frac{(v_s - U)}{2v_s}[u_0(\alpha + a) - u_0(\alpha - a)]\right\}. \tag{i}$$

Remember that α and β are given by (10.2.13) and (10.2.14). The first two terms in this expression are recognized as impulses propagating along the C^- characteristics originating

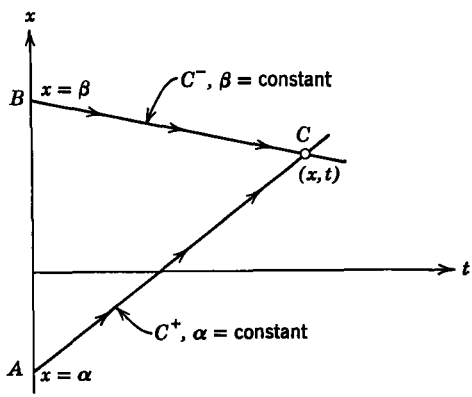

Fig. 10.2.3 Characteristics that intersect at a general point in space and time (x, t) showing the points A and B at which the initial conditions determine the dependent variables at C.

at $x = -a$ and $x = a$, respectively. The last two terms are impulses propagating along the C^+ characteristics. We can obtain the displacement ξ by integrating this equation with respect to x. The resulting values of ξ in two cases are shown in Figs 10.2.4 and 10.2.5. In the first of these figures U is less than v_s and we see that the original pulse divides into a part propagating slowly in the $-x$-direction (upstream) and a part that is propagating rapidly in the $+x$-direction. In Fig. 10.2.5 the convection velocity U is greater than the propagation velocity v_s and, although the pulse divides into two parts, both parts are carried downstream by the convection. Note that the convection also makes the ξ_+ and ξ_- waves unequal in magnitude. In fact, when U exceeds v_s, the ξ_+ wave is inverted, as shown in Fig. 10.2.5.

We are now in a position to make an important observation about the appropriate initial conditions and boundary conditions when the differential equation of motion is (10.2.9). We first observe that this expression is a partial differential equation that is second-order in both time (t) and space (x). Consequently, we need two initial conditions and two boundary conditions to evaluate all the constants in the solution. Where these conditions can be applied depends on whether the convection velocity U is greater or less than the propagation velocity v_s and is essentially the question whether a disturbance can propagate upstream (in the negative x-direction).

Consider first the case in which $U < v_s$ and disturbances can propagate upstream. As an example, assume that the string deflection is fixed at $x = l$. Then we can say that $\xi = 0$ along the line $x = l$ in the x-t plane. This is one boundary condition. A second boundary condition is that at $x = 0$ the string position is driven independently

$$\xi(0, t) = \xi_d(t). \tag{10.2.15}$$

It is helpful to picture these conditions as shown in Fig. 10.2.6. The two initial conditions can be specified as the initial displacement $\xi(x, 0)$ and the initial transverse velocity $(\partial\xi/\partial t)(x, 0)$. The solution for $\xi(x, t)$ at an arbitrary point C can be found as follows. First, the value of $\xi_+(\alpha)$ that propagates from A to B along a C^+ characteristic is determined by the initial conditions at point A. Similarly, the $\xi_-(\beta)$ wave propagating along a C^- characteristic from E to D is found from the initial conditions at point E. These incident waves, together with the boundary conditions at B and D, determine the reflected waves that travel from B to C along a C^- characteristic [a $\xi_-(\beta)$ wave] and from D to C along a C^+ characteristic [a $\xi_+(\alpha)$ wave] described in Section 9.1.1*b*. Hence we have found the solution for the displacement at point C. From similar arguments, perhaps involving many reflections of the waves, we can find the solution at any point in the x-t plane in the interval of space $0 < x < l$.

Consider next the case in which $U > v_s$. As indicated by Fig. 10.2.6*b*) both the C^+ and C^- characteristics point downstream (positive x-direction) as t increases and no disturbances can propagate upstream. Consequently, we expect that initial conditions and boundary conditions applied downstream

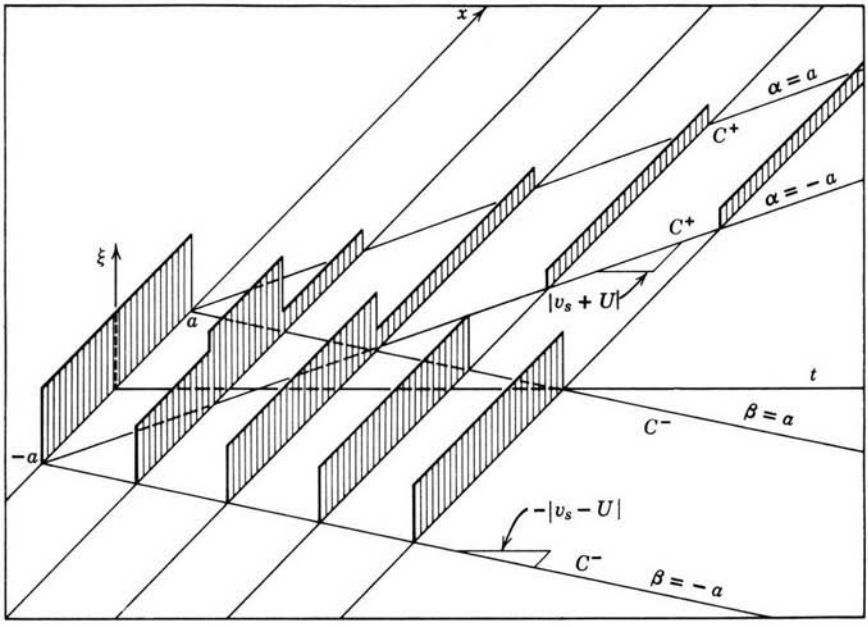

Fig. 10.2.4 Propagation of an initially static displacement pulse on a string moving with the velocity $U = v_s/2$.

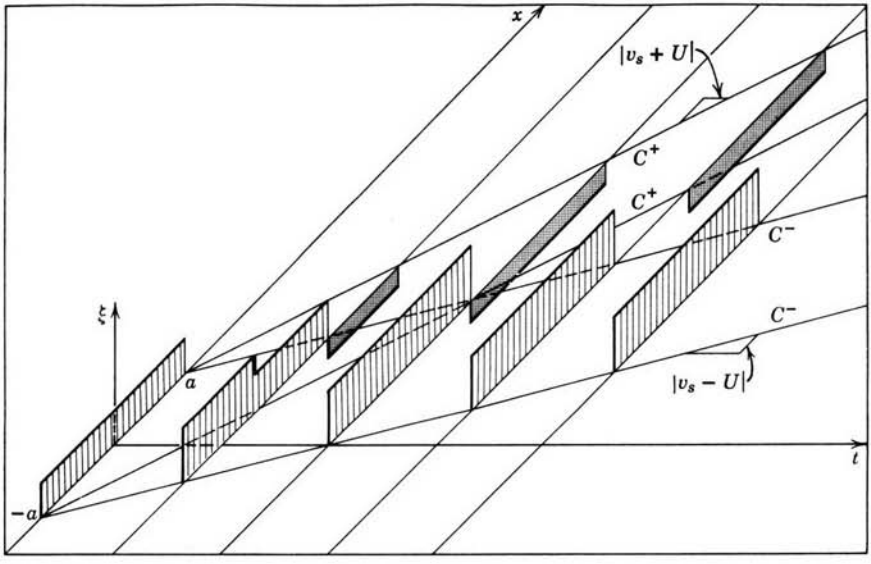

Fig. 10.2.5 Propagation of an initially static displacement pulse on a string moving with the velocity $U = 2v_s$.

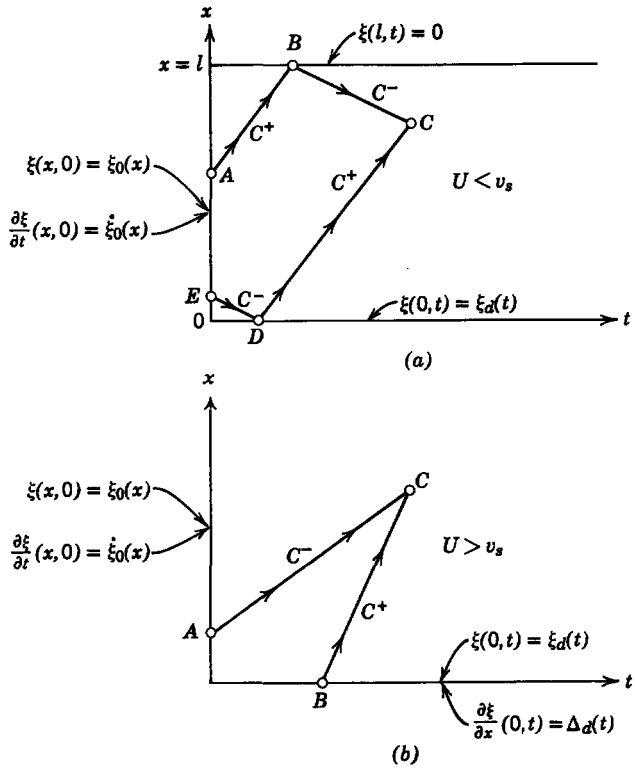

Fig. 10.2.6 Boundary and initial conditions to establish solution $\xi(x, t)$ at a point C: (*a*) $U < v_s$; (*b*) $U > v_s$.

from point C will not affect the displacement ξ at point C because the effects of initial and boundary conditions are transmitted in space and time by waves that propagate along the characteristics. To make this discussion explicit we refer to Fig. 10.2.6*b* and ask for the displacement at an arbitrary point C. Note that the solution at C can depend on only conditions at A and B. Hence causality is introduced as a physical law that must be obeyed by our mathematical solution, and we assume that solutions evolve from left to right (in the direction of increasing time) in Fig. 10.2.6. Hence it is necessary to impose two conditions at A and two conditions at B. Note that this means that boundary conditions along the $(x = 0)$-axis have the same nature as initial conditions along the $(t = 0)$-axis. In addition to the two initial conditions when $t = 0$, we can impose

$$\xi(0, t) = \xi_d(t) \tag{10.2.16}$$

and the slope at $x = 0$,

$$\frac{\partial \xi}{\partial x}(0, t) = \Delta_d(t). \tag{10.2.17}$$

With the initial and boundary conditions thus specified, we can calculate the $\xi_+(\alpha)$ wave that propagates along the C^+ characteristic from B to C and the $\xi_-(\beta)$ wave that propagates along the C^- characteristic from A to C in Fig. 10.2.6*b*. Thus we have found the displacement at point C.

A comparison of Figs. 10.2.6*a* and *b* shows that the essential difference between the two cases is that with $U < v_s$ boundary conditions must be specified both upstream and downstream from the point in question because waves propagate in both directions. For the case $U > v_s$ waves propagate downstream only; thus the boundary conditions must be specified upstream from the point in question.

In the supersonic case ($U > v_s$) it would violate causality to impose only one boundary condition at $x = 0$ and the second condition at $x = l$. Waves propagating along the C^+ and C^- characteristics would have to know in advance that they had to satisfy a boundary condition at C in Fig. 10.2.6*b*. This is an important point because there can be no mathematical objection to a solution to (10.2.9) with $U > v_s$ which satisfies one upstream and one downstream boundary condition. Rather our objection is based on the physical requirement of causality.*

10.2.1b Sinusoidal Steady State

To appreciate fully the drastic effect of the convection it is important to recognize the manner in which a sinusoidal steady-state condition is established on the "supersonic" string. Suppose that with $U > v_s$ a sinusoidal excitation is applied when $t = 0$ at $x = 0$. This is shown in Fig. 10.2.7, in

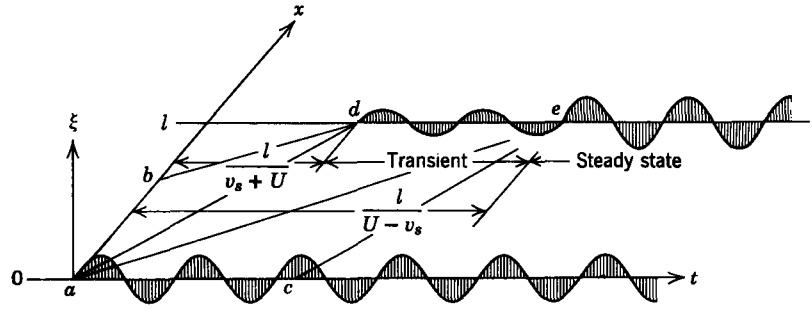

Fig. 10.2.7 A sinusoidal excitation turned on at $x = 0$ when $t = 0$ is applied to a moving string ($U > v_s$). At the downstream position $x = l$ the sinusoidal steady state is established when the slow wave arrives [$t = l/(U - v_s)$].

* Nonlinear disturbances can propagate upstream even when $U > v_s$. In the language of gas dynamics these are "shock waves" that travel faster than the speed v_s of small amplitude disturbances. These nonlinear phenomena are beyond the scope of this work and are not predicted by our simple, linear model. See, for example, R. Courant and K. O. Friedrichs, *Supersonic Flow and Shock Waves*, Interscience, New York, 1948, Part II.

which two sinusoidal driving conditions are imposed along the t-axis when $t > 0$ and when $t = 0$ the string has a dynamical state specified by the initial conditions.

Consider the string deflections that would be observed at the downstream position $x = l$. We have learned in this section that the solution at any given time is determined by a superposition of fast and slow waves propagating downstream on the C^+ and C^- characteristics, respectively. These characteristics originate either on the x-axis, where the initial conditions are arbitrary, or on the t-axis, where the boundary conditions are in the sinusoidal steady state. From this it follows that there is no response to the sinusoidal drive observed at $x = l$ until the fast wave initiated by the excitation at (*a*) in Fig. 10.2.7 arrives at (*d*). Hence, if the initial conditions are zero, there is no response until $t = l/(U + v_s)$. In the interval of time between the points *d* and *e* at $x = l$ the slow wave is determined by the initial conditions, whereas the fast wave is determined by the sinusoidal driving conditions. After the slow wave arrives when $t = l/(U - v_s)$, however, both characteristic lines, which determine the solution at a given point along the line $x = l$, originate in the sinusoidal steady-state driving condition. Because the conditions that determine the solution are then periodic in time, it follows that so also is the solution; that is, after the time $t = l/(U - v_s)$ when the slow wave arrives at $x = l$ the sinusoidal steady-state condition has been established. After this time there is no evidence of the initial conditions.

Recall the nature of the response to the initial conditions, as described in Section 10.1, in which the string has no longitudinal velocity. There the effect of initial conditions was described in terms of the normal modes, and the consequences of the initial conditions persisted in the form of these modes for an indefinite period of time. As we saw in the examples of Section 10.1, these modes are purely oscillatory unless other effects, such as damping, are introduced.

In the sections that follow we introduce additional forces on the string, with the longitudinal convection included ($U > v_s$). Hence the examples considered involve the same transverse forces that are developed in Section 10.1 but in addition include the effect of convection. With this in mind, remember that in the examples in Section 10.1 the normal modes, with amplitudes specified by the initial conditions, determine whether the string deflections become unbounded in time. In any of these cases the sinusoidal steady-state solution can be found, but in cases in which the system is unstable this steady-state solution is eventually dominated by the unstable normal modes. With the convection, this dominance of the transient resulting from the initial conditions is not possible. The sinusoidal steady-state solution is all that remains after the time $l/(U - v_s)$, which means that in the supersonic case ($U > v_s$) it is not possible for deflections to become unbounded with time at a given position x.

The significance of these remarks becomes more evident in Section 10.2.3. In any case it should be evident that with $U > v_s$ the driven response assumes primary importance

If once again we assume complex waves (10.0.1) as solutions, substitution into (10.2.9) shows that the dispersion relation between the frequency ω and wavenumber k is

$$(\omega - kU)^2 = v_s^2 k^2. \tag{10.2.18}$$

Note that this is the relation obtained in Section 10.1.1, except that now $\omega \to \omega - kU$, which reflects the fact that the effect of the convection is to replace the time derivative with the convective derivative. (As we emphasize in Section 10.2.4, care must be taken in transforming from one frame of reference to another using this simple substitution by noting the parts of the system that are moving.)

The dispersion equation has the graphical form of two straight lines, as can be seen by solving (10.2.18) for ω:

$$\omega = k(U \pm v_s). \tag{10.2.19}$$

The subsonic and supersonic cases are shown in Fig. 10.2.8. The effect of increasing U is to rotate the two straight lines of Fig. 10.1.1 until finally, when $U > v_s$, as shown in Fig. 10.2.8*b*, both straight lines are in the first and third quadrants of the ω-k plane.

The dispersion equation can be used to find the response of the string to a drive with the frequency ω_d by solving (10.2.19) for the wavenumbers k, given that $\omega = \omega_d$:

$$k = \eta \pm \gamma, \tag{10.2.20}$$

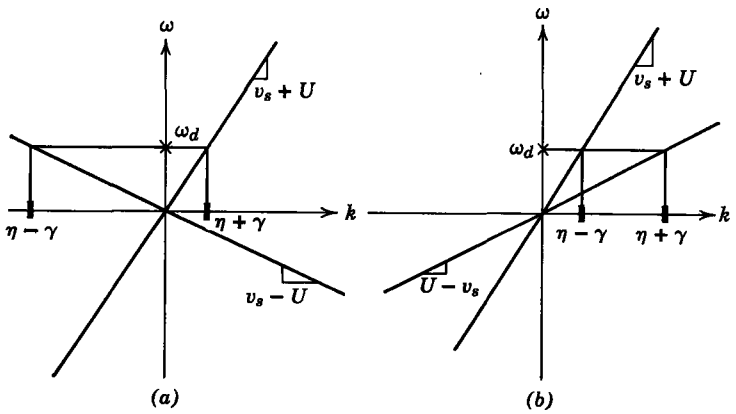

Fig. 10.2.8 Dispersion relations for waves on a string moving with the equilibrium velocity U in the positive x-direction. Although the geometry for the subsonic and supersonic cases is the same as that for the characteristic lines in Fig. 10.2.2, the axes here are ω-k, whereas in Fig. 10.2.2 they are x-t: (*a*) $U < v_s$; (*b*) $U > v_s$.

where for the string without additional forces

$$\eta = \frac{U}{v_s}\gamma, \qquad \gamma = \frac{\omega_d v_s}{U^2 - v_s^2} \tag{10.2.21}$$

A graphic representation of these two wavenumbers corresponding to the frequency ω_d is given in Fig. 10.2.8. Remember that the phase velocity of a wave is ω/k. With $U < v_s$, phases of one wave propagate rapidly downstream with the velocity $v_p = U + v_s$, whereas those of the other propagate upstream at the lesser velocity $v_p \doteq v_s - U$. With $U > v_s$, as shown in Fig. 10.2.8*b*, phases of both waves propagate downstream. These results are not surprising in view of the wave dynamics found in Section 10.2.1*a*.

Consider the sinusoidal steady-state dynamics resulting when $U > v_s$. Then, upstream boundary conditions in the form of (10.2.16) and (10.2.17) are appropriate. In particular, suppose that

$$\xi(0, t) = 0 \tag{10.2.22}$$

$$\frac{\partial \xi}{\partial x}(0, t) = \Delta_0 \cos \omega_d t. \tag{10.2.23}$$

Then we can take a linear combination of waves with wavenumbers given by (10.2.20) to satisfy the first of these conditions:

$$\xi(x, t) = \text{Re}\, A e^{j(\omega_d t - \eta x)} \sin \gamma x. \tag{10.2.24}$$

The remaining arbitrary constant A is determined by the second condition to be $A = \Delta_0/\gamma$, and so the required sinusoidal steady-state driven response is

$$\xi(x, t) = \frac{\Delta_0}{\gamma} \cos(\omega_d t - \eta x) \sin \gamma x. \tag{10.2.25}$$

We have found that when sinusoidal steady-state waves are excited on the supersonic string they combine to form an envelope with nulls spaced by the distance $\pi/\gamma = \pi(U^2 - v_s^2)/\omega_d v_s$. Within this envelope points of zero phase on the string move in the x-direction with the velocity $\omega_d/\eta = (U^2 - v_s^2)/U$. The deflections are shown at an instant in time in Fig. 10.2.9.

The periodic envelope of the waves is stationary in space and therefore has the same character as the standing waves found for the stationary string. These peaks and nulls in the deflection are sometimes referred to as beats*

* The beating of two sinusoidal signals is commonly encountered in demodulation processes, such as those that occur in the ear when tuning two musical instruments. Tones that differ slightly in frequency beat together at the difference frequency. This illustrates how phenomena observed as functions of time are found as functions of space when the supersonic motion of a medium is involved.

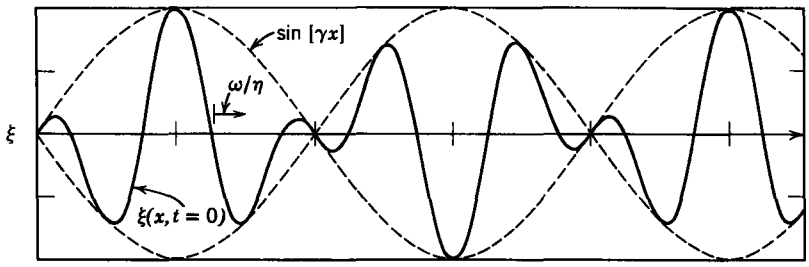

Fig. 10.2.9 Fast and slow waves interfere to form beats in space when $U > v_s$. The deflection is as the string appears if illuminated once each period of excitation $2\pi/\omega_d$.

because they result from interference between the two waves propagating downstream. At some positions the deflections from the two waves tend to add, whereas at others the deflections cancel.

In the sections that follow we undertake to show the effect of convection on each of the classes of interactions developed in Section 10.1. In cases in which the convection is equivalent to the entire system being in a state of uniform translation this is a simple matter, since the effect of the convection is represented by replacing the time derivatives in the differential equation with convective derivatives.

10.2.2 Evanescence and Oscillation with Convection

The developments of Section 10.2.1 pertained to the effect of convection on the dynamics of an ordinary string. In the absence of convection this string supports waves that propagate without dispersion. In this section we begin a discussion of the effects of convection on dispersive waves. In particular, we reconsider the systems that support the cutoff or evanescent waves described in Section 10.1.2. Now the system is as shown in Fig. 10.1.2, except that the wire has an equilibrium longitudinal velocity U. Because the magnetic restoring force is the same, whether evaluated in the frame moving with the string or in a fixed frame, the equation of motion found in Section 10.1.2 (10.1.6) is valid in a frame moving with the velocity U in the x-direction. As illustrated in Section 10.2, the equation of motion in the fixed frame is obtained by replacing the time derivative with the convective derivative. From this it follows that the dispersion equation with convection is obtained by simply replacing ω in the dispersion equation for the fixed system (10.1.7) with $\omega - kU$. Hence the required dispersion equation with convection is

$$(\omega - kU)^2 = v_s^2k^2 + \omega_c^2. \tag{10.2.26}$$

The graphical repres tion of this equation is shown in Fig. 10.2.10, in which $U < v_s$ and $U > v_s$ are shown. These plo' give complex values of k

for real values of ω. It should be clear from the plots and the fact that the dispersion equation is quadratic in ω that only real values of ω are given by (10.2.26) for real values of k.

The asymptotes of the dispersion equation are the two straight lines of Fig. 10.2.8*a*, *b*. Hence the result of increasing the velocity U is to rotate the hyperbolas in a counterclockwise direction. To make further deductions about the dispersion equation, it is helpful to solve (10.2.26) for k.

$$k = \eta \pm \gamma, \tag{10.2.27}$$

where

$$\eta = \frac{\omega_d U}{U^2 - v_s^2}, \qquad \gamma = \frac{\sqrt{v_s^2 \omega_d^2 + (U^2 - v_s^2)\omega_c^2}}{U^2 - v_s^2}. \tag{10.2.28}$$

This makes it evident that in the case in which $U < v_s$, there is a range of driving frequencies over which the wavenumbers are complex. From the last two equations, this is the range of ω_d over which the quantity under the radical is negative.

$$|\omega_d| < \left| \frac{(v_s^2 - U^2)\omega_c^2}{v_s^2} \right|^{1/2}. \tag{10.2.29}$$

The complex values of k are shown in Fig. 10.2.10*a*, in which the imaginary part of k takes the form of an ellipse and the real part of k (the straight line) is the same for both waves.

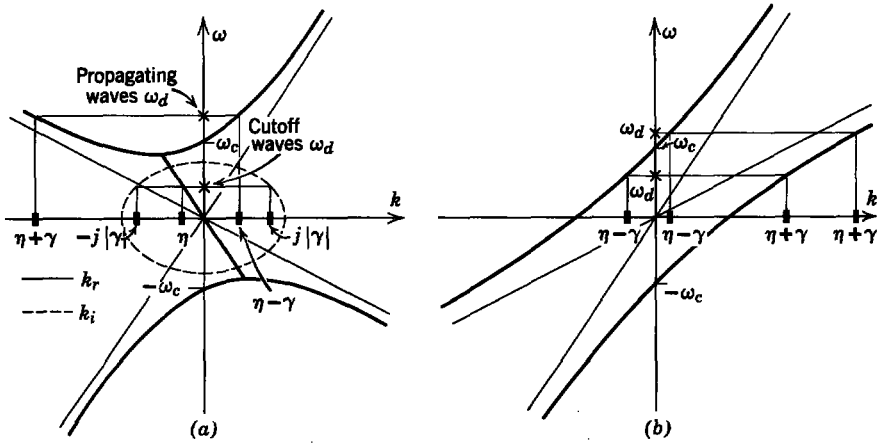

Fig. 10.2.10 Dispersion relations for system of Section 1.2, with the addition of a longitudinal velocity U. When U exceeds v_s, both waves propagate without decay, regardless of the frequency, and the effect of the convection is to eliminate the evanescence. (*a*) $U < v_s$; (*b*) $U > v_s$.

Two cases are shown in Fig. 10.2.10*a*. At the lower of the two driving frequencies waves with wavenumbers whose real part is η and imaginary parts, $\pm j|\gamma|$ are cutoff. At the larger driving frequency both wavenumbers are real. Note that the effect of the convection has been to make the cutoff wavenumbers complex rather than purely imaginary, as they were when the string was stationary.

As U is raised, the ellipse of Fig. 10.2.10*a* becomes smaller, until under the critical condition that $U = v_s$ it disappears and only real values of k are possible. Hence in Fig. 10.2.10*b* there are two real wavenumbers corresponding to a given driving frequency ω_d.

It is evident from what we have found that the effect of the convection has been to eliminate the evanescence. Two cases are illustrated in Fig. 10.2.10*b*. At the larger of the two driving frequencies both wavenumbers are positive and points of constant phase on the waves propagate downstream. At the lower driving frequency, however, the phase velocity of the slow wave is in the negative x-direction (upstream). This is perhaps our first disenchantment with the physical significance of the phase velocity. In fact, a pulse initiated at some point along the moving string would not propagate upstream in the face of the convection. The phase velocity does *not* indicate the manner in which a wavefront would propagate.

We introduced a discussion of the propagation of pulses on the moving string in Section 10.2 because it clearly indicated the direction in which a disturbance would propagate on the string. The string alone, however, is a rather special case in that such sinusoidal steady-state quantities as the phase velocity are identical with the actual propagational velocity of wavefronts. This is why the string merits the designation "dispersionless medium." In general, the phase velocity has no more significance than that associated with the dynamics of the sinusoidal steady state. We return to a discussion of propagational velocities in Section 10.3. For now, suffice it to say that regardless of the types of dispersion introduced with the examples of this and the preceding section wavefronts propagate with the velocities $U + v_s$ and $U - v_s$. Hence boundary conditions are imposed in accordance with the relative values of U and v_s, just as they are with the string alone.

If U is less than v_s, a pulse on the string can propagate upstream. Hence in Fig. 10.2.10*a* it is appropriate to use the wavenumbers to provide solutions that satisfy one upstream and one downstream boundary condition. Just as in the case considered in Section 10.1.2 the complex wavenumbers indicate that the deflections excited at one end decay spatially from the point of excitation. In the supersonic case shown in Fig. 10.2.10*b* it is appropriate to impose two boundary conditions at an upstream position. The sinusoidal steady state is then established in essentially the same way as for the moving string alone (Fig. 10.2.7). In fact, the wavenumbers now have the same form

considered in Section 10.2.1 (10.2.20), except that η and γ are defined by (10.2.27). Without any further mathematical developments, we can see that driving conditions in the sinusoidal steady-state form of (10.2.22) and (10.2.23) lead to the deflections given by (10.2.24) and shown in Fig. 10.2.9. The waves combine to form spatial beats as an envelope. The most salient consequences of the dispersion introduced by the addition of the magnetic restoring force can be seen if we consider the limit in which the tension on the string is of negligible importance. Then $v_s \to 0$ and η and γ, as given by (10.2.28), reduce to

$$\eta = \frac{\omega_d}{U}, \qquad \gamma = \frac{\omega_c}{U}. \tag{10.2.30}$$

It follows that the string deflections for the sinusoidal steady-state solution of (10.2.25) become

$$\xi(x, t) = \frac{\Delta_0 U}{\omega_c} \cos\left[\omega_d\left(t - \frac{x}{U}\right)\right] \sin\frac{\omega_c x}{U}. \tag{10.2.31}$$

The envelope of the waveform is determined by the cutoff frequency ω_c, whereas the phase velocity of the waves within this envelope is simply the convection velocity U.

In the absence of a tension f each section of the string is subject only to the spring like restoring force of the magnetic field. Because each section has a mass, the resulting dynamics can be pictured in terms of the mechanical model shown in Fig. 10.2.11. Here the mass has been lumped at discrete positions so that it is clear that each section of the string behaves as a simple mass-spring oscillator. As in Section 10.1.2, the spring represents the effect of the field. The convection carries these oscillators in the x-direction with the velocity U.

The resonance frequency of the mass-spring oscillators is ω_c. We can see this by recognizing that in the moving frame the equation of motion takes the form found with a simple harmonic oscillator.

$$\frac{\partial^2 \xi}{\partial t'^2} = -\omega_c^2 \xi. \tag{10.2.32}$$

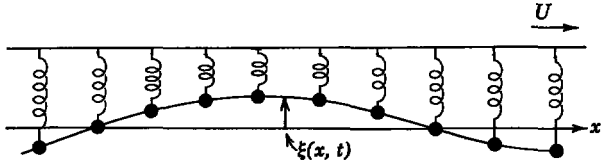

Fig. 10.2.11 When $f \to 0 (v_s \to 0)$, the moving string subject to the restoring force of the magnetic field is equivalent to a distribution of mass-spring oscillators with the resonance frequency ω_c and moving with the velocity U in the x-direction.

The example that follows illustrates how this type of dynamics develops in dealing with electron beams.

Example 10.2.2. The dynamics of moving oscillators is of importance in dealing with interactions between streaming electrons and various media, such as distributed circuits, plasmas, and solid-state lattice structures. The similarity between the electron and string dynamics treated in this section can be illustrated by considering a simple one-dimensional example.

Suppose that a given region of space is filled with electrons with the number density n_e and ions with the number density n_i. We assume that these particles do not interact with one another, except through their electric fields. In the equilibrium situation both the electrons and the ions are static. Moreover, the ion charge density is equal to the electron charge density, so that there is no net charge so long as the system of particles is in equilibrium; for example, if both the ions and electrons have a single electronic charge e, the ion charge density en_i just balances the electron charge density $-en_e$ when the system is in equilibrium.

We are concerned here about the dynamics of the electrons, which have a much smaller mass then the ions. For this reason, it is a good approximation to consider the more massive ions as fixed, hence as having a constant number density. Then the perturbation from equilibrium charge density is

$$\rho_e = (n_i - n_e)e = -ne, \tag{a}$$

where $n(x, t)$ is the amount by which the number density of electrons exceeds the equilibrium value n_e at any given (x, t).

To describe the electric part of this interaction it is recognized that the charge density is related to the electric field intensity by Gauss's law. In one dimension this is

$$\frac{\partial E}{\partial x} = -\frac{ne}{\epsilon_0}. \tag{b}$$

In addition, conservation of charge in one dimension becomes

$$\frac{\partial J_f}{\partial x} + \frac{\partial \rho_e}{\partial t} = 0, \tag{c}$$

where J_f is the current density. In the present case currents arise only because of the motion of the electrons in the x-direction; hence

$$J_f = -(n_e + n)ev \simeq -n_e ev, \tag{d}$$

where v is the longitudinal (x) electron velocity and the last approximate equality results from a linearization.

The mechanical equation of motion is Newton's law expressed for each of the electrons (having the mass m).

$$m\frac{\partial v}{\partial t} = -eE. \tag{e}$$

Now, a combination of (a) through (e) gives

$$\frac{\partial^2 n}{\partial t^2} + \omega_p{}^2 n = 0, \tag{f}$$

where

$$\omega_p = \left(\frac{n_e e^2}{\epsilon_0 m}\right)^{1/2}. \tag{g}$$

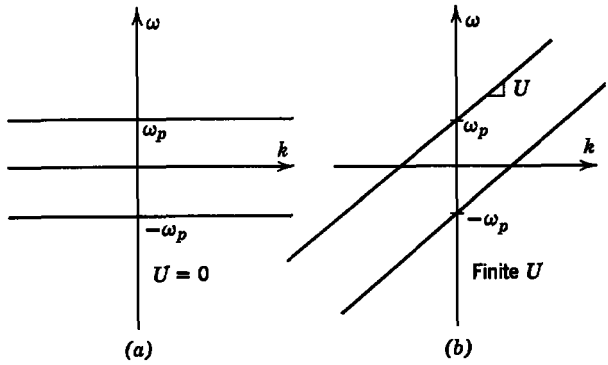

Fig. 10.2.12 Dispersion plot for electron oscillations having the plasma frequency ω_p: (*a*) the electrons with a fixed equilibrium state; (*b*) electrons with an equilibrium velocity U in the x-direction.

On the basis of the developments in this and the preceding section, it is a simple matter to see that if the electrons have an equilibrium state of motion in the x-direction with the velocity U (f) is altered to

$$\left(\frac{\partial}{\partial t} + U\frac{\partial}{\partial x}\right)^2 n + \omega_p{}^2 n = 0. \tag{h}$$

The dispersion equations for these two situations are shown in Fig. 10.2.12. The plasma frequency ω_p plays the same role here as the cutoff frequency ω_c in the discussion of this section. The string dynamics in the magnetic field are described by the same dispersion equation found here in the limit in which $v_s \to 0$. Note, however, that the electron motions considered here are longitudinal, whereas the deflections of the oscillators (Fig. 10.2.11) are transverse.

In electron beam devices similar oscillations are obtained on a beam with finite cross-sectional dimensions by imposing a large longitudinally directed magnetic field. The Lorentz force $-e\mathbf{v} \times \mathbf{B}$ then tends to confine these space-charge oscillations to the longitudinal direction.*

10.2.3 Convective Instability or Wave Amplification

Continuum instability is the subject of Section 10.1.3, in which the simple string, under the influence of a destabilizing magnetic force (Fig. 10.1.9), sustained deflections that grew exponentially with time.

In this section we shall find that if the unstable medium moves fast enough the instability will be carried downstream and a perturbation can grow in amplitude, but not at the same point in space at which it originated. This

* For a discussion of electron beam dynamics, see C. C. Johnson, *Field and Wave Electrodynamics*, McGraw-Hill, 1965, p. 277. The analogy between the moving string and the electron beam should make it clear to those who are familiar with the two-cavity klystron that the moving string with $U > v_s$ can be used to make a "stringtron" or amplifier using the longitudinal kinetic energy of the string as a source of energy.

type of instability can be excited in the sinusoidal steady state, in which case it appears as a spatially growing wave. Hence this *convective instability* is also called an *amplifying wave*, since it can be used to amplify a driving signal.

Some electron-beam devices, such as traveling wave tubes (TWT), make practical use of amplifying waves. In addition, convective instabilities play important roles in a variety of physical situations, ranging from fluid dynamics (boundary layer dynamics) to physical acoustics (ultrasonic amplification). In some cases the convective instability can be put to work, and in others the convective instability occurs inherently in a system and must be understood.

We can illustrate the basic nature of the amplifying wave by considering the effect of convection on the instability studied in Section 10.1.3. We now include the fact that the string is moving in the x-direction with the velocity U.

The effect of the convection is accounted for by replacing the time derivative in the equation of motion by the convective derivative. Hence (10.1.25) becomes

$$\frac{1}{v_s^2}\left(\frac{\partial}{\partial t} + U\frac{\partial}{\partial x}\right)^2 \xi = \frac{\partial^2 \xi}{\partial x^2} + k_c^2 \xi. \tag{10.2.33}$$

Remember, k_c^2 is proportional to the current I in the wire and the gradient of the imposed magnetic field.

Substitution of the traveling wave solution (10.0.1) into this equation of motion yields

$$(\omega - kU)^2 = v_s^2(k^2 - k_c^2). \tag{10.2.34}$$

We could just as well have obtained this dispersion equation by replacing ω in the dispersion equation of Section 10.1.3 with $\omega - kU$. The effect of the convection is simply to translate the entire system in the x-direction with the velocity U. As in Section 10.2.2, however, the excitations and frame of observation remain fixed, and it is this fact that makes the situation inherently different from the case with no convection.

Equation 10.2.34 is quadratic in either ω or k. Solving it for ω shows that there are "unstable" values of ω for real values of $k(|k| < |k_c|)$

$$\omega = kU \pm \sqrt{v_s^2(k^2 - k_c^2)}. \tag{10.2.35}$$

We have seen situations in which a negative imaginary value of ω resulting from a real value of k indicates that the deflections become unbounded with time (Section 10.1.3). In fact, if $U = 0$ and the string is fixed at each end, the allowed values of $k = n\pi/l$, and the associated eigenfrequencies are given by (10.2.35). With the string moving with a velocity U that exceeds v_s, it is no longer consistent with causality to impose a downstream boundary condition. This means that the response to initial conditions is no longer defined in terms of eigenmodes, but rather that it has the character described

in Section 10.2.1. With $U > v_s$, we impose two boundary conditions at $x = 0$. At any downstream position the transient response to the initial conditions is over when a slow wavefront arrives from $x = 0$. Hence the deflections of the string can no longer become unbounded with time at a fixed position x. If the boundary conditions at $x = 0$ are both zero, the response will be zero once the transient is completed.

Consider the consequences of a sinusoidal steady-state boundary condition at $x = 0$. Solution of the dispersion equation shows that for $\omega = \omega_d$, the wavenumbers k are

$$k = \eta \pm j\gamma, \tag{10.2.36}$$

where

$$\eta = \frac{\omega_d U}{U^2 - v_s^2},$$

$$\gamma = \frac{v_s\sqrt{(U^2 - v_s^2)k_c^2 - \omega_d^2}}{U^2 - v_s^2}.$$

The dispersion equation is shown graphically in Fig. 10.2.13. In this ω-k plot complex values of k are shown as functions of real values of ω. As can be seen from (10.2.36), over the range of frequencies

$$\omega_d^2 < (U^2 - v_s^2)k_c^2, \tag{10.2.37}$$

the wavenumbers are complex. Each wavenumber has the same real part over this range, which depends linearly on ω, as shown by the straight line in Fig. 10.2.13. As a function of ω, the imaginary part of k forms an ellipse. Of

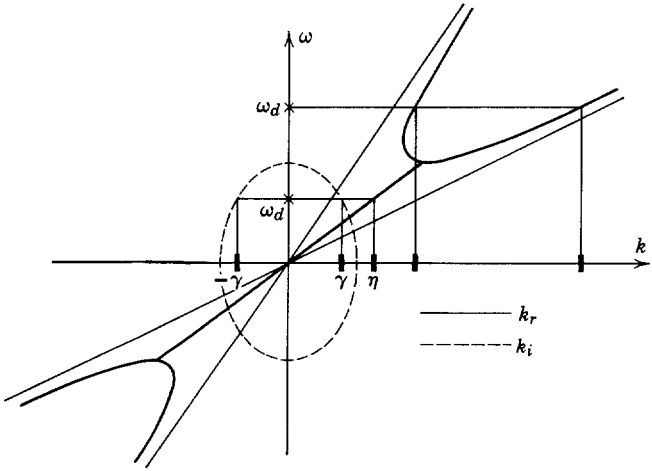

Fig. 10.2.13 Dispersion plot for supersonic string with a destabilizing magnetic force that shows complex values of k for real values of ω.

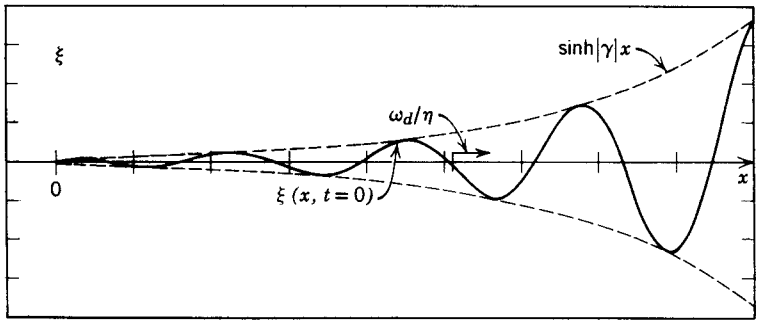

Fig. 10.2.14 Instantaneous view of string deflections when they are convectively unstable.

course, if the driving frequency exceeds a maximum value (10.2.37), both wavenumbers become real and the driven response takes on the form discussed in Section 10.2.1*b*.

To appreciate the significance of what we have found, consider once again the sinusoidal steady-state response to the boundary conditions of (10.2.22) and (10.2.23). Following the procedures outlined in Section 10.2.1b, we take a linear combination of the two waves which satisfies the boundary conditions at $x = 0$.

$$\xi(x, t) = \frac{\Delta_0}{|\gamma|} \sinh |\gamma| x \cos (\omega_d t - \eta x). \tag{10.2.38}$$

Here we have assumed that the driving frequency ω_d is the lower of the two shown in Fig. 10.2.13 so that the wavenumbers are complex.

The displacement given by (10.2.38) is shown as a function of x at a given instant of time in Fig. 10.2.14.*

Points of zero deflection move downstream with the phase velocity ω_d/η. Most important, the displacements have an envelope that grows exponentially with increasing x. The effect of the motion on the instability is now apparent. Rather than having an amplitude that is a monotonically increasing function of time at a given point in space, the displacements are now bounded in time but exhibit an exponential growth in space. The convection is responsible for washing the instability downstream.

The convective and absolute instabilities impose very different limitations on the engineering of systems. The largest amplitude obtained by the string within a given length is determined by the input of signals, perhaps in the form of noise, to the system. The more nearly the excitations are eliminated from the system, the more nearly will the string maintain its equilibrium

* The reason for the term "amplifying wave" is that an output transducer downstream from the excitation can extract a signal of the same frequency as the excitation but at a higher power level. The source of power is the moving medium.

position. This is by contrast to the case of absolute instability, in which, inadvertently, no matter how carefully the conditions of the string are set, initial noise will result in displacements that become unbounded in time.

The following example affords an opportunity to gain further physical insight into the nature of the convective instability.

Example 10.2.3. In Section 10.1.3 (on absolute instability) an example was considered in which a highly conducting membrane stressed by an electric field was found to be absolutely unstable (Example 10.1.2). Figure 10.2.15 shows a somewhat similar situation in which a jet of water passes between plane-parallel electrodes. The jet moves in the x-direction with the equilibrium velocity U. Transverse or kinking motions of the stream can be modeled by the string equation with the effect of convection included. In the jet the tension f is due to surface tension.

The jet is grounded, but the plates are at the same constant potential V shown in the figure. This is an electric field system, and because the time required for free charges to

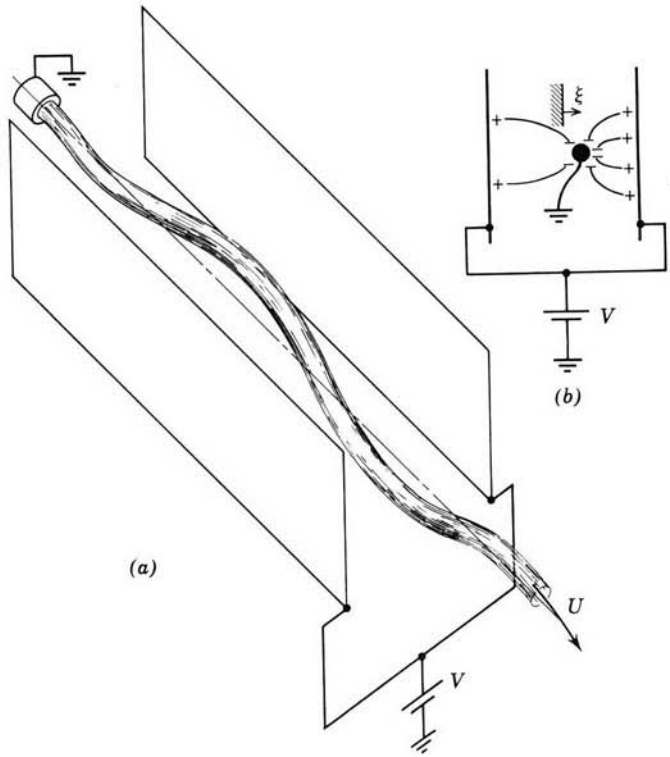

Fig. 10.2.15 (*a*) A jet of water has a streaming velocity U midway between plane-parallel electrodes. A potential difference V is applied between the plates and the jet. (*b*) As the jet is deflected toward one of the plates, an unbalance in the electric force of attraction tends to carry it even farther in the direction of deflection. The instability resulting from this force is washed downstream to form the convective instability sketched in Fig. 10.2.16.

relax from one point to another on the water jet is extremely short compared with dynamical times of interest, the jet can be regarded as perfectly conducting; that is, the potential difference between any point on the jet and either of the electrodes is the constant V. This is the same electrical situation as in Example 10.1.2, in which the membrane and electrodes retained a constant potential difference even as the membrane deflected. The dependence of the electric force on the jet displacement is much the same as in the membrane.

A cross section of the jet and plates is shown in Fig. 10.2.15*b*. When the jet is centered, charges induced on its surface are attracted equally toward their images on each of the plates. Hence there is no net transverse force on the jet so long as it remains centered. If, however, it moves off center by the amount ξ, there is a net force. More charges are induced on the side of the jet that is nearer one of the plates (remember that the potential difference is constant and so the jet and plates form a constant potential capacitor). This surplus of

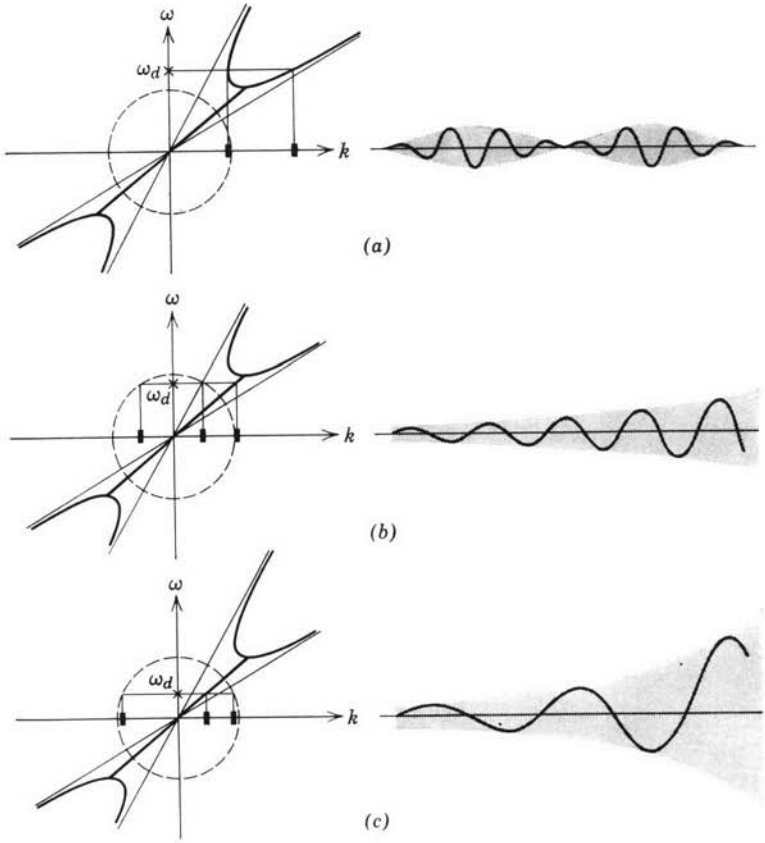

Fig. 10.2.16 Sinusoidal excitation of jet shown in Fig. 10.2.15. Driving frequency decreases from (*a*) to (*c*). This experiment together with animated ω-k plots can be seen in the film "Complex Waves II," produced for the National Committee on Electrical Engineering Films by the Education Development Center, Newton, Mass.

charge is attracted toward its image on the plate. Hence the force is (to linear terms) proportional to ξ and in the same direction as ξ. Both the amount of surface charge and the electric field are proportional to V, hence the force, which is proportional to the product of these quantities, is proportional to V^2. We conclude that the force per unit length acting on the jet transverse to its direction of streaming has the form

$$S_z = bV^2\xi, \tag{a}$$

where b is a geometric constant.

If we combine the electric force of (a) with the equation of motion for the jet alone (10.2.9), it follows that the equation for the jet in the electric field will take the form of (10.2.33) with

$$k_c^2 = \frac{bV^2}{f}. \tag{b}$$

A jet of tap water with the diameter of a pencil and moving with a longitudinal velocity of 2 m/sec has a convection velocity U that exceeds v_s by a factor of 10 or more. Hence in the presence of the electric field the jet is subject to convective instability. It can be excited in the sinusoidal steady state at the upstream end to obtain the response illustrated by (10.2.38) and sketched in Fig. 10.2.16.

In the sequence of sketches the driving frequency ω_d is reduced, as indicated on the corresponding ω-k plots. Hence in Fig. 10.2.16*a* the frequency is high enough that wavenumbers are real and beats form on the jet, as described in Section 10.2.2. In Fig. 10.2.16*b*,*c* the frequency is reduced to the point at which the wavenumbers are complex and the waves exhibit spatial growth. Note that as the frequency is reduced the wavelength is increased and the rate of spatial growth is increased. This is consistent with the prediction of the ω-k plot, since the rate of growth is proportional to the imaginary part of k, whereas the wavelength is inversely proportional to the real part of k.

The physical significance of the complex wavenumbers found in this section is altogether different from that for the evanescent waves. In Section 10.1.2 complex wavenumbers were used to represent waves that decayed spatially away from the point of excitation. Here the deflection amplitude grows as a function of distance from the excitation.

The contrast between evanescent and amplifying waves must be emphasized, for even though these waves are physically very different they can be confused mathematically; for example, we could arbitrarily impose two upstream sinusoidal steady-state boundary conditions on the evanescent waves found in Section 10.1.2. The resulting mathematical solution would exhibit spatial growth and would appear to be an amplifying wave. Similarly, we could use the waves represented by (10.2.34) with $U > v_s$ to satisfy boundary conditions at two points in space and to conclude that waves decay away from the point of excitation. What we have called a convective instability in this section would then appear to be an evanescent wave. Both sinusoidal steady-state solutions, however, would be inconsistent with causality. The boundary conditions would make it impossible to establish the sinusoidal steady-state solution with the past always affecting the future and not vice versa.

The dispersion equation, as we have used it here, simply guarantees that solutions with the form $\exp j(\omega t - kx)$ satisfy the equation of motion. To make appropriate use of these solutions requires that proper regard be taken of the physical realizibility of boundary conditions imposed on the solutions. The examples considered here are so simple that we could use physical intuition or a knowledge of how the system behaves without dispersion effects to establish the correct boundary conditions. Our arguments hinge essentially on observing how the system responds from the moment it is "turned on" until the sinusoidal steady state has been established. If the sinusoidal steady state can be established without violating conditions of causality, it is physically significant. We return to this topic in Section 10.3, in which propagation in the presence of dispersion is considered.*

10.2.4 "Resistive Wall" Wave Amplification

As shown in Section 10.2.3, the instability of continuous media in motion can give rise to amplifying waves. In the frame of reference attached to the moving medium the convective instability appears to grow in time, but in the fixed frame it is bounded in time. Hence it can be excited in the sinusoidal steady state with an attendant spatial growth.

Although the combination of material convection and absolute instability is one way of obtaining a convective instability, it is by no means true that this is the only way in which convective instabilities arise. Convective instabilities or amplifying waves often result when a stream interacts with a fixed structure. This is how amplifying waves are obtained in a traveling wave (electron beam) tube. A beam of electrons is coupled to a fixed electromagnetic transmission line. Similarly, beams of electrons or holes can couple to solid-state crystal structures to produce amplifying waves. These systems are more complicated than those introduced in this section because they involve more than two waves. Not only do the beams support waves, but so also do the fixed structures. Here we can illustrate this class of phenomenon by coupling the moving continuum to a fixed structure that does not support waves—simply a resistive wall. In fact, resistive wall instabilities are also found in electron beam devices and particle accelerators.†

With the developments of Section 10.1.4 in view, it is a simple matter to illustrate how convection, in conjunction with the damping, can produce wave amplification. Consider once again the situation in which the string is

* For a general discussion of this topic see A. Bers and R. J. Briggs, "Criteria for determining absolute instabilities and distinguishing between amplifying and evanescent waves," *Bull. Amer. Phys. Soc.*, Ser 2, **9**, 304 (1964) or R. J. Briggs, *Electron-Stream Interaction With Plasmas*, M.I.T. Press, Cambridge, Mass., 1964, pp. 8–46.

† F. H. Clauser, *Symposium on Plasma Dynamics*, Addison-Wesley, Reading, Mass., 1960, pp. 78–118.

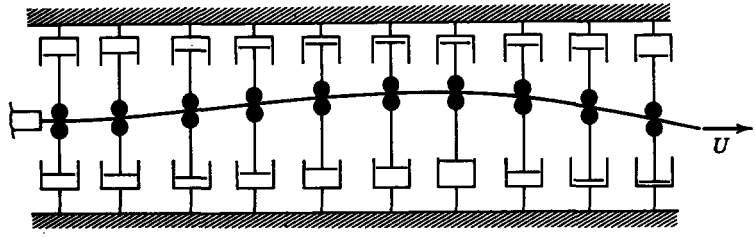

Fig. 10.2.17 The string moves unimpeded in the x-direction with the velocity U, and transverse motions are retarded by dashpots that interact with the string through rollers. The dashpots are fixed to the laboratory frame of reference.

immersed in a viscous liquid. Now, however, the string has a longitudinal velocity U. We assume that the convection of the string in the x-direction is unimpeded by the viscous fluid, even though the transverse motions lead to transverse viscous retarding forces. For conceptual purposes it is helpful to think of the system as being equivalent to that shown in Fig. 10.2.17.

The damping remains in the fixed frame. This means that the effect of the string motion is not simply accounted for by replacing time derivatives in (10.1.33) with convective derivatives, as would be appropriate with the total system in motion. We do, however, know the equation of motion for the string alone (10.2.8). Because the damping force does not depend on the motions, it remains as given by (10.1.32). Hence the equation of motion is (10.1.33) with the second time derivative (acceleration term) replaced by the second convective derivative but with the damping term left unaltered.

$$\left(\frac{\partial}{\partial t} + U\frac{\partial}{\partial x}\right)^2 \xi = v_s^2 \frac{\partial^2 \xi}{\partial x^2} - \nu \frac{\partial \xi}{\partial t}. \tag{10.2.39}$$

As in Section 10.1.4, the wavefront velocity v_s and damping frequency ν are

$$v_s = \left(\frac{f}{m}\right)^{1/2},$$

$$\nu = \frac{B}{m}.$$

It follows from (10.2.39) that traveling wave solutions must satisfy the dispersion equation

$$(\omega - kU)^2 = v_s^2 k^2 + j\omega\nu, \tag{10.2.40}$$

which has the same form as (10.1.36), except that the ω on the left has been replaced by $\omega - kU$. Now, this dispersion equation, like others introduced in this and the preceding section, is simply quadratic in ω and k. Hence we

can solve for either ω or k. Observe first that $\omega(k)$ is

$$\omega = kU + \frac{j\nu}{2} \pm \left[\left(kU + \frac{j\nu}{2}\right)^2 - (U^2 - v_s^2)k^2\right]^{1/2}. \qquad (10.2.41)$$

If U exceeds v_s, this result shows that for real values of k there are negative imaginary values of ω. The ω-k plot, which shows complex values of ω for real values of k, is sketched in Fig. 10.2.18. This plot should be compared with Fig. 10.1.19 to appreciate the effect of convection. The convection is responsible for replacing the damping found (in Section 10.1.4) with $U < v_s$ by an instability. It would be erroneous, however, to assume on the basis of (10.2.41) that deflections of the string would become unbounded with time at a fixed position x. As in Section 10.2.3, the fact that U exceeds v_s requires that two upstream boundary conditions be imposed. In a manner similar to that discussed in Section 10.2.1*b*, the response to initial conditions vanishes in a finite time at a given position. Hence a sinusoidal steady state can be established, and the corresponding mathematical solution is found by solving (10.2.40) for k as a function of ω.

$$k = \frac{\omega U \pm \sqrt{v_s^2\omega^2 + (U^2 - v_s^2)(j\omega\nu)}}{(U^2 - v_s^2)}. \qquad (10.2.42)$$

This dispersion equation is shown in Fig. 10.2.19, in which complex values of k are shown for real values of ω. Note that the phase velocity of both waves is now downstream. More significant is the fact that because $U > v_s$ the wave with a positive imaginary wavenumber grows spatially. With the

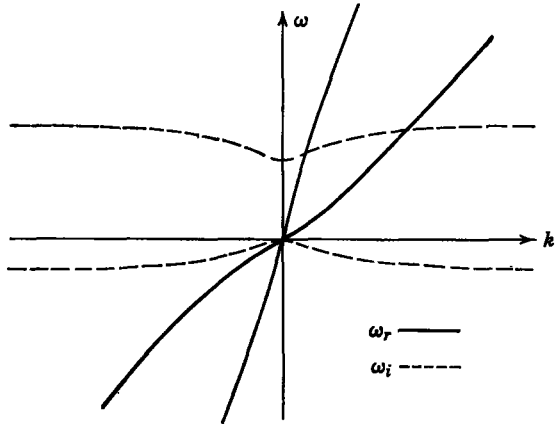

Fig. 10.2.18 Dispersion equation for resistive wall instability. Complex values of ω are shown for real values of k. Although this plot indicates that the string deflections are unstable, the instability is exhibited as a growth in space rather than in time.

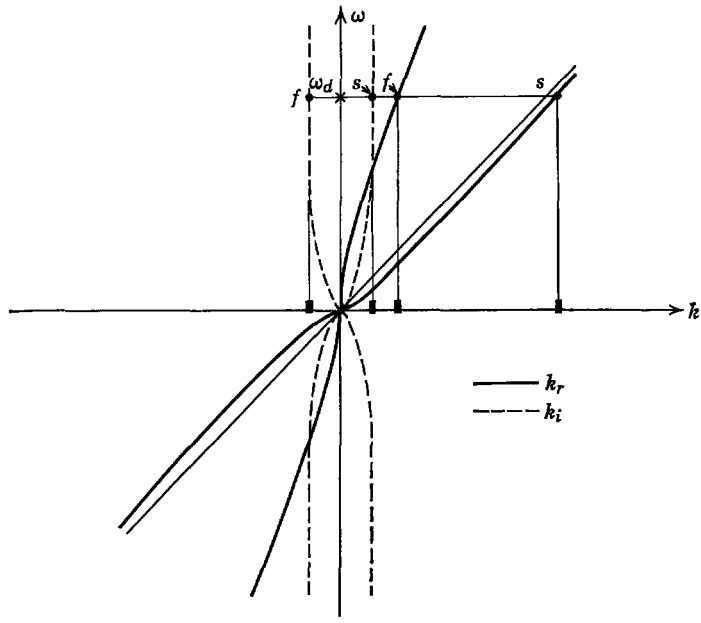

Fig. 10.2.19 Dispersion relation for resistive wall instability. Complex values of k are shown as functions of real values of ω. The effect of convection is apparent if this plot is compared with that shown in Fig. 10.1.17 (where $U = 0$).

damping removed, this is the wave that tries to buck the convection and, because $U > v_s$, propagates slowly downstream. The amplifying slow wave is denoted by (s) in Fig. 10.2.19; the spatially decaying fast wave is labeled (f). This amplifying wave has been termed a resistive wall instability because it is often found in electron beam devices when the beam is coupled to a resistive wall. The mechanical dampers might also be viewed as a resistive wall. The same effect as the dampers, however, is produced by coupling the continuum through a magnetic field to a dissipative structure, as shown in Example 10.1.3. With motion, that example quite literally illustrates a resistive wall instability, as discussed in the following example.

Example 10.2.4. Consider once again the perfectly conducting membrane shown in Fig. 10.1.7. Recall that the membrane is immersed in a longitudinal magnetic field that is uniform when the membrane is undeflected. Because the edges of the membrane make contact with side walls, which in turn form electric circuits above and below the membrane, deformations are accompanied by currents that tend to conserve the total flux above and below the membrane. We consider here the effect of convection when the resistance of the walls is so high that the self-inductance of the external current loops is unimportant. This limit was discussed in Example 10.1.3, in which it was found that the wall had the effect of damping the transverse motions.

We now introduce the additional complication that the membrane is moving in the x-direction with a velocity $U > v_s$. The resistive walls remain fixed. Consequently, the equation of motion, which for the membrane without convection takes the form of (e) in Example 10.1.3, becomes

$$\left(\frac{\partial}{\partial t} + U\frac{\partial}{\partial x}\right)^2 \xi = v_s^2 \frac{\partial^2 \xi}{\partial x^2} - \nu \frac{\partial \xi}{\partial t}, \tag{a}$$

where $v_s = \sqrt{S/\sigma_m}$ and $\nu = 2\sigma_s(\mu_0 H_0)^2/\sigma_m$. The left-hand side of this equation reflects the effect of convection on the moving membrane, whereas the damping force on the right remains unaffected. This can be shown by using a contour of integration for Faraday's law [contour (a) or (b) in Fig. 10.1.8] just as in Example 10.1.1 but with the segment through the membrane moving in the x-direction with velocity U. Because the membrane is perfectly conducting $E' = 0$ over that segment and, moreover, there is no addition to the rate of change of the flux linked by the contour.

Because (a) has the same form as (10.2.39), we conclude that the moving membrane coupled to the resistive wall is subject to convective instability.

A physical picture of the variety of convective instability studied in Section 10.2.3 is not difficult to obtain. In a frame of reference moving with the string the amplitude becomes unbounded with time for the same reason that it does when the string is stationary. Without the motion, however, the system we consider in this section is stable. In fact, we normally think of damping as a stabilizing influence. Yet the combination of the convection and damping leads to instability!

An understanding of this instability can be obtained by considering string deflections in a frame of reference moving with the string, represented by Fig. 10.2.20. In this frame the string appears to have no longitudinal velocity but the resistive wall (the dampers) moves in the $-x$-direction with the velocity U. The viscous force, expressed in terms of the coordinates (x', t'), is

$$S_z = -B\left(\frac{\partial}{\partial t'} - U\frac{\partial}{\partial x'}\right)\xi. \tag{10.2.43}$$

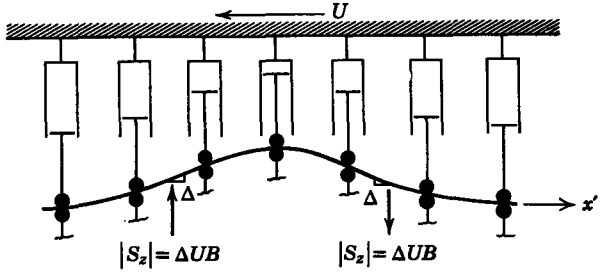

Fig. 10.2.20 A pulse is initially stationary when viewed from a frame moving with the string. Then, as the dashpots move to the left, they produce a force with a sign determined by the slope of the string.

The first term, familiar as the retarding force due to the transverse velocity, will always act in a direction opposite to that in which ξ is temporally increasing. The second term enters because, with the dashpots moving to the left, the plungers must change their positions at a rate determined by U and the slope of the string; for example, suppose that the pulse is instantaneously stationary in the x'-frame. The moving dampers will tend to increase the deflection when the slope is positive and decrease it when the slope is negative. Hence the back of the pulse tends to grow, whereas the front of the pulse is flattened by the moving dampers. As the regions of positive slope grow, they move to the right when viewed in the fixed frame, and we have the ingredients of a convective instability.

10.3 PROPAGATION

The situations developed in the last two sections provide an ample background for embarking on a discussion of wave propagation in distributed systems exhibiting dispersive waves. In retrospect, it is clear that we have either confined attention to sinusoidal steady-state behavior or, when transient conditions were considered, to nondispersive waves (with and without convection); for example, in Section 10.2.1 we used the moving string without external forces to illustrate how conditions of causality restrict the boundary conditions that can be imposed. Throughout our discussion we have assumed that even with dispersive waves (an extreme example is the convective instability) we are justified in imposing two upstream conditions if $U > v_s$ and one upstream and one downstream condition if $U < v_s$. In fact, our assumption is correct but this is not obvious. One way to ask the question is this: if a pulse is initiated on the string, does any part of it propagate upstream? If so, we must impose a downstream boundary condition. We have illustrated that the phase velocity of a periodic wave is not a reliable basis for answering this question. We begin by reviewing this point.

10.3.1 Phase Velocity

Suppose that we restrict attention to waves that are purely sinusoidal in space and time so that both ω and k are real. Then points of constant phase propagate with the velocity,

$$v_p = \frac{\omega}{k}. \tag{10.3.1}$$

On an ω-k plot this phase velocity has the geometrical significance shown in Fig. 10.3.1. As long as we are dealing with nondispersive waves, the phase velocity is identical with the velocity of propagation of wavefronts, which is

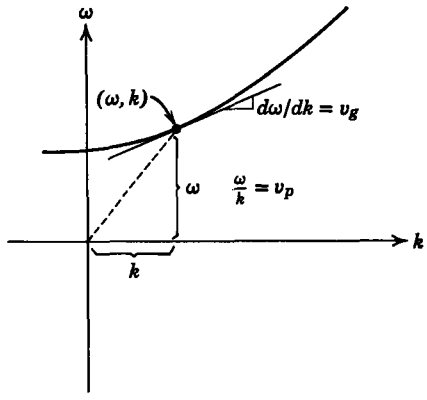

Fig. 10.3.1 The slope of the line joining the point (ω, k) and the origin is the phase velocity. The tangent of the ω-k curve at this same point is the group velocity.

why the ω-k plots of Fig. 10.2.8 appear so similar to the characteristic lines in the x-t plane, shown in Fig. 10.2.2. For the moving string without external forces wavefronts propagate with the velocities $U \pm v_s$ (the slopes of the characteristics), and these are the phase velocities of the fast and slow waves in the sinusoidal steady state.

It would be an assumption to say that the phase velocity is always the velocity of propagation of a wavefront, and we have examples from which to choose to show that this assumption is not well founded. In the case in which we have the possibility of evanescent waves (Fig. 10.1.3) the phase velocity approaches infinity as $k \to 0$, and it is certainly unreasonable to assume that a pulse will propagate with this velocity. Even more obvious, since v_p is a function of ω or k, which value do we select as the velocity of a wavefront? Considerations of this type lead us to consider other velocities such as the group velocity.

10.3.2 Group Velocity

The group velocity of waves with frequencies in the neighborhood of ω is defined as

$$v_g = \frac{d\omega}{dk} \tag{10.3.2}$$

or as the slope shown in Fig. 10.3.1. The velocity v_g has the physical significance of being the velocity of propagation of a group of waves with essentially the same wavenumber and frequency.

A straightforward way to show the dynamical meaning of the group velocity is to consider an excitation in the form of

$$\xi(0, t) = \xi_0[1 + \cos \omega_m t] \cos \omega_s t, \tag{10.3.3}$$

which is recognized as amplitude modulation of a sinusoidal excitation with a frequency ω_s. The amplitude of the excitation varies between $2\xi_0$ and 0 with a frequency ω_m. The nature of the resulting waves is most easily demonstrated if it is assumed that the string has an infinite extent in the x-direction and excitations are applied in such a way that only one of the two possible waves is excited.

A trigonometric identity* converts (10.3.3) to

$$\xi(0, t) = \xi_0 \cos \omega_s t + \tfrac{1}{2}\xi_0[\cos(\omega_s + \omega_m)t + \cos(\omega_s - \omega_m)t], \quad (10.3.4)$$

which is the familiar statement that a sinusoidal signal with a frequency ω_s, amplitude modulated at the frequency ω_m, is equivalent to three signals with frequencies ω_s, $\omega_s + \omega_m$, and $\omega_s - \omega_m$. Because the wavenumber depends on the frequency of excitation, each of the terms in (10.3.4) excites a wave with a different wavelength.

Attention is confined to situations in which $\omega_m \ll \omega_s$. Then the wavenumbers corresponding to $\omega_s \pm \omega_m$ are given approximately by $k = k_s \pm \omega_m/v_g$. Figure 10.3.2 shows graphically the relationship between frequencies and wavenumbers. The wavenumbers adjacent to k_s are obtained by assuming that in the vicinity of the point (ω_s, k_s) the dispersion equation can be approximated by a straight line whose slope v_g is the same as that in the ω-k plot.

If only one wave is excited, the first term in (10.3.4) gives rise to the string deflections

$$\xi(x, t) = \xi_0 \cos(\omega_s t - k_s x). \quad (10.3.5)$$

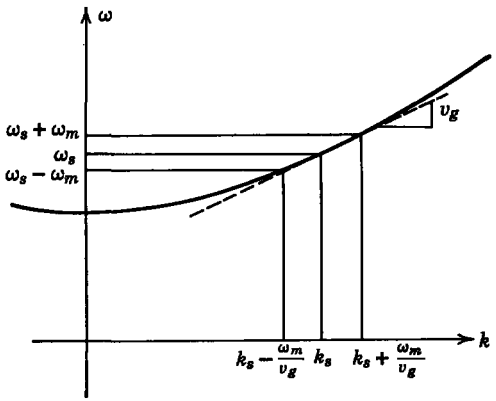

Fig. 10.3.2 For waves with very nearly the same frequency the group velocity v_g can be used to represent the dispersion.

* $\cos A \cos B = \frac{1}{2}[\cos(A + B) + \cos(A - B)]$.

The excitations at the sum and difference frequencies $\omega_s \pm \omega_m$ lead to similar waves with wavenumbers $k_s \pm \omega_m/v_g$ which are now superimposed to find waves resulting from the total excitation.

$$\xi(x, t) = \xi_0 \cos(\omega_s t - k_s x) + \tfrac{1}{2}\xi_0 \cos\left[(\omega_s t - k_s x) + \omega_m\left(t - \frac{x}{v_g}\right)\right] + \tfrac{1}{2}\xi_0 \cos\left[(\omega_s t - k_s x) - \omega_m\left(t - \frac{x}{v_g}\right)\right]. \qquad (10.3.6)$$

We again use a trigonometric identity* to write this expression as

$$\xi(x, t) = \xi_0\left[1 + \cos\omega_m\left(t - \frac{x}{v_g}\right)\right]\cos(\omega_s t - k_s x), \qquad (10.3.7)$$

so that it is clear that displacements take the form of a wave, with a frequency ω_s, which is modulated by another wave with a frequency ω_m. At an instant of time the string appears as shown in Fig. 10.3.3. A point of constant phase (a zero crossing) moves to the right with the phase velocity ω_s/k_s. By contrast, a point of constant phase on the *envelope* moves to the right with group velocity v_g. The group velocity is therefore interpreted as the velocity at which the group of waves, defined by the envelope, propagates in the x-direction. Note that because the phase and group velocities are different the waves will appear to move with respect to the envelope. In the ω-k plot of Fig. 10.1.3 (which was the subject of Section 10.1.2) the group velocity is less than the phase velocity; hence the phases move downstream more rapidly than the envelope.

Our analysis presumes that the wavetrain of Fig. 10.3.3 extends to infinity in the x-direction and that the sinusoidal steady state has been established.

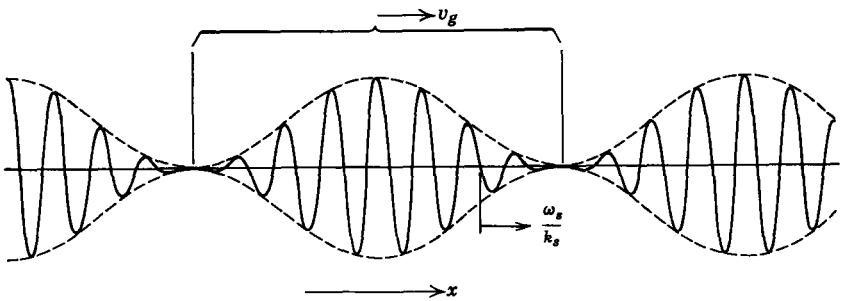

Fig. 10.3.3 Wavetrain amplitude modulated at a frequency that is much lower than the wave frequency. The string appears as shown by the solid line at an instant in time.

* $\cos(A + B) = \cos A \cos B - \sin A \sin B$.

Hence it does not directly indicate the manner in which a pulse propagates. Suppose, however, that we were concerned with the propagation of the pulse obtained by eliminating all the wavetrain except the one full pulse in Fig. 10.3.3 bounded on either end by the nulls in the envelope. It is not possible to describe this signal as the superposition of three sinusoidal signals, but, if we take the Fourier transform of this signal*

$$\hat{\xi}(\omega, k) = \int_{-\infty}^{+\infty} \int_{-\infty}^{+\infty} \xi(x, t) e^{-j(\omega t + kx)}\, dx\, dt, \tag{10.3.8}$$

we find that its major frequency and wavenumber components are in the neighborhood of (ω_s, k_s). Provided that the spectrum of frequency (hence, because of the dispersion equation, the wavenumbers) of a pulse is confined essentially to a small region, the group velocity gives a measure of the velocity of the pulse. In terms of (x, t) this pulse is almost a pure sinusoid, except for a slowly varying envelope.

From this discussion it should be clear that the group velocity can be used to ascertain the "over-all" velocity of a high-frequency pulse, but because only those portions of the pulse that have a slowly varying envelope can be so described the group velocity is not the velocity of a wavefront. As we have seen, in the region of a wavefront deflections vary rapidly and, in fact, can be discontinuous. Hence the group velocity is not appropriate for determining the boundary conditions consistent with causality. As for the phase velocity, we might have suspected this limitation from the outset, since the group velocity is a function of ω or k. We hope that the question whether two upstream boundary conditions or one upstream and one downstream boundary condition should be used is independent of the dynamical quantities ω and k.

We must make one further reservation concerning the physical significance of the group velocity. It does not give a reliable indication of pulse propagation, even subject to the limitations outlined, if the system is unstable.† This is true whether the instability is convective or nonconvective. We have not attempted to prove this here but have used the examples of the two previous sections to make this further limitation plausable. The ω-k plot for the unstable string is shown in Fig. 10.1.11. Note that as $k \to k_c$ the group velocity approaches infinity. It would be unreasonable to conclude that a pulse could be made to propagate with an arbitrarily large velocity.

With convection (Fig. 10.2.13) the insignificance of v_g becomes even more apparent. In this case we can select ω or k to give any value of v_g, positive,

* R. G. Brown and J. W. Nilsson, *Introduction to Linear Systems Analysis*, Wiley, New York, 1962, p. 209.

† R. J. Briggs, *Electron-Stream Interaction With Plasmas*, M.I.T. Press, Cambridge, Mass., 1964, p. 33.

negative, zero, and infinite! From this it is clear that the notion of a group velocity must be used with care. Cases in which instability can develop make this particularly clear. A pulse of finite extent contains all wavenumbers. The group velocity is meaningful if the dynamics are dominated by signal components confined to a small range of wavenumbers. The wavenumber spectrum that is unstable tends to amplify and cannot be ignored.

10.3.3 Characteristics and the Velocity of Wavefronts

Wavefronts propagate along the characteristic lines in the x-t plane. This is illustrated by considering a convecting string with a destabilizing force, discussed in Section 10.2.3. The equation of motion (10.2.33) is

$$\left(\frac{\partial}{\partial t} + U\frac{\partial}{\partial x}\right)^2 = v_s^2\left[\frac{\partial^2 \xi}{\partial x^2} + k_c^2 \xi\right]. \tag{10.3.9}$$

A general discussion of how characteristics can be found for a given differential equation would lead us afield.* Thus for our purposes we view the characteristics as a convenient transformation of independent variables from the coordinate system (x, t) to the new coordinate system (α, β) according to the relations

$$\alpha = x - (U + v_s)t, \tag{10.3.10}$$

$$\beta = x - (U - v_s)t. \tag{10.3.11}$$

The resulting simplification in the differential equation and its interpretation and solution justify the transformation.

Note that the characteristic lines are the same as those used in Sections 9.1.1*a* and 10.2.1, in which nondispersive waves were studied.

To write (10.3.9) in terms of the new independent variables α and β, we use (10.3.10) and (10.3.11) to evaluate the partial time derivative as

$$\frac{\partial \xi}{\partial t} = \frac{\partial \xi}{\partial \alpha}\frac{\partial \alpha}{\partial t} + \frac{\partial \xi}{\partial \beta}\frac{\partial \beta}{\partial t} = -(U + v_s)\frac{\partial \xi}{\partial \alpha} - (U - v_s)\frac{\partial \xi}{\partial \beta}. \tag{10.3.12}$$

In a similar manner

$$\frac{\partial \xi}{\partial x} = \frac{\partial \xi}{\partial \alpha}\frac{\partial \alpha}{\partial x} + \frac{\partial \xi}{\partial \beta}\frac{\partial \beta}{\partial x} = \frac{\partial \xi}{\partial \alpha} + \frac{\partial \xi}{\partial \beta}. \tag{10.3.13}$$

* For a general discussion of the method of characteristics see, for example, R. Courant and K. O. Friedrichs, *Supersonic Flow and Shock Waves*, Interscience, New York, 1948, Chapters, II, III, and IV.

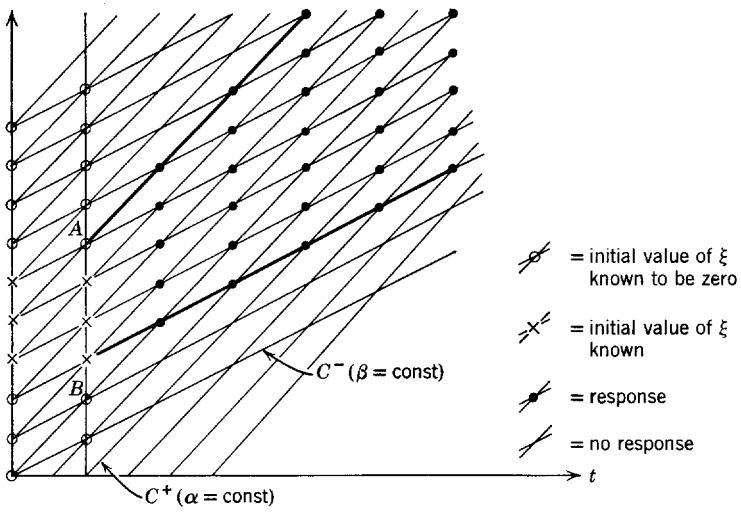

Fig. 10.3.4 Grid of characteristics in the x-t plane for $U > v_s$.

A repetition of the process and transformation of the derivatives in (10.3.9) yields

$$\frac{\partial^2 \xi}{\partial \alpha \, \partial \beta} + \frac{k_c^2}{4} \xi = 0. \tag{10.3.14}$$

This form of the equation of motion makes it particularly clear why $\xi(\alpha)$ and $\xi(\beta)$ are both solutions when $k_c = 0$.

In the x-t plane the C^+ characteristics (α = constant) are parallel straight lines with the slope $U + v_s$ and the C^- characteristics (β = constant) are parallel straight lines with slope $U - v_s$. These characteristics fill the x-t plane as illustrated in Fig. 10.3.4. In Fig. 10.3.5 the four intersections of two pairs of closely spaced characteristics are shown. This configuration can be used to obtain an approximate integral of (10.3.14). The solution thus obtained yields both numerical answers and insight into how disturbances propagate.

We assume that the displacements at points A, B, and D in Fig. 10.3.5 are

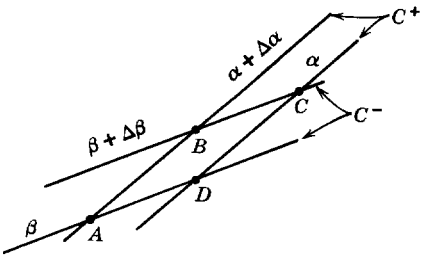

Fig. 10.3.5 Intersections A, B, C, and D of two pairs of characteristics with $U > v_s$.

known and we wish to evaluate the displacement at point C (at some future time at a downstream point) When $\Delta\alpha$ and $\Delta\beta$ are small, we can write

$$\frac{\partial\xi}{\partial\alpha}(\alpha, \beta + \Delta\beta) \approx \frac{\xi(\alpha + \Delta\alpha, \beta + \Delta\beta) - \xi(\alpha, \beta + \Delta\beta)}{\Delta\alpha} = \frac{\xi_B - \xi_C}{\Delta\alpha}, \tag{10.3.15}$$

$$\frac{\partial\xi}{\partial\alpha}(\alpha, \beta) \approx \frac{\xi(\alpha + \Delta\alpha, \beta) - \xi(\alpha, \beta)}{\Delta\alpha} = \frac{\xi_A - \xi_D}{\Delta\alpha} \tag{10.3.16}$$

Continuation of this process one step further yields

$$\frac{\partial^2\xi}{\partial\alpha\,\partial\beta}(\alpha, \beta) \approx \frac{(\partial\xi/\partial\alpha)(\alpha, \beta + \Delta\beta) - (\partial\xi/\partial\alpha)(\alpha, \beta)}{\Delta\beta} \tag{10.3.17}$$

or

$$\frac{\partial^2\xi}{\partial\alpha\,\partial\beta}(\alpha, \beta) \approx \frac{(\xi_B - \xi_C) - (\xi_A - \xi_D)}{\Delta\alpha\,\Delta\beta} \tag{10.3.18}$$

The use of this approximate derivative in (10.3.14) and solution for ξ_C yield the desired result*:

$$\xi_C = \xi_B + \xi_D - \xi_A\left(1 - \frac{k_c^2\Delta\alpha\,\Delta\beta}{4}\right). \tag{10.3.19}$$

The solution to our problem $\xi(x, t)$ or $\xi(\alpha, \beta)$ can be viewed in a three-dimensional plot as the height of a surface above the x-t or α-β plane. Hence the initial conditions $\xi(x, 0)$ and $(\partial\xi/\partial t)(x, 0)$ give the height of the surface and its slope in the t-direction near the x-axis In approximate terms this is equivalent to giving the value of ξ at the intersections of characteristics on and adjacent to the x-axis, as shown in Fig. 10.3.4. From this initial data (10.3.19) can be used to find ξ at the next (third) vertical column of intersections in the x-t plane of Fig. 10.3.4. These values, in turn, can be used to calculate ξ at the next vertical column of intersections.

In Fig. 10.3.4 we have indicated an initial pulse by an $\times$ at the characteristic intersections; that is, ξ has some finite value at these points. The initial displacements are zero at intersections marked $\circ$. The approximate solution (10.3.19) of the equation of motion then shows that there is no deflection ξ except possibly at the intersections marked. Hence the initial deflection in the interval AB results in wavefronts propagating within the region in the x-t plane bounded by the C^+ characteristic originating at A and the C^- characteristic originating at B. Because $U > v_s$, the initial disturbance propagates downstream, as we assumed in Section 10.2.3.

* Note that the term $k_c^2\xi/4$ has been approximated by $k_c^2\xi_A/4$. The error implicit in this approximation becomes more and more significant as iterative use is made of (10.3.19).

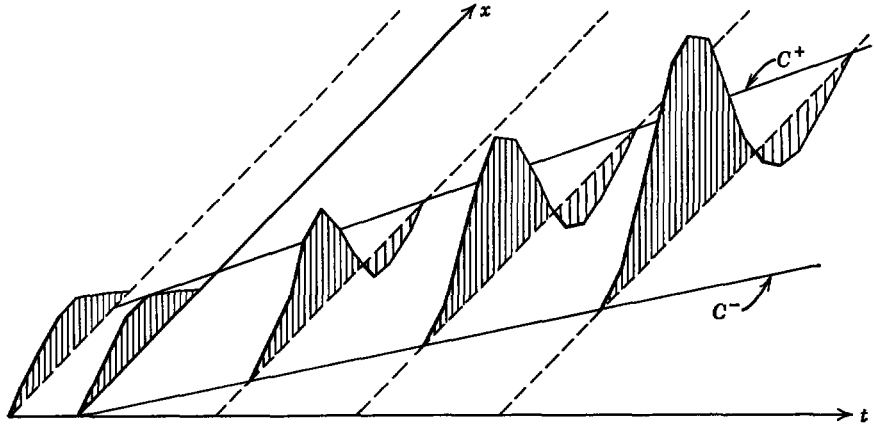

Fig. 10.3.6 Transient deflection following the initiation of a static pulse on a moving unstable string ($U = 3v_s$). The deflection is convectively unstable.

It can be seen that as long as both families of characteristics go downstream as t increases, a driving condition (along the t-axis) that involves two conditions on ξ is no different mathematically from the two initial conditions along the x-axis considered here.

Our approximate solution for the equation of motion shows also that waves are likely to grow. Consider the case in which points A, B, and D all have the deflection $\xi = \xi_0$ (the initial condition of a static, spatially uniform pulse of height ξ_0). Then

$$\xi_C = \xi_0\left(1 + \frac{k_c^2 \Delta\alpha\, \Delta\beta}{4}\right), \tag{10.3.20}$$

and the amplitude has increased by the time the pulse reaches the point C.

A numerical example is shown in Fig. 10.3.6. For all values of $t < 0$ the initial pulse has the same x-dependence, as shown; that is, the pulse is initially static. For this transient solution seven grid points have been used to describe the initial pulse and $k_c^2 \Delta\alpha\, \Delta\beta/4 = 0.1$. The pulse grows in amplitude but propagates downstream. At any given position x, the deflection remains bounded. These are the salient features of a convective instability.

The leading edge of the pulse becomes inverted, as is expected from the results found in Example 10.2.1 for an initially static pulse in a stable situation but with $U > v_s$ (see Fig. 10.2.5).

10.4 DYNAMICS IN TWO DIMENSIONS

The techniques described for dealing with continuum electromechanical interactions are not limited to a single space dimension, as implied by the

examples given. In this section we consider several cases that show how the dispersion equation also accounts for motions that depend on two or three dimensions.

10.4.1 Membrane Dynamics: Two-Dimensional Modes

A classic demonstration of wave propagation, as it depends on two dimensions, is given by considering a membrane. In the absence of external surface forces the equation of motion (as derived in Section 9.2) is

$$\frac{\partial^2 \xi}{\partial t^2} = v_s^2 \left(\frac{\partial^2 \xi}{\partial x^2} + \frac{\partial^2 \xi}{\partial y^2} \right), \tag{10.4.1}$$

where

$$v_s = \left(\frac{S}{\sigma_m} \right)^{1/2}.$$

Solutions to this equation have the general form

$$\xi = \text{Re}\, \hat{\xi}\, e^{j(\omega t - k_x x - k_y y)}, \tag{10.4.2}$$

where we must now distinguish between the wavenumber k_y, which indicates the dependence on y, and k_x, which indicates the x-dependence. Substitution of (10.4.2) into (10.4.1) shows that ω is related to k_y and k_x by the dispersion equation

$$\omega^2 = v_s^2 (k_x^2 + k_y^2). \tag{10.4.3}$$

Now suppose that the edges of the membrane at $y = 0$ and $y = b$ are fixed, as shown in Fig. 10.4.1; that is, deflections satisfy the boundary conditions

$$\xi(x, 0, t) = 0, \tag{10.4.4}$$

$$\xi(x, b, t) = 0. \tag{10.4.5}$$

Any linear combination of solutions with the traveling waveform of (10.4.2) and (ω, k_x, k_y) satisfying the dispersion equation (10.4.3) will satisfy the equation of motion. In particular, we take the linear combination

$$\xi = \text{Re}\, [\hat{\xi}_1 \sin k_y y + \hat{\xi}_2 \cos k_y y] e^{j(\omega t - k_x x)}. \tag{10.4.6}$$

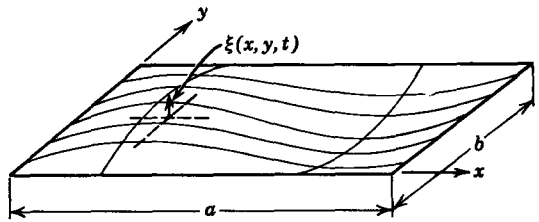

Fig. 10.4.1 Membrane having static equilibrium in x-y plane.

Here it is more convenient to write the complex exponential dependence on y in terms of trigonometric functions because it is clear from (10.4.4) that $\hat{\xi}_2 = 0$. Moreover, if boundary condition (10.4.5) is to be satisfied,

$$k_y = \frac{n\pi}{b}. \tag{10.4.7}$$

We have found that modes satisfying the transverse boundary conditions take the form

$$\xi(x, y, t) = \text{Re } \hat{\xi}_1 \sin\left(\frac{n\pi y}{b}\right) e^{j(\omega t - k_x x)}, \tag{10.4.8}$$

where in view of (10.4.7) the dispersion equation relating (ω, k_x) for any given mode (n) is

$$\omega^2 = v_s^2\left[k_x^2 + \left(\frac{n\pi}{b}\right)^2\right]. \tag{10.4.9}$$

This expression takes the same form as the dispersion equation (10.1.7) developed in Section 10.1.2, in which evanescent waves were studied. Hence for each mode the dispersion equation takes the geometrical form shown in Fig. 10.1.3. The cutoff frequency is [compare (10.1.7) and (10.4.9)]

$$\omega_c^2 = v_s^2\left(\frac{n\pi}{b}\right)^2. \tag{10.4.10}$$

Suppose that the membrane is driven at one end by a sinusoidal steady-state excitation with a frequency $\omega = \omega_d$. Then we have found that the response is composed of an infinite number of waves, each having n half-wavelengths in the y-direction. If $\omega_d < \omega_c$, the waves in the x-direction are evanescent. Hence for any given driving frequency a finite number (or, if $\omega_d < v_s\pi/b$, none) of the waves will propagate (have real values of k_x), whereas all others will be evanescent.

The evanescent or cutoff waves are a consequence of the stiffening effect of the transverse boundaries. Curvature of the membrane leads to an elastic restoring force (remember the membrane is under the longitudinal and transverse tension S). Because of the transverse boundaries, the membrane cannot deform without incurring a curvature. Waves are cutoff if the elastic restoring force resulting from this curvature (proportional to k_y^2) outweighs the effect of inertia.

If, in addition to the boundary conditions already imposed, the membrane is fixed at $x = 0$ and $x = a$, it is appropriate to look for the natural modes or eigenmodes of the membrane. This time we take a linear combination of solutions in the form of (10.4.8) to determine that

$$\xi(x, y, t) = \text{Re } \hat{\xi}_3 \sin\left(\frac{n\pi y}{b}\right) \sin\left(\frac{m\pi x}{a}\right) e^{j\omega t}, \tag{10.4.11}$$

where k_x has been made $m\pi/a$; hence the dispersion equation gives the eigenfrequencies as

$$\omega_{mn} = \pm v_s\left[\left(\frac{n\pi}{b}\right)^2 + \left(\frac{m\pi}{a}\right)^2\right]^{1/2}. \tag{10.4.12}$$

The indices (n, m) can have any integer values. Note, however, that if both n and m are zero the solution is trivial, since (10.4.11) then shows that the deflections are zero.

The eigenfrequencies of the membrane constrained on all of its edges have the same physical significance as those of the simple string; for example, if the membrane is driven in some manner by a sinusoidal steady-state forcing function, there will be a resonance in the response at the eigenfrequencies, with the membrane assuming the corresponding deflections given by (10.4.11). Figure 10.4.2 is a graphic example of membrane modes $n = 1$. A soap film is attached to a rectangular wire frame by surface tension. Each of the modes is then excited by vibrating the frame by hand.

10.4.2 Moving Membrane: Mach Lines

We have seen that convection can have a marked effect on the dynamics of one-dimensional continua. This is especially true if the motion is supersonic, in the sense that the convection velocity (U) is greater than the propagation velocity (v_s) of small disturbances. The moving membrane provides an opportunity to determine how these effects are displayed in two dimensions.

With the membrane moving in the x-direction with the velocity U, the equation of motion is

$$\left(\frac{\partial}{\partial t} + U\frac{\partial}{\partial x}\right)^2 \xi = v_s^2\left(\frac{\partial^2 \xi}{\partial x^2} + \frac{\partial^2 \xi}{\partial y^2}\right). \tag{10.4.13}$$

Here we have replaced the time derivative with the convective derivative, as justified in Section 10.2.

Now suppose we consider the case in which the *Mach number* M is greater than unity,

$$M = \frac{U}{v_s} > 1, \tag{10.4.14}$$

and in which steady-state conditions prevail ($\partial/\partial t = 0$). Then (10.4.13) becomes

$$(M^2 - 1)\frac{\partial^2 \xi}{\partial x^2} = \frac{\partial^2 \xi}{\partial y^2}. \tag{10.4.15}$$

This expression has the same familiar form as the wave equation. The time dependence, however, has been replaced by a dependence on the second dimension y. With this in mind, we expect that deformations of the membrane,

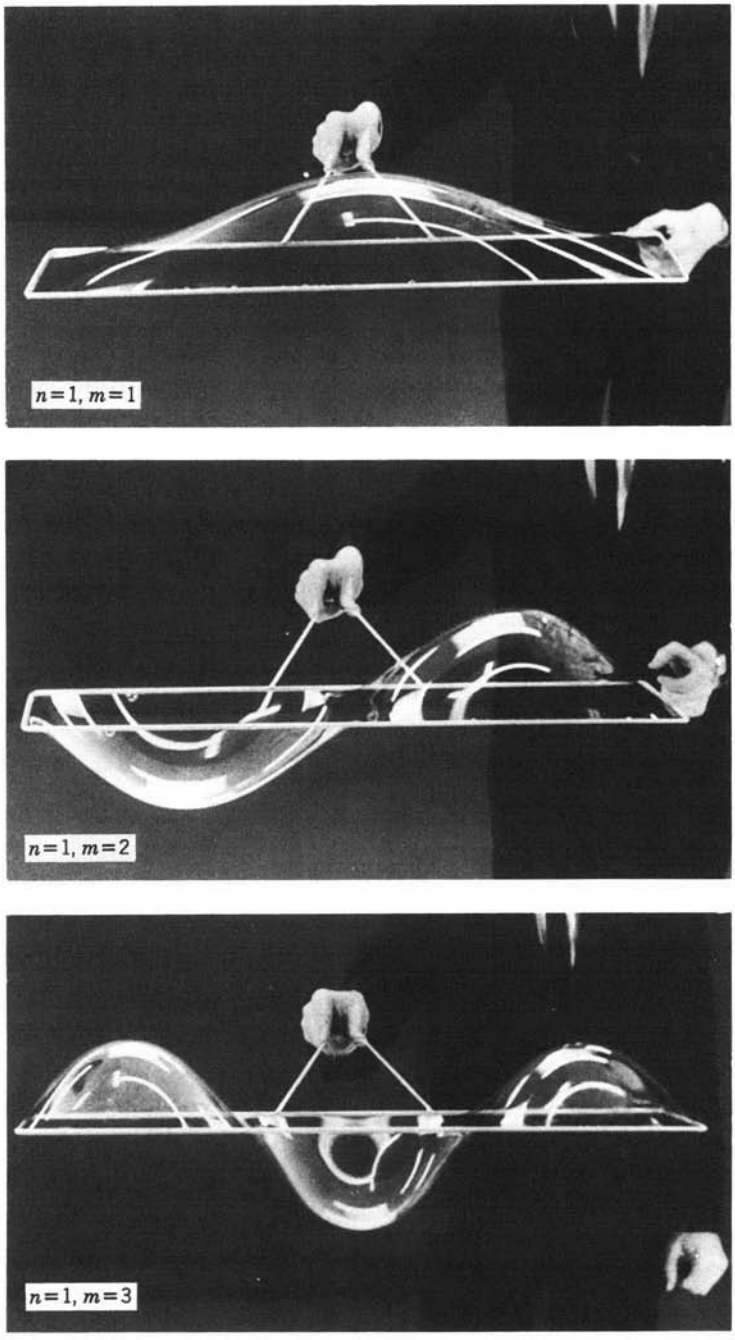

Fig. 10.4.2 Membrane motions illustrated by soap film on a vibrating wire frame. Pictures from film "Soap Film Oscillations." Courtesy of A. M. Hudson, Occidental College and Film Studio, Education Development Center, Inc., Newton, Mass.

as they depend on (x, y), will assume the same wavelike character found in Section 9.1.1*a*.

Solution of (10.4.15) is completely analogous to the solution of the wave equation in (x, t) coordinates. Reference to Section 9.1.1*a* shows that we have solutions

$$\xi = \xi_+(\alpha) + \xi_-(\beta), \tag{10.4.16}$$

where

$$\alpha = x - \sqrt{M^2 - 1}\, y, \tag{10.4.17}$$

$$\beta = x + \sqrt{M^2 - 1}\, y. \tag{10.4.18}$$

The lines α = constant and β = constant are again the characteristic lines along which we expect that the membrane can undergo abrupt deformations. These lines along which the equivalent of wavefronts in the x-y space can exist are referred to as *Mach lines*.* Their physical significance is more apparent in the context of a simple example.

Example 10.4.1. A sheet of molten plastic is to be given the cross-sectional shape shown in Fig. 10.4.3*a*. It is proposed that this be done by ejecting the molten plastic as a sheet

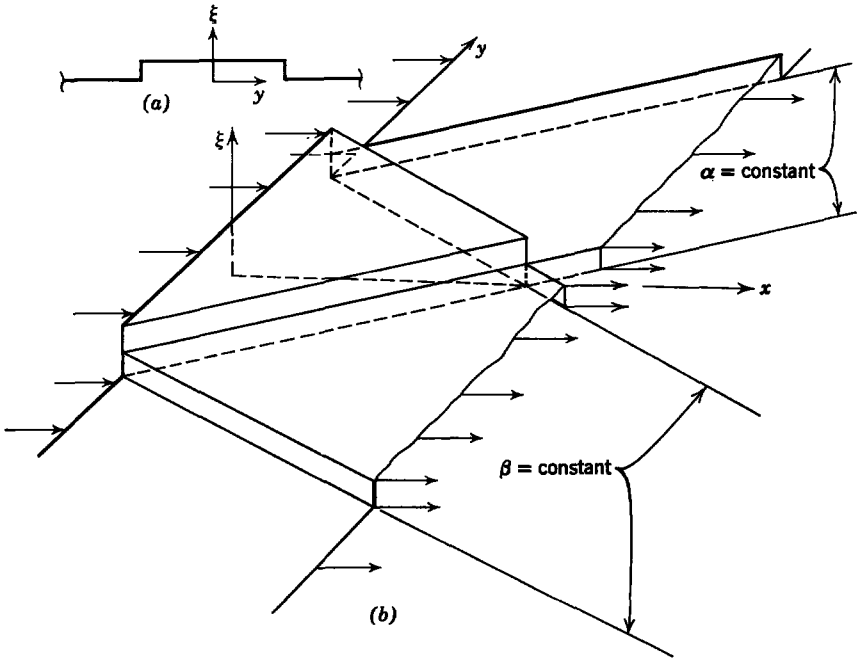

Fig. 10.4.3 (*a*) A membrane is constrained to have the shape shown at $x = 0$; (*b*) the resulting deflections for $M > 1$.

* A. H. Shapiro, *The Dynamics and Thermodynamics of Compressible Fluid Flow*, Ronald, New York, 1953, Vol. I, p. 462.

through an orifice in the shape of Fig. 10.4.3*a*. As long as the sheet is molten and thin, it is reasonable to obtain an idea of the likely success of our method by modeling the sheet as a membrane with $M > 1$ because the effect of surface tension, hence v_s, is small. The membrane is constrained at $x = 0$ so that $\xi(0, y)$ has the form shown in Fig. 10.4.3*a* and

$$\frac{\partial \xi}{\partial x}(0, y) = 0. \tag{a}$$

This problem then reduces to one that is essentially the same as that discussed in Example 9.1.2. The deformations of the membrane, as they depend on (x, y), are shown in Fig. 10.4.3*b*. The pulse that originates at $x = 0$ divides into two pulses that tend toward infinity in the $\pm y$-directions as x increases. On the basis of this finding, we expect that our technique of forming the plastic would not be a good one unless the plastic could be made to solidify within a distance short compared with that required for the pulses to separate from one another.

10.4.3 A Kink Instability

Two-dimensional motions of a wire are very different from those of a membrane and provide an excellent model for demonstrating electromechanical coupling between propagating modes. A wire is shown in Fig. 10.4.4. It is now free to deflect in the x- or y-direction; hence we can, in general, find the wire at the transverse position

$$\boldsymbol{\xi} = u(z, t)\mathbf{i}_x + v(z, t)\mathbf{i}_y. \tag{10.4.19}$$

Note that the motions still involve only two independent variables (z, t) by contrast with the two-dimensional motions of the membrane. Now,

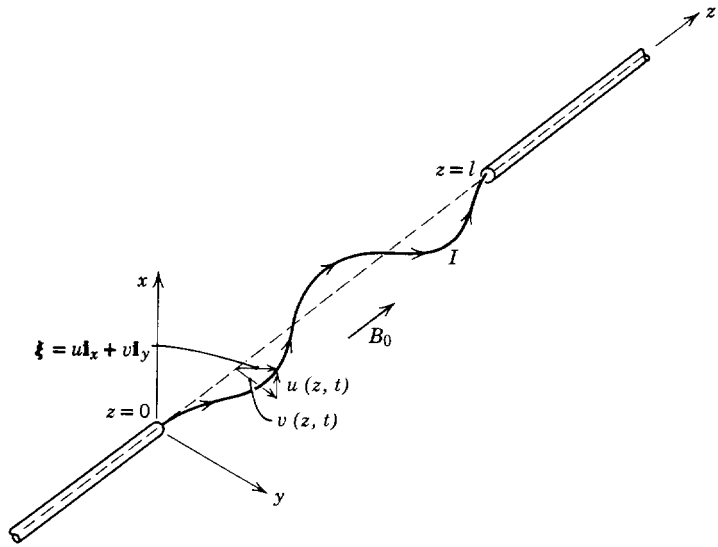

Fig. 10.4.4 A wire stretched along the z-axis.

however, there are two dependent variables $u(z, t)$ and $v(z, t)$, the displacements along the x- and y-axes, respectively.

We have already found that motions in the x- or y-direction are defined by the string equation (Table 9.2). To linear terms deflections v in the y-direction do not produce an x-directed force on the wire, and vice versa; hence the string equation remains valid for two-dimensional motions. A force equation for deflections in the x- and y-directions is

$$m\frac{\partial^2\boldsymbol{\xi}}{\partial t^2} = f\frac{\partial^2\boldsymbol{\xi}}{\partial z^2} + \mathbf{S}. \tag{10.4.20}$$

The external force per unit length $\mathbf{S}$ has components S_x and S_y. With $\mathbf{S} = 0$ motions in the x- and y-directions are uncoupled. In either case they are governed by a simple wave equation and disturbances propagate with the velocity $v_s = \sqrt{f/m}$.

We now use a magnetic field interaction to couple the motions in the x- and y-directions. In the process the continuum model of a constant-current constraint is illustrated.

The elastic wire is assumed to be conducting and is stretched between the pole pieces of a magnet (along the z-axis). As shown in Fig. 10.4.4, a current I is carried by the wire. In static equilibrium this current is in the same direction as an imposed magnetic flux density B_0; hence there is no magnetic force per unit length $\mathbf{I} \times \mathbf{B}_0$. Any slight perturbation of the current path (the wire position), however, will result in a radial component of current, and this component produces an $\mathbf{I} \times \mathbf{B}$ force that tends to rotate the wire about the z-axis. We see that motions of the wire cannot be purely in the x-z or y-z plane but must involve all three space dimensions.

Our constant current approximation is implicit in the statement that the current in the wire has the same direction as the wire. To linear terms we write

$$\mathbf{I} = \mathbf{i}_x\frac{\partial u}{\partial z}I + \mathbf{i}_y\frac{\partial v}{\partial z}I + \mathbf{i}_z I. \tag{10.4.21}$$

Here we have assumed that the cross section of the wire is small enough to make currents induced by the motion negligible. In general, the motion would produce currents that close on themselves in the x-y plane (eddy currents), and they could be crossed with the imposed magnetic field to give a transverse force on the wire. In Section 7.1 we obtained the condition that the currents induced by the motion of a conductor (conductivity σ) in a magnetic field are small if

$$\mathrm{R}_m = \frac{\mu_0\sigma\omega d^2}{2} \ll 1, \tag{10.4.22}$$

where in our case d is the diameter of the wire and ω is the frequency of vibration. Our constant current approximation is the limit of small R_m.

We make the additional assumption that the magnetic flux density B_0 imposed by the external magnet is much larger than the equilibrium flux density generated by the current I. This allows us to compute the force on the wire as

$$\mathbf{S} = \mathbf{I} \times B_0 \mathbf{i}_z \tag{10.4.23}$$

or from Eq. (10.4.21)

$$\mathbf{S} = B_0 I \frac{\partial v}{\partial z} \mathbf{i}_x - B_0 I \frac{\partial u}{\partial z} \mathbf{i}_y. \tag{10.4.24}$$

We now use these forces, and the components of (10.4.20) become

$$\frac{\partial^2 u}{\partial t^2} = v_s^2 \frac{\partial^2 u}{\partial z^2} + \frac{B_0 I}{m} \frac{\partial v}{\partial z}, \tag{10.4.25}$$

$$\frac{\partial^2 v}{\partial t^2} = v_s^2 \frac{\partial^2 v}{\partial z^2} - \frac{B_0 I}{m} \frac{\partial u}{\partial z}. \tag{10.4.26}$$

This pair of equations is sufficient to describe the dynamics of the current-carrying wire. As our intuition suggested, the magnetic field produces a force in the x-direction [the last term in (10.4.25)] in proportion to the tilt of the wire in the y-direction. The equations are now coupled. A motion in one transverse direction cannot occur without involving a motion in the other transverse direction. Put another way, waves polarized in either the x- or y-directions are now coupled as they propagate along the z-axis, and we expect that the coupling will affect the dynamics of both waves.

There are still two waves that propagate in each direction on the wire. We can find them if we assume solutions with the variable separable form

$$u = \text{Re}\,[\hat{u} \exp j(\omega t - kz)] \quad \text{and} \quad v = \text{Re}\,[\hat{v} \exp j(\omega t - kz)].$$

The equations of motion are satisfied by these solutions if

$$\hat{u}(\omega^2 - v_s^2 k^2) - \hat{v}\left(\frac{jkB_0 I}{m}\right) = 0, \tag{10.4.27}$$

$$\hat{u}\left(\frac{jkB_0 I}{m}\right) + \hat{v}(\omega^2 - v_s^2 k^2) = 0. \tag{10.4.28}$$

These equations are homogeneous in the amplitudes $\hat{u}$ and $\hat{v}$. Unless both amplitudes are zero (not an interesting situation), the determinant of the coefficients must be zero. It is concluded that ω and k are related by

$$(\omega^2 - v_s^2 k^2) = \pm\left(\frac{kB_0 I}{m}\right). \tag{10.4.29}$$

We have found the dispersion equation for waves on the wire, and the nature of these waves is made evident by solving (10.4.29) for ω^2:

$$\omega^2 = k^2\left[v_s^2 \pm \left(\frac{B_0 I}{km}\right)\right]. \tag{10.4.30}$$

Evidently four waves can propagate on the wire, which is consistent with what we find if there is no magnetic field.

Equation 10.4.30 shows that one pair of waves (+ sign) has a phase velocity that increases with the magnetic field, whereas the other pair has a phase velocity that decreases with the magnetic field. The slower waves can, in fact, be unstable if

$$\left|\frac{B_0 I}{v_s^2 m}\right| > k, \tag{10.4.31}$$

for then $\omega = \pm j\alpha$, where α is a real number. If all real values of k were allowed by the boundary conditions, the wire would be unstable, no matter how small $B_0 I$, since there would always be a small enough wavenumber (long enough wave) to satisfy the condition for instability. The boundary conditions, however, are satisfied only by certain discrete values of k, which we enumerate shortly.

For the purpose of establishing the physical significance of the waves we have found, consider the case in which the wire is excited in the sinusoidal steady state at the (real) frequency ω. Then (10.4.29) is

$$k^2 \pm k\left(\frac{B_0 I}{v_s^2 m}\right) - \frac{\omega^2}{v_s^2} = 0, \tag{10.4.32}$$

and we can solve this relation to find four possible wavenumbers. Using the + sign in (10.4.32), we obtain

$$k = k_2, -k_1, \tag{10.4.33}$$

and using the minus sign we obtain

$$k = k_1, -k_2, \tag{10.4.34}$$

where k_1 and k_2 are the positive real numbers

$$k_1 = \frac{B_0 I}{2v_s^2 m} + \left[\left(\frac{B_0 I}{2v_s^2 m}\right)^2 + \frac{\omega^2}{v_s^2}\right]^{1/2}, \tag{10.4.35}$$

$$k_2 = -\frac{B_0 I}{2v_s^2 m} + \left[\left(\frac{B_0 I}{2v_s^2 m}\right)^2 + \frac{\omega^2}{v_s^2}\right]^{1/2}. \tag{10.4.36}$$

(Just to keep things straight, we assume for now that $B_0 I > 0$.) Note that $k_1 > k_2$. The dispersion equation (10.4.29), together with (10.4.27) or (10.4.28), shows that

$$\hat{v} = \pm j\hat{u} \tag{10.4.37}$$

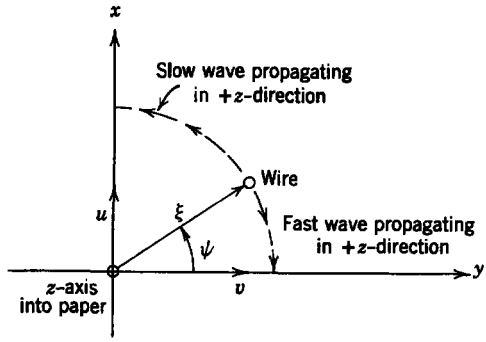

Fig. 10.4.5 Polar coordinates of wire deflection. At a given position along the z-axis the wire appears to rotate about it. The fast and slow waves have opposite directions of rotation.

We must remember to use the upper sign with those waves with wavenumbers given by (10.4.33) and the lower sign with those given by (10.4.34). Hence, if we have a wave given by

$$u = \text{Re}\,[\hat{u}_+^a e^{j(\omega t - k_1 z)} + \hat{u}_+^b e^{j(\omega t - k_2 z)} + \hat{u}_-^a e^{j(\omega t + k_1 z)} + \hat{u}_-^b e^{j(\omega t + k_2 z)}], \tag{10.4.38}$$

it follows from (10.4.37) that

$$v = \text{Re}\,j[\hat{u}_+^a e^{j(\omega t - k_1 z)} - \hat{u}_+^b e^{j(\omega t - k_2 z)} - \hat{u}_-^a e^{j(\omega t + k_1 z)} + \hat{u}_-^b e^{j(\omega t + k_2 z)}]. \tag{10.4.39}$$

The first two terms in these equations are waves with points of constant phase propagating in the $+z$-direction. Because $k_1 > k_2$, the (a) wave propagates more slowly than the (b) wave. The third and fourth terms are similar waves propagating in the $-z$-direction.

To obtain some insight into the nature of these waves, consider the first wave alone with $\hat{u}_+^a = -ju_0$. Then

$$\boldsymbol{\xi} = u\mathbf{i}_x + v\mathbf{i}_y = u_0[\sin(\omega t - k_1 z)\mathbf{i}_x + \cos(\omega t - k_1 z)\mathbf{i}_y]. \tag{10.4.40}$$

This deflection is easier to interpret if we consider the magnitude ξ and angle ψ defined in Fig. 10.4.5. Then

$$\begin{aligned} \xi &= \sqrt{u^2 + v^2}, \\ \psi &= \tan^{-1}\left(\frac{u}{v}\right) = \omega t - k_1 z. \end{aligned} \tag{10.4.41}$$

At an instant in time the deflection given by this wave is a spiral that circles the z-axis in the clockwise direction, as shown in Fig. 10.4.6b. Points of constant phase advance in the z-direction with the velocity ω/k_1. The phases of the (b) wave, which propagates in the $+z$-direction, move more rapidly with the velocity ω/k_2. If we repeat the arguments that led to (10.4.41),

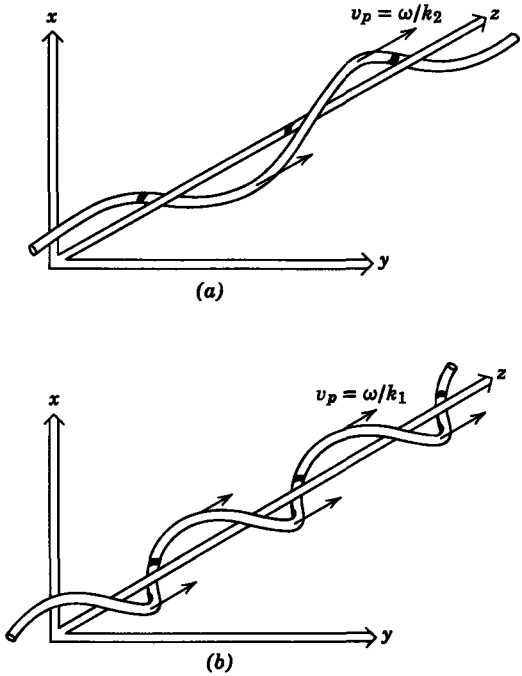

Fig. 10.4.6 Waves propagating in the $+z$-direction: (*a*) fast wave with a wavelength $2\pi/k_2$; and (*b*) slow wave with a wavelength $2\pi/k_1$.

using the u_+^b wave, we obtain a spiral that at an instant in time circles the z-axis in the counterclockwise direction (Fig. 10.4.6*a*). At any position z the wire will circle the z-axis in the counterclockwise direction for the slow wave and in the clockwise direction for the fast wave. Except that the propagation is in the opposite direction, the u_- waves have the same physical appearance.

We address ourselves now to superimposing these four wave solutions to find the free modes that satisfy the boundary conditions of Fig. 10.4.4 in which the wire is fixed at $z = 0$ and at $z = l$. This is done by finding the allowed eigenvalues k and then using (10.4.30) to find the associated eigenfrequencies.

In a boundary value problem of this type it is easier to work with trigonometric functions than with the complex exponentials. Hence we use the fact that $e^{j\theta} = \cos\theta + j\sin\theta$ and write the solution given by (10.4.38) as

$$u = \text{Re}\,\{e^{j\omega t}[A\sin k_1 z + B\cos k_1 z + C\sin k_2 z + D\cos k_2 z]\}, \quad (10.4.42)$$

where we have defined a new set of four constants as

$$\begin{aligned} A &= j(\hat{u}_-^a - \hat{u}_+^a), & C &= j(\hat{u}_-^b - \hat{u}_+^b), \\ B &= (\hat{u}_+^a + \hat{u}_-^a), & D &= (\hat{u}_+^b + \hat{u}_-^b). \end{aligned} \quad (10.4.43)$$

In terms of these same constants the solution for the y-deflection becomes (10.4.39)

$$v = -\text{Re}\,\{e^{j\omega t}[A\cos k_1 z - B\sin k_1 z - C\cos k_2 z + D\sin k_2 z]\}. \quad (10.4.44)$$

The four constants are, of course, determined by the boundary conditions

$$\begin{aligned} u(0,t) &= 0, \qquad v(0,t) = 0, \\ u(l,t) &= 0, \qquad v(l,t) = 0. \end{aligned} \quad (10.4.45)$$

The advantage of the trigonometric form that we have used for our solution is the simplicity of the relation among the constants that results from the boundary conditions at $z = 0$. Because the sine functions are zero at the origin,

$$\begin{aligned} B &= -D, \\ A &= C. \end{aligned} \quad (10.4.46)$$

The remaining two conditions at $z = l$ require that

$$\begin{aligned} A(\sin k_1 l + \sin k_2 l) + B(\cos k_1 l - \cos k_2 l) &= 0, \\ A(\cos k_1 l - \cos k_2 l) - B(\sin k_1 l + \sin k_2 l) &= 0. \end{aligned} \quad (10.4.47)$$

Because A and B are not zero, the determinant of the coefficients must be zero; that is,

$$(\sin k_1 l + \sin k_2 l)^2 + (\cos k_1 l - \cos k_2 l)^2 = 0. \quad (10.4.48)$$

Recall that $\sin^2\theta + \cos^2\theta = 1$ and $\cos\theta\cos\gamma - \sin\theta\sin\gamma = \cos(\theta + \gamma)$, and (10.4.48) reduces to the simple condition

$$\cos l(k_1 + k_2) = 1. \quad (10.4.49)$$

It follows that the argument $l(k_1 + k_2)$ must have values $0, 2\pi, 4\pi, \ldots, 2n\pi, \ldots$. If $k_1 + k_2$ is replaced by the sum of (10.4.35) and (10.4.36), we obtain an expression that determines the eigenfrequencies ω_n:

$$\omega_n^2 = \frac{v_s^2}{4}\left[\left(\frac{2n\pi}{l}\right)^2 - \left(\frac{B_0 I}{v_s^2 m}\right)^2\right], \qquad n = 1, 2, \ldots. \quad (10.4.50)$$

We have left out the case $n = 0$ because this solution is trivial; that is, there is no deflection when $n = 0$, as can be seen by taking the limiting case in which there is no magnetic field.

We have found that if we set the wire into vibration in one of its natural modes and then turn on the magnetic field and current, the frequency will decrease in magnitude. As we raise the magnetic field, the equilibrium is first unstable in the $n = 1$ mode. The system is unstable if

$$\left|\frac{B_0 I}{v_s^2 m}\right| > \frac{2\pi}{l}. \quad (10.4.51)$$

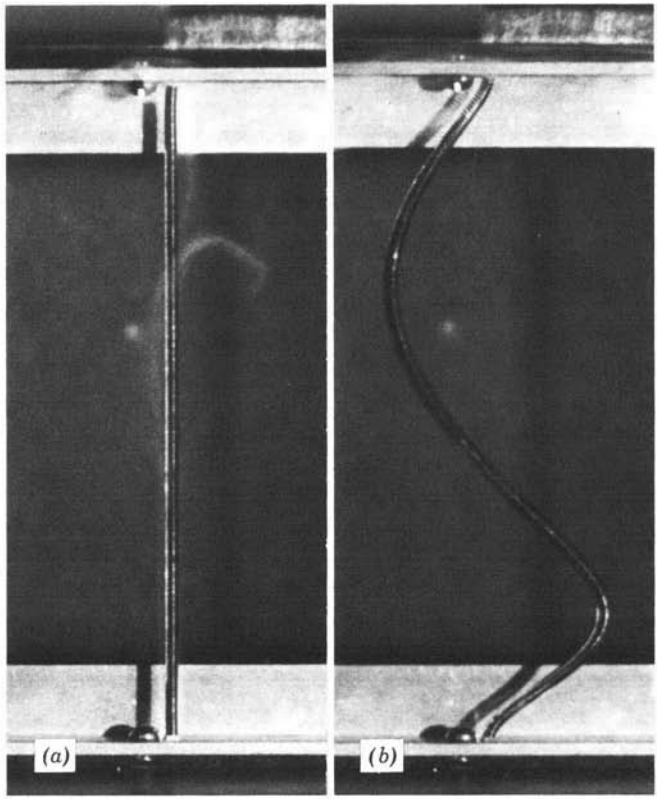

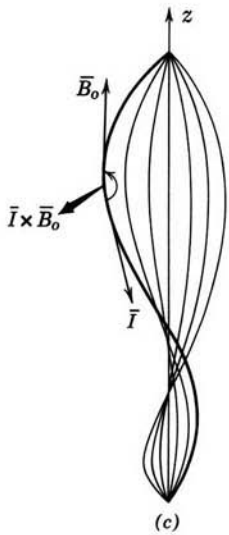

Fig. 10.4.7 (*a*) Experiment in which a conducting spring is stretched between pole faces of a magnet. There is a vertical field B_0 and a current has just been applied to the spring. (*b*) A moment later instability occurs. (*c*) Predicted $n = 1$ mode at point of impending instability. (From Film "Complex Waves I, Propagation, Evanescence and Instability," produced by Education Development Center, Inc., Newton, Mass., for the National Committee on Electrical Engineering Films.)

We have established that the value of k that should be used in (10.4.31) is $2\pi/l$.

Finally, it is worthwhile to see what the physical form of a natural mode is. Given one of the constants, the other three can be determined from (10.4.46) and (10.4.47). For this particular problem, however, the compatability condition (10.4.49) ensures that the coefficients of both A's and B's in (10.4.47) are zero, as can be determined by using trigonometric identities. This means that all conditions are satisfied if A and B are specified independently. Consider the case in which A, hence [from (10.4.46)] C is zero. Then, since $B = -D$, if we determine the time phase by taking B as a real number, (10.4.42) and (10.4.44) become [here, use is made of (10.4.35) and (10.4.36) and the fact that $k_1 + k_2 = 2n\pi/l$.]

$$\begin{aligned} u &= -2B \cos \omega t \sin \frac{n\pi z}{l} \sin \frac{B_0 I}{2v_s^2 m} z, \\ v &= 2B \cos \omega t \sin \frac{n\pi z}{l} \cos \frac{B_0 I}{2v_s^2 m} z. \end{aligned} \tag{10.4.52}$$

In terms of the polar variables of (10.4.41) and Fig. 10.4.5,

$$\begin{aligned} \psi &= -\frac{B_0 I}{2v_s^2 m} z, \\ \xi &= 2B \cos \omega t \sin \frac{n\pi z}{l}. \end{aligned} \tag{10.4.53}$$

If we had used the constant A, rather than B, it would have shifted this deflection by 90° about the z-axis.

A plot of (10.4.53) is shown in Fig. 10.4.7*c* for the first eigenmode with $B_0 I < 0$. Note that because of the condition for instability (10.4.51) the maximum twist ψ that the standing wave can undergo is 180°. Hence the mode shown in Fig. 10.4.7*c* is at the point at which instability occurs for the $n = 1$ mode.

The wave dynamics that we have found in this section are related to several types of electromechanical interaction. The "pinch" confinement of a plasma, proposed as a scheme for containing a controlled thermonuclear reaction, suffers from an instability with the same kinked property as the one found here.* The plasma is likely to behave more nearly as a perfectly conducting medium or as one with a high rather than a low magnetic Reynolds number. If, however, a current is passed through a liquid column of mercury (where R_m is small) in the presence of an axial magnetic field, an instability with

* D. J. Rose and M. Clarke, Jr., *Plasmas and Controlled Fusion*, M. I. T. Press and Wiley, New York, 1961, p. 336.

essentially the same features as that described here will result.* Often the twisting motions that characterize the dynamics of the wire are found in other electromechanical systems that involve an imposed magnetic field. An example is the cyclotron wave of electron beam theory.†

10.5 DISCUSSION

In this chapter we have explored the consequences of continuum electromechanical coupling with simple elastic continua. This has produced mathematical analyses and physical interpretations of evanescent waves, absolute instabilities, and waves and instabilities in convecting systems. The unifying mathematical concept is the dispersion relation presented graphically in the ω-k plots.

Although our examples have been framed in terms of simple physical situations, the phenomena we have discussed occur in the wide variety of practical situations indicated in Section 10.0 and throughout the chapter.